EXPLORING MORE SUSTAINABLE ROUTES

TO ACRYLATE MONOMER MANUFACTURE

LAURA JAYNE SCHOFIELD, MSc.

Thesis submitted to the University of Nottingham
for the degree of Doctor of Philosophy

JULY 2016

Declaration

I, Laura Jayne Schofield, declare that this Thesis has been composed by myself and that the work reported is my own and was conducted over the period September 2011 to March 2015. Where work was carried out in collaboration, the relevant researchers have been acknowledged. This thesis has not been accepted in partial or complete fulfilment of any other degree or professional qualification.

Abstract

Acrylic based monomers are used to create a wide range of organic polymers with applications from false nails to lighting panels and from lightweight, scratch-proof laptop screens to viewing windows in aquariums and submarines. Petrochemicals have been the predominant feedstock for these monomers since their introduction, but moves to make the industry "cleaner" and "greener" have led to a growing interest in renewable resources. Exploiting such resources for bulk plastic manufacture is the focus of this project.

This thesis describes the hydrothermal conversion of di- and tri-carboxylic acids into acrylic acid and methacrylic acid. In order to produce these chemicals via sustainable routes, the di- and tri-carboxylic acid precursors used in this work are all available from biomass or from known biological processes that convert biomass into useful precursors.

Previous work in this area has focussed on the production of methacrylic acid from itaconic acid and its isomers or from citramalic acid. However, the first section of this thesis investigates the production of acrylic acid from malic acid. Malic acid is readily available from biomass sources and can produce acrylic acid after decarboxylation and dehydration akin to the previously-reported route from citramalic acid to methacrylic acid. However, significant levels of by-products and unselective extractions meant we were unable to present an industrially viable route that could compete with current processes. The focus of the project then returned to the production of methacrylic acid.

Fermentation of sugar molasses using Aspergillus terreus yields itaconic acid. This acid can then be used in the continuous production of

methacrylic acid in high temperature water (>200 °C), at elevated pressure (>2000 psi) in the presence of sodium hydroxide. Our research looks at the stability of methacrylic acid under these reaction conditions, showing the hydration to 2-hydroxyisobutyric acid and decomposition to acetone. By investigating the effect of temperature and residence time on the stability of methacrylic acid and 2-hydroxyisobutyric acid, it is suggested that reactions do not exceed 260°C and have a residence time shorter than 360 s.

Finally, this thesis describes a proposed new process for methacrylic acid production to include the recycling of a sodium hydroxide catalyst. Subsequent acidification of reaction exit solutions releases free methacrylic acid that can be extracted with a suitable organic solvent. Previous work in this area demonstrated this process with the use of sulfuric acid to release free methacrylic acid and yield the free acid as well as aqueous sodium sulfate waste. However, by using an acidic precursor, such as itaconic acid, to acidify the exit solution, methacrylic acid can be extracted and the remaining aqueous solution can be cycled through the continuous flow equipment, recycling the base catalyst as sodium itaconate. This process is demonstrated up to 20 cycles, and collected methacrylic acid has been esterified and polymerised to yield a sample of poly(methyl methacrylate), demonstrating proof of the concept behind our new process as a route to bulk plastic manufacture from renewable resources.

Acknowledgements

It is with great pleasure that I begin this long list of thanks with my supervisor, Professor Sir Martyn Poliakoff. To Martyn, I owe my career in Science. During a chance meeting on an open day many moons ago, he captured my imagination and I am glad to call him not only a colleague, but a friend.

I would like to extend my gratitude to Dr Mark Waugh, Dr Graham Eastham, Dr David Johnson and many other employees at Lucite International for their involvement in this project. Thanks also go to Lucite International and the EPSRC for funding such an exciting and successful CASE project. I send great thanks to Dr Tom Huddle for the initial training and for being a willing sounding board for my visions of the project.

To my colleagues and the Masters students that I have had the pleasure of working with through this project, I thank you all for making my years in Nottingham so pleasurable and I wish you the best in all your future endeavours. I would especially like to thank Dr Peter Bayliss for training me in the lab and for being so entertaining over the last five years; please never change.

I thank Mr Martin Dellar, Mr Peter Fields, Mr Richard Wilson, Mr David Litchfield, Mr Kevin Hind and Mr Mark Guyler for their hard work and dedication to aid my experimental work and for keeping the department running. I would also like to express my appreciation to Di Mann for her unwavering organisation of the entire group. Her early morning smiles will always cheer my soul.

To the friends I had before and those I've made along the way, I thank you for being my biggest and loudest cheerleaders, and for being the most beautiful and hilarious bunch of people I could ever wish to know!

To my family, you are my heroes. You've been there since the beginning and moulded me into the person I am today. This thesis is for all of you:

Dad, for always pretending to understand me, assuring me that the world is my lobster and always making me laugh, merci buckets. Mum, thank you for instilling in us the mentality to always go after what we want and for encouraging a love of books from a young age. Hayley, you set the bar high, gave me something to aim for and are always an inspiration to your little sis. To my grandparents, aunts, uncles and cousins, thank you for being my biggest fans and for pandering to my (not so) inner nerd.

And finally, to Paul, you knew it wasn't going to be the easiest of rides after *that* second date, but you stuck by me. I could not have completed this work without your constant support and frequent badgering. I adore you.

Congratulations!
Today is your day.
You're off to Great Places!
You're off and away!

And will you succeed?
Yes! You will, indeed!
(98 and ¾ per cent guaranteed.)
KID, YOU'LL MOVE MOUNTAINS!
- Dr Seuss

Contents

DECLARATION ..... **I**

ABSTRACT ..... **III**

ACKNOWLEDGEMENTS ..... **V**

CHAPTER 1 - INTRODUCTION **1**

The Chemical Industry *2*

Green and Sustainable Reactions *2*

Green Chemistry and the Polymer Industry *7*

METHACRYLIC ACID (MAA) 9

Properties and Uses *9*

Production of MAA *12*

Renewable Processes for Methacrylic Acid *19*

ACRYLIC ACID 26

Properties and Uses *26*

Production of Acrylic Acid *27*

Renewable Processes to Acrylic Acid *28*

AIMS AND OBJECTIVES 32

CHAPTER 2 - EXPERIMENTAL METHODS **34**

EQUIPMENT 34

MATERIALS 46

ERRORS 48

STANDARD OPERATING PROCEDURE 52

EXPERIMENTAL PROCEDURE 55

CHAPTER 3 - A NOVEL APPROACH TO ACRYLIC ACID PRODUCTION 62

STRATEGY 69

RESULTS AND DISCUSSION 70

Malic Acid Decomposition 70

Acrylic Acid Stability 77

Acrylic Acid Extraction 87

SUMMARY 99

CHAPTER 4 - METHACRYLIC ACID STABILITY 100

STRATEGY 105

RESULTS AND DISCUSSION 107

MAA Stability 107

HIB Stability 119

SUMMARY 128

CHAPTER 5 - A RECYCLABLE PROCESS 129

STRATEGY 135

RESULTS AND DISCUSSION 136

Comparison of Isomeric Precursors 148

PMMA Production 163

Scale Up 164

SUMMARY 170

CONCLUSIONS AND FURTHER WORK 171

Aim 1 171

Aim 2 ..... *173*

Aim 3 ..... *174*

Aim 4 ..... *175*

Aim 5 ..... *177*

FINAL REMARK 179

REFERENCES 180

APPENDIX 187

Chapter 1 - Introduction

The modern UK chemical industry dates back to the eighteenth century,[1] when the demand for sulfuric acid highlighted the need for the large scale production of chemicals. Since then, the chemical industry has grown to an enormous scale, with the current UK chemical industry boasting an annual turnover that tops £58 billion.[2, 3]

Petrochemicals have been the predominant feedstock for many processes since their introduction, but moves to make the industry "cleaner" and "greener" have led to a growing interest in renewable resources. As fossil fuel reserves are rapidly being depleted and the World's energy consumption continues to rise,[4] the chemical industry is being forced to look towards biomass and other renewable sources for their feedstocks.

Not only has the nature of feedstocks been affected but, since the introduction of the 12 Principles of Green Chemistry,[5] efforts have been made to make industrial processes as a whole more sustainable. Research into "greener" synthesis has made progress towards eradicating the use of harsh solvent systems and using less hazardous and less toxic chemicals in industrial reactions.

The research outlined in this thesis describes the production of acrylic based monomers in high temperature and high pressure water for polymer manufacture. More specifically the research looks at aqueous acidic solutions undergoing decarboxylation and dehydration reactions to form acrylic acid and methacrylic acid (MAA). The overall intention of this research is to present novel and sustainable routes to acrylic acid and MAA from biomass precursors using a simple base catalyst.

The Chemical Industry

Manufacturing chemicals is a potentially hazardous enterprise, with most processes involving the use or formation of harmful or toxic chemicals, and elevated temperatures and pressures being used during reactions. As such the industry is heavily regulated and many safety regulations have been put into place to reduce risks.

Regulations are also enforced on the introduction of living biologics, or biological products, in the processing of chemicals. The use of living entities can lead to more desirable reaction conditions, reducing risks including high temperatures. However, such living entities are susceptible to mutation and must be monitored closely.

In its simplest form, the risk of a chemical process can be defined as the level of hazard multiplied by the level of exposure, seen in Equation 1.1:

$$Risk = Hazard \times Exposure$$

Equation 1.1 The term "risk" in chemical reactions is often described as a function of the hazards of the reaction, such as the nature of reagents and products and the conditions required for the reaction pathway, and later, the exposure through the handling and disposal of chemicals.

In most cases, when assessing risk one would act to reduce exposure to limit the overall risk. However, a new shift to reduce the hazards of reactants, reactions and products has been led by the introduction of so called "Green Chemistry".

Green and Sustainable Reactions

As an employee of the United States Environmental Protection Agency, Paul Anastas promoted the term "Green Chemistry" and described an energy efficient process that not only minimised the use of toxic materials

but also eliminated waste production. Anastas went on with John Warner to expand this definition as a set of 12 Principles of Green Chemistry[5] and quickly became regarded as the father of "Green Chemistry".

Prevents waste	**I**nherently non-hazardous and safe
Renewable materials	**M**inimise material diversity
Omit derivatisation steps	**P**revention instead of treatment
Degradable chemical products	**R**enewable material and energy inputs
Use safe synthetic methods	**O**utput-led design
Catalytic reagents	**V**ery simple
Temperature, pressure ambient	**E**fficient use of mass, energy, space & time
In-process monitoring	**M**eet the need
Very few auxiliary substances	**E**asy to separate by design
E-factor, maximise feed in product	**N**etworks for exchange of local mass & energy
Low toxicity of chemical products	**T**est the life cycle of the design
Yes, it's safe	**S**ustainability throughout product life

Figure 1.1 The 12 Principles of Green Chemistry and 12 Principles of Green Engineering have been shortened to form the mnemonics "PRODUCTIVELY" and "IMPROVEMENTS" respectively.[5-8] The principles were introduced to steer chemical reactions, both on a lab scale and larger, industrial scales, towards minimising risk by reducing the hazards associated with a reaction or process.

The principles have since been condensed into a mnemonic "PRODUCTIVELY"[6] and have inspired further principles, including the 12 Principles of Green Engineering.[7] The engineering principles were written to complement Anastas's original ideals by working to create end processes that could be tuned to different output levels, minimise risks and be built from the correct material to be durable throughout its lifetime. These

principles have also been condensed to form a second mnemonic of "IMPROVEMENTS".[8]

The 12 Principles of Green Chemistry focus on minimising waste and increasing energy efficiency and were inspired by such terms as "ideal synthesis", "Atom Economy" and "E factor". In 1975, Hendrickson defined the "ideal synthesis" as one that prevents waste by using building blocks that simply click together to form the desired product.[9]

> *"The ideal synthesis…would start from available small molecules so functionalised as to allow constructions linking them together directly, in a sequence only of successive construction reactions involving no intermediary refunctionalisations, and leading directly to the structure of the target, not only its skeleton but also its correctly placed functionality. If available, such a synthesis would be the most economical, and it would contain only construction reactions."* – James B. Hendrickson[9]

Barry Trost quantified the selectivity of a reaction by introducing "Atom Economy",[10] a measure of the overall efficiency of a process:

$$Atom\ Economy = \frac{Molecular\ Mass\ of\ Desired\ Product}{Molecular\ Mass\ of\ all\ Reactants}\ x\ 100\ \%$$

Equation 1.2 To calculate the ratio of waste compared to product. A perfect process will score 100 % for atom efficiency and would describe a very neat reaction where all reactants are incorporated into the desired product.

The "Atom Economy" is a percentage value based on the sum of the molecular mass of desired products divided by the molecular mass of all reactants. The term was introduced to describe the weight of atoms from reactants that end up in the final product. Equation 1.2 does not directly quantify the waste of a process and while it can be assumed that any reactants that do not end up in the products are waste, it does not make

allowances for processes that recycle any unreacted starting materials, or account for solvents or catalysts.

To better account for the problem of waste in the chemical industry, Roger Sheldon introduced the "E factor".[11] The "E factor" or "Environmental factor" defines the amount of waste from any given process where waste includes everything except the desired product. The waste includes solvents, unreacted reagents, unwanted by-products and, in more complete calculations, the fuel consumption of the process.

$$E\ factor = \frac{Total\ waste\ (kg)}{Total\ product\ (kg)}$$

Equation 1.3 When evaluating a process, a smaller "E factor" value corresponds to a more sustainable process, which would have a very small E factor as the total mass of products far outweighs the total waste of the product but the equation does not look at the nature of the waste and so a more desirable E factor may not correlate to the least hazardous reaction.

A measure of "Atom Efficiency" or "E factor" alone would be criticised because they do not concern themselves with the nature of waste. A process that releases a small amount of highly toxic waste would seem much more appealing than a process that produces a larger amount of a non-toxic, benign chemical; however, the 12 Principles of Green Chemistry state that the release of hazardous chemicals should be minimised and pollution should be prevented. It is only by linking these measures together that a process can truly call itself green.

A new branch of organic chemistry has introduced the ideas behind Green Chemistry to the pharmaceutical industry through "Click Chemistry".[12] In order to synthesise complex molecules, modular reactions join smaller molecular units together with carbon-heteroatom links that exhibit high atom efficiencies. This branch of chemical synthesis follows

several of the 12 Principles of Green Chemistry, including the generation of only "inoffensive byproducts", "simple reaction conditions" using "no solvent or a solvent that is benign", "give very high yields" and be "stereoselective".

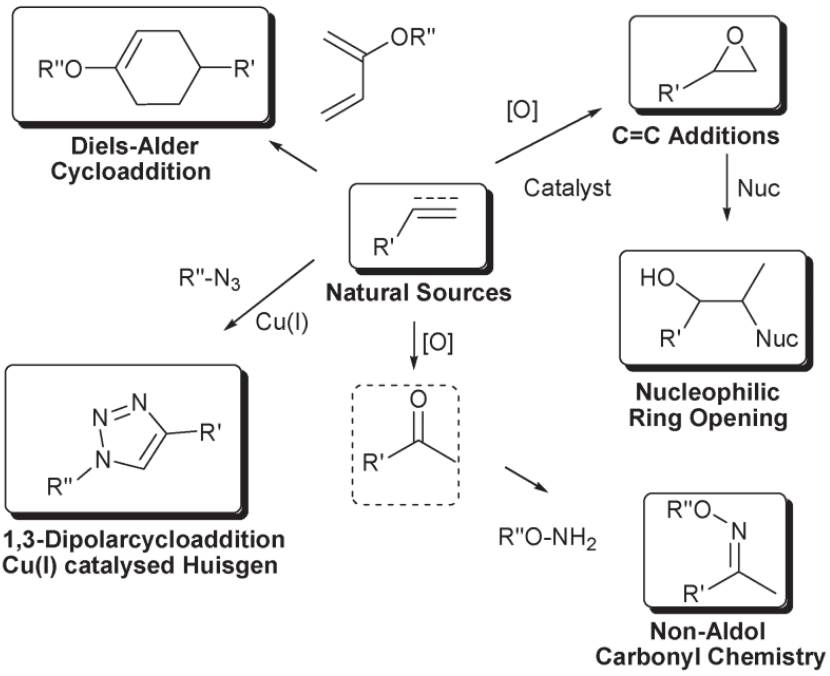


Figure 1.2 A collection of suitable reactions that follow the guidelines set out by Click Chemistry.[13]

A variety of reactions are shown in Figure 1.2 to demonstrate the application of Click Chemistry.[13-18] The reactions typically begin with widely available alkenes or alkynes and react them to form widely used products that are not only produced in high yields, but also stereoselectively.

The main criticism of Green Chemistry is the lack of economic concern, that is to say, the "greenest" reaction may not be economically viable. Perhaps Sustainable Chemistry is a more appropriate term to describe an ideal reaction as it encompasses three pillars: social, economic and environmental. It can be defined as "meeting the needs of the present generation without compromising the needs of future generations to meet their own needs".[19] At present our use of fossil fuels is far from sustainable

and as their depletion reaches critical levels, the chemical industry must turn their focus towards new fuels and feedstocks for both fine and bulk chemicals.

Green Chemistry and the Polymer Industry

The price of bulk chemicals, such as polymers, is very sensitive to the price of oil and the cost of manufacturing such materials fluctuates with the market value. If a renewable source could be found for their manufacture, it would be possible for the Chemical Industry to stabilise prices and the use of these products would become more sustainable.



Figure 1.3 Objects made from Parkesine in the 19th Century and stored in the archives at the Science Museum in London.[22]

It is not a new idea to use biomass in the production of polymers. In 1856, Alexander Parkes patented his nitrocellulose polymer, "Parkesine".[20] The polymer was soon blended with camphor and "celluloid" was born.[21]

The global plastics industry uses 4% of the world's annual production of oil as a feedstock[23] and, in 2013, produced 299 Mtonnes of plastic.[24]

- Benzene is used as a precursor to styrene, the monomer of polystyrene.
- Ethene yields polythene after polymerisation. Ethene can also be chlorinated to form vinyl chloride or oxidised to form ethylene glycol which can be further reacted with dimethyl terephthalate to yield poly(ethylene terephthalate) or PET.
- Methyl methacrylate (MMA) is commonly synthesised from isobutylene or acetone and is used to produce Perspex.

In an effort to become more sustainable, the chemical industry is striving to find replacements for low cost bulk chemicals, such as plastics and hence the monomers they are made from, or to redesign the synthetic routes. It is predicted that the annual global demand for bio-plastics will rise to 960,000 tonnes in 2017.[25]

One such chemical replacement is 2,5-furandicarboxylic acid as a substitute for terephthalic acid in polyesters. By switching to 2,5-furandicarboxylic acid, it is possible to make a biologically derived polymer since both the monomer and ethylene glycol can be sourced from biomass.[26] A further example is the new method for obtaining biomass-based monomers from lignocellulosic material *via* a reaction with trifluoroacetic acid.[27] An example of redesigning a synthetic method is the possible switch from the Alpha Process to make the perspex precursor, MAA, *via* a more biological route, as discussed in section 1.4.

Methacrylic Acid

Properties and Uses

MAA is a colourless liquid that is almost exclusively produced as a precursor to various methacrylate monomers and polymers. MAA can be polymerised to form poly(methacrylic acid) (PMAA), which has a number of uses including semi-rigid packaging and coatings for golf balls,[28] as well as biomedical uses, as bone cement for fixing orthopaedic replacements and improving wound healing.[29]

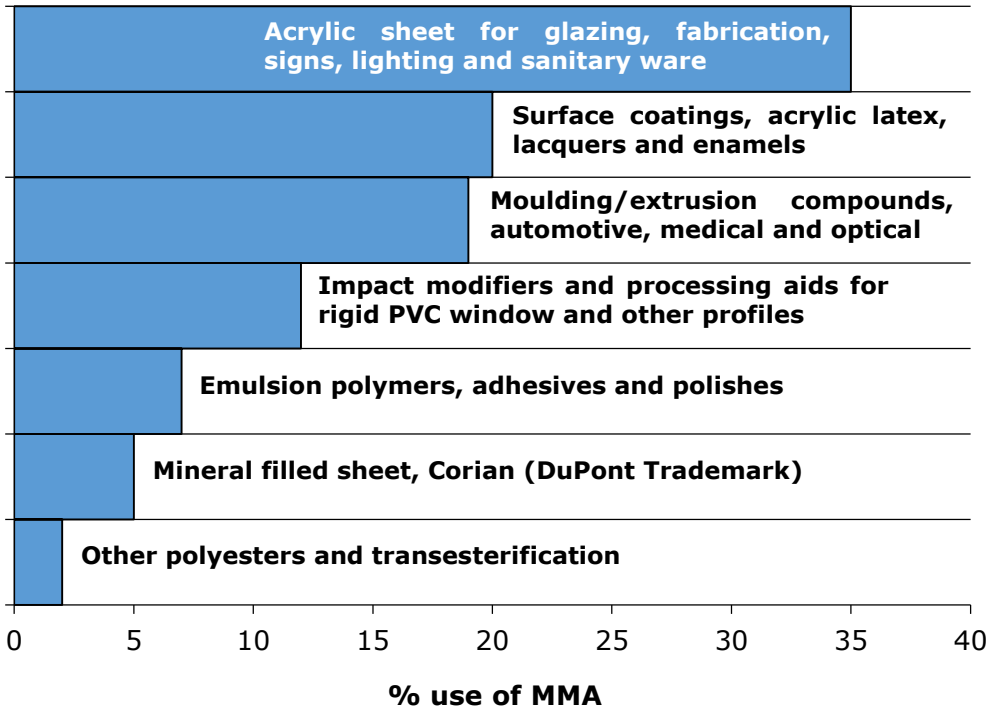


Figure 1.4 The primary uses of the 3.8 Mtonnes of MMA produced by Lucite International in 2011.[30]

However, MAA is more commonly used after esterification, most notably to methyl methacrylate (MMA). The presence of a double bond in the methacrylate molecules enables the polymerisation of these monomers; for example, MMA forming poly(methyl methacrylate) (PMMA).[31] PMMA is often described as an organic or acrylic glass as it is a tough, clear plastic

that can be recycled and goes by various brand names, such as Plexiglass®, Perspex® and Lucite®.

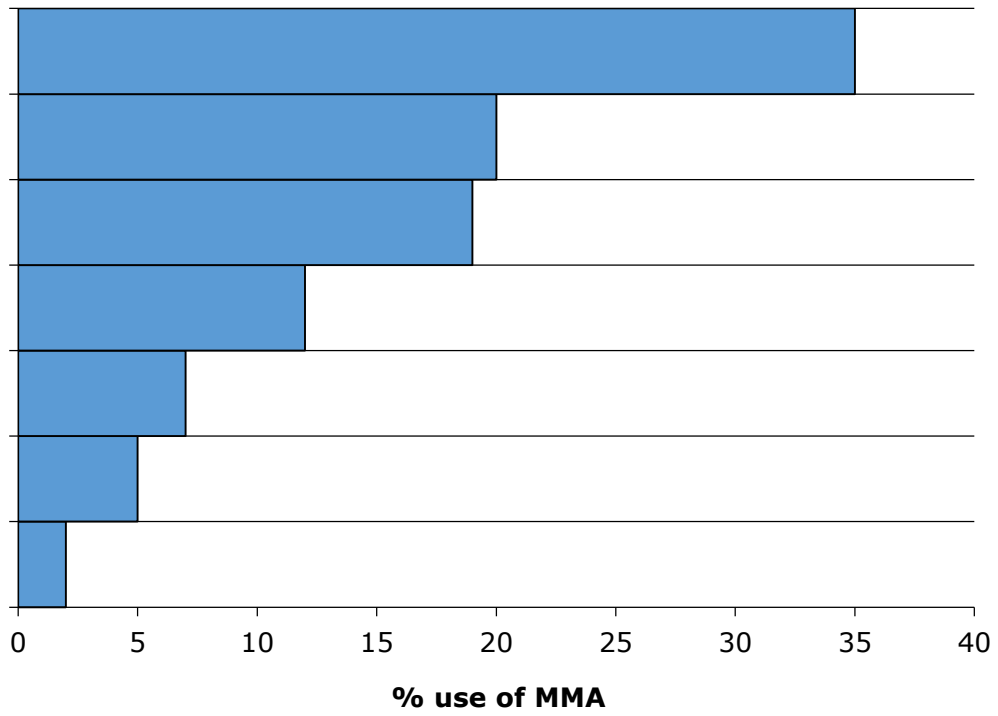


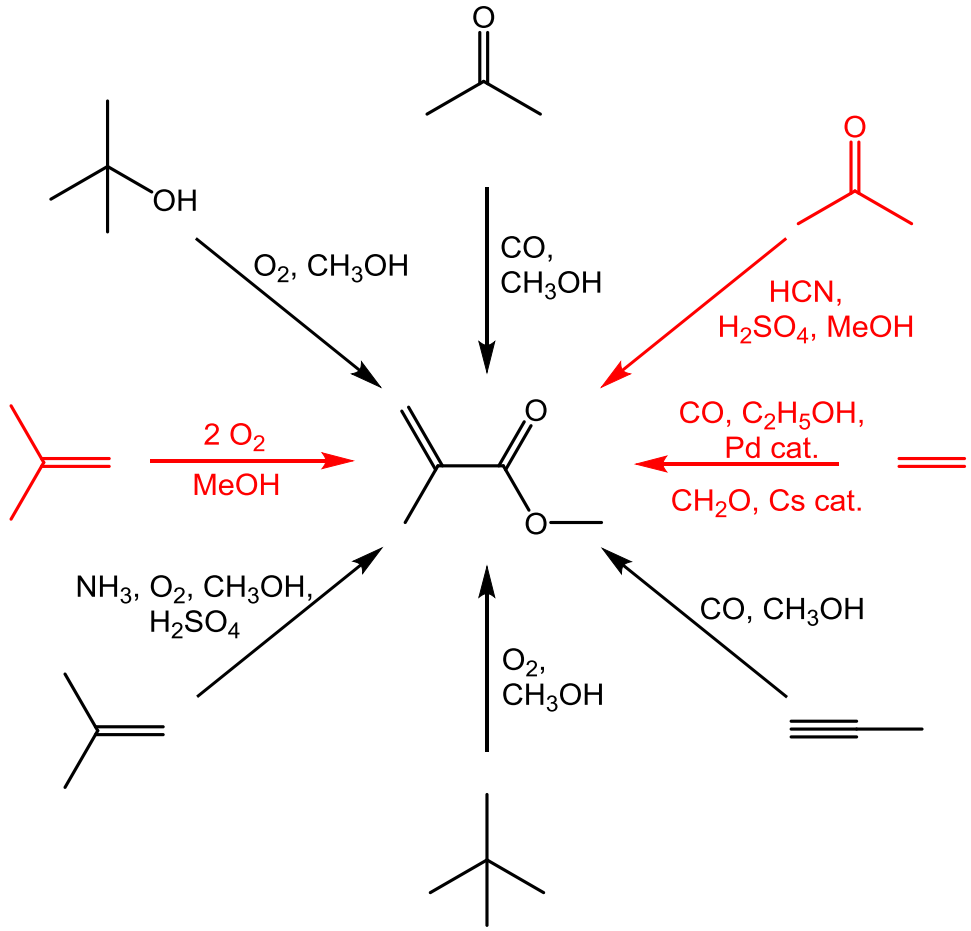
Figure 1.4 shows the primary uses for PMMA in 2011. Its uses are ubiquitous, from dental components[32, 33] to the cement used in hip replacements;[33] from viewing windows in ice hockey rinks[33] to high molecular weight surfactants;[34] and from signs and displays[33, 35] to shatterproof mobile phone screens. In 2010, an advert featured a Nissan 370Z replica car made from PMMA by Asylum SFX (see Figure 1.5).[36] The advert exploited the high optical clarity of the material and was used to show the inner workings of an engine without the need for computer generated graphics.



Figure 1.5 A replica Nissan 370Z was made from PMMA to highlight the inner workings of an engine.[36] PMMA was chosen as the material due to its high optical clarity.

Production of MAA

Over 3 million tonnes of MMA were produced in 2011, with demand growing year on year and is expected[37] to top 3.94 million tonnes in 2017. Some of the common synthetic routes[38] to MMA are shown in Scheme 1.1. The more industrially significant processes, highlighted in red, are described below.



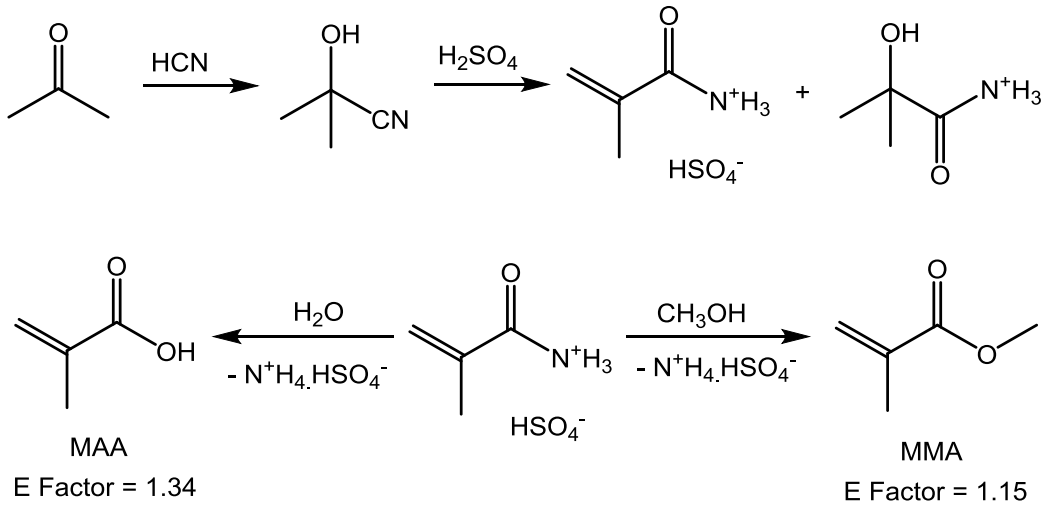
Scheme 1.1 The most common synthetic routes to MMA.[38] Those highlighted in red are described in detail in this chapter.

ACH Process

In 1934 ICI was granted a patent for the production of methacrylamide sulfate from acetone cyanohydrin (ACH) using concentrated sulfuric acid.[39]

The process involves the conversion of acetone and hydrogen cyanide first to ACH and then on to form methacrylamide sulfate using sulfuric acid. This can be hydrolysed to give MAA or reacted with methanol to give MMA. This process is known as the ACH route and is still a common route to MMA in many countries today.

In the first step of this process (see Scheme 1.2), acetone and hydrogen cyanide are reacted together in the presence of base, at 80 – 110 °C to form acetone cyanohydrin. Anhydrous sulfuric acid is then added to the ACH, while the mixture is continuously stirred to prevent decomposition. At this stage, the temperature is increased to 125 – 160 °C for a brief thermal cracking period. This stage converts any α-hydroxyisobutyramide that may have been formed by hydrolysis of methacrylamide sulfate. Finally, the methacrylamide sulfate is reacted with either excess water to produce MAA, or with aqueous methanol to form MMA through esterification.[9]

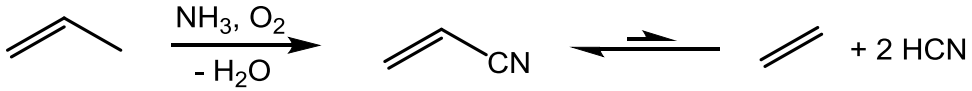


Scheme 1.2 Reaction scheme showing the production of MAA and MMA from acetone and hydrogen cyanide. Shown under each product is a calculated E Factor value.

While this process is still the most common for MMA production, it has clear disadvantages, including the use of petrochemicals as a feedstock.

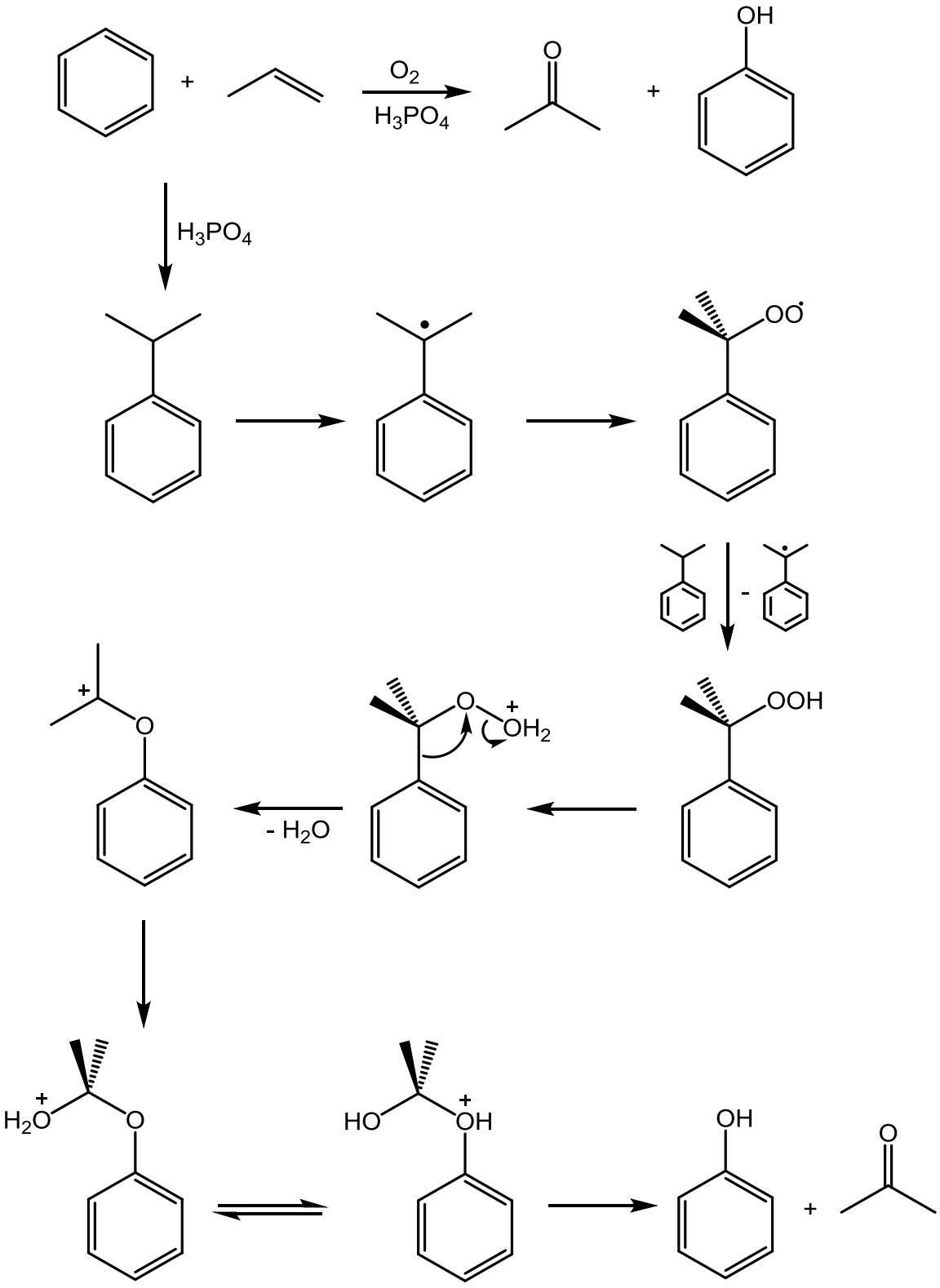
Scheme 1.2 shows E Factor values for both MMA and MAA production *via* the ACH route. MMA production shows a low E Factor value of just 1.15, making the process appear desirable. However, the toxicity of both hydrogen cyanide and concentrated sulfuric acid present inherent risks to the reaction.[40] On large industrial scales, the production, storage and disposal of these chemicals can be very costly and will limit the size of the plant to minimise the hazards of chemical containment.

However, the addition of a sulfuric acid regeneration plant can reduce the cost of disposal as it converts the ammonium sulfate back into sulfuric acid, which can be recycled back into the MMA plant, and ammonia. Both acetone and hydrogen cyanide can be purchased from other industrial processes that synthesise the chemicals as by-products. Hydrogen cyanide is a by-product of acrylonitrile production, seen in Scheme 1.3[41] and acetone is a by-product of the synthesis of phenol, seen in Scheme 1.4.[42]



Scheme 1.3 Reaction scheme showing the production of hydrogen cyanide as a byproduct of acrylonitrile synthesis.

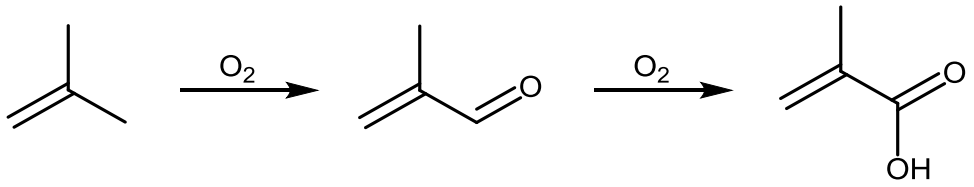
While these materials can be sourced from other process, there are often problems with matching the scales of the linked processes. Another issue of this association is the safe transfer of hydrogen cyanide from the acrylonitrile plant to the MAA plant, which would be costly due to the high toxicity of the liquid. To overcome this, the plants could be located next to each other, but in the majority of cases HCN is produced *in situ* in MMA manufacture.



Scheme 1.4 Showing the co-production of acetone during the synthesis of phenol in the Cumene process.[42]

i-C4 Process

In an attempt to overcome the hazards of containment of such toxic reagents and byproducts, the i-C4 process was developed in Japan to produce MAA in a two-step oxidation of isobutylene.[43, 44] The i-C4 process is widely used in Japan, and plants have now opened in South Korea, Singapore and Thailand. The i-C4 process can be seen in Scheme 1.5.



Scheme 1.5 Reaction scheme showing the production of MAA from isobutylene.

In the first step of the reaction, isobutylene is reacted with molecular oxygen to yield methacrolein, which is then further oxidised in a second step to MAA. Both steps require the use of a catalyst and, although much research has been done into catalytic improvements,[45-50] the overall selectivity remains at 65-70%. The product from the first step can either be extracted from the oxidation gas before being fed into a second vessel to complete the reaction, or simply fed in through a continuous flow.

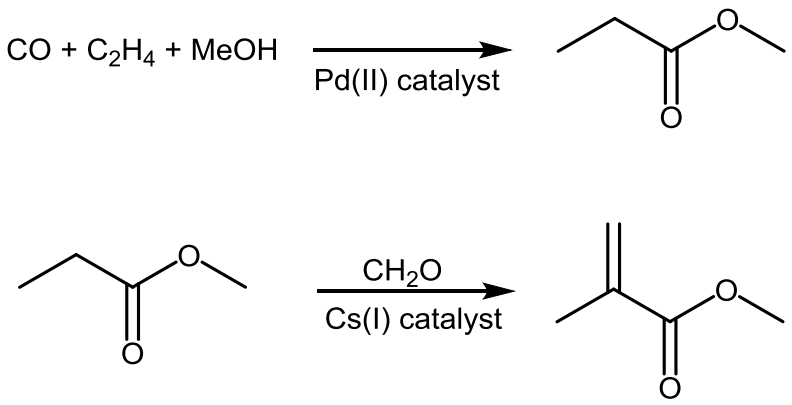
While the process uses excess oxygen in both steps, it is possible for the oxygen gas to be recycled, because both methacrolein and MMA are liquids at room temperature and could be siphoned off at the end of the reaction. This reduces the E Factor and improves the sustainability of the process.

A limited supply of hydrogen cyanide and low demand for isobutylene means the i-C4 process is very popular in Japan and its neighbours. However, isobutylene has been used in Western countries as a fuel additive;[51] and although its use in fuels is no longer as popular, the i-C4 process remains largely limited to Asia.

Alpha Process

Possibly the most significant advance in MAA and MMA production in recent years has been the introduction of the Alpha Process by Lucite International.[52] This process uses much more abundant feedstocks (ethylene, ethanol and carbon monoxide) than previous processes and all of the precursors can be obtained from biomass. In addition, the process generates little waste and is a much less toxic method than the ACH Process, meaning that Alpha plants are not limited in size and offers economy of scale.

The process is, like the i-C4, a two-step process and again requires a catalyst for both steps. In the first step, ethylene undergoes a carbonylation step in the presence of a palladium (II) biphosphine catalyst[53, 54] to yield >99.9% methyl propionate (MeP).[55] The second step first vaporises MeP with formaldehyde and then converts them to MMA over a heterogeneously supported caesium oxide catalyst with a 95% selectivity.[52] The product stream is then passed through several columns before the MMA is sufficiently separated.



Scheme 1.6 The production of MMA by the Alpha Process, from ethylene, ethanol and carbon monoxide.

The Alpha process demonstrates several improvements in line with the 12 Principles of Green Chemistry compared to previous processes, such as the

sourcing of reactants from syngas and biomass, the low hazard rating of the chemicals, the moderate heat and pressure required for the first stage of the reaction, an increase in selectivity to MMA from 70% in the i-C 4 process to 85%[52] and the benign nature of the by-product, water. These factors contribute to an overall reduction in operating cost of around 40%.[56]

During the second stage of the Alpha Process, the catalyst is reversibly poisoned. In order to run the process continuously, the Alpha Process uses two parallel reactor vessels. By switching between reactors, the catalyst can be heated and activity restored by controlled regeneration.[28] Alternating regularly between the two reactors means the high catalytic activity can be maintained.

Lucite International unveiled a 120 kte yr^{-1} plant using Alpha technology in Singapore in 2008 and a second 250 kte yr^{-1} plant is due to open in Saudi Arabia in 2017.[57, 58] However, Lucite International are among many interested in a more environmentally sustainable route to MMA production, steering away from a reliance on petrochemicals and syngas, and looking towards biomass products of fermentation.

Renewable Processes for Methacrylic Acid

Hydrothermal Processing

This thesis involves the use of hydrothermal processing for the manufacture of both acrylic and methacrylic acids. A hydrothermal process has been defined as a "chemical reaction in the presence of an aqueous solvent above the room temperature and at pressure greater than 1 atm in a closed system".[59] "Hydrothermal" comes from the Greek "hydros" meaning water and "thermos" meaning heat and was first used by Sir Roderick Murchison in the 1840s to describe the action of water at elevated temperatures and pressures to form rocks and minerals in the Earth's crust.[60]

Hydrothermal processing was used throughout the 19th and 20th centuries and continues to be used in many different disciplines into the 21st century. Many different fields utilise the technology today, including the production of advanced materials, geotechnology and biotechnology.[61]

A near-critical or subcritical fluid is a substance held below its critical temperature (T_c) and critical pressure (p_c). At a substances critical temperature and critical pressure - the critical point – the boundary between gaseous and liquid phases no longer exists. Beyond this point, the substance is said to be in its supercritical phase. A supercritical fluid has properties between those of a liquid and a gas and can be carefully fine-tuned by altering the temperature and pressure of the system. The critical point for water is T_c = 647 K, p_c = 22.1 MPa, ρ_c = 322 kg m^{-3}.[62] Figure 1.6 shows the effect of temperature on the density, dielectric constant and ionic product of water, key factors that help determine its properties as a solvent.

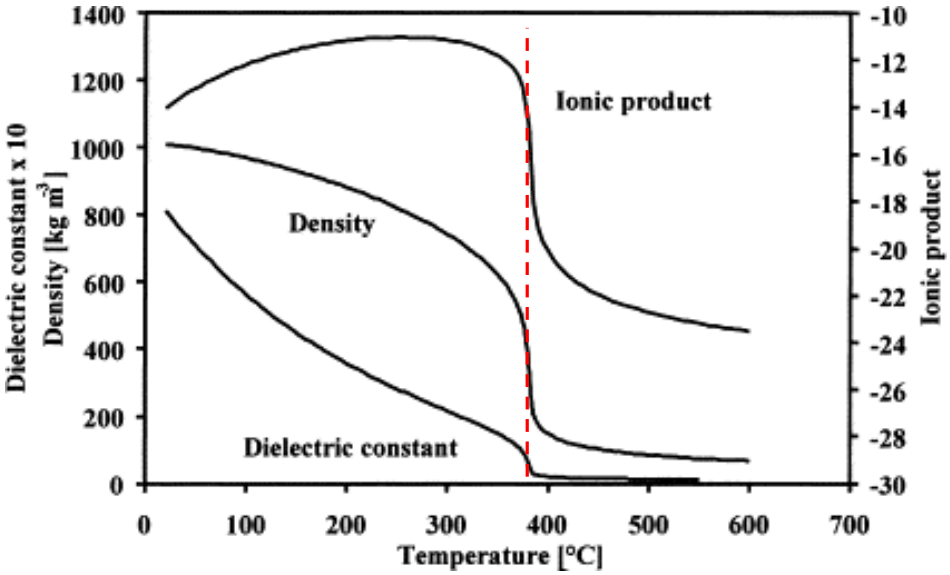


Figure 1.6 The changing properties of water with temperature at a fixed pressure of 23.7 psi. The critical temperature (647 K) is shown by the red dashed line.[63]

A steady decrease in density occurrs with increasing temperature, as can be seen in Figure 1.6, before falling off rapidly around the critical temperature. The same can be seen for the dielectric constant, falling rapidly with increasing temperature and then falling off to near zero at the critical point.[62] Unlike the density and dielectric constant, the ionic product shows an increase with temperature[62] up to the near-critical region and then falls dramatically above the critical point. However, this drop in ionic product at the critical point can be linked to the drop in density. As will be demonstrated later in this thesis, these properties lend themselves well to the production of MAA, offering a good environment for both dehydration and decarboxylation reactions.

Batch and Continuous Flow Processing

Hydrothermal synthesis is well suited to both batch and continuous flow systems, which can be designed to suit the requirements of the process. For example, short reactions in batch reactors are limited by the time

taken for the reactor to reach temperature and pressure, known as the equilibration period. This period is dictated by the volume of the reactor, with larger reactors taking much longer to reach equilibration. There is no upper limit to the reaction time of a batch reactor and many common batch reactions run for hours or days at a time.

Unlike the long reactions often found with batch reactors, continuous flow processing lends itself well to much shorter residence times of seconds up to a few hours. The use of heated capillary tubes means almost instant heat transfer and so very short residence times can be achieved. Reaching longer reaction times requires a lower flow rate or a larger reactor volume, which is often limited by the size of the available equipment and safety issues.

Lowering flow rates in continuous flow reduces the Reynold's number (Re) of the fluid. The Re can be used to predict the flow regime, whether it will be laminar or turbulent. Turbulent flow is preferable as it ensures that the fluids achieve good mixing, while a laminar flow will mean that the fluid may not be heated or mixed evenly. This problem is overcome by using small reactors with high flow rates. In batch systems, a stirrer can be integrated into the design and ensures even mixing throughout the duration of the experiment.

$$Re = \frac{\underset{/\ kg.m^{-3}}{density\ of\ fluid} \times \underset{/\ m.s^{-1}}{velocity\ of\ fluid} \times \underset{/\ m}{pipe\ diameter}}{dynamic\ viscosity/\ kg.m^{-1}.s^{-1}}$$

Equation 1.4 Reynold's numbers (Re) are calculated to predict the flow patterns of a fluid in a pipe using the equation above. The flow can be considered as turbulent when the Reynolds Number exceeds 4000. The dynamic viscosity measures the internal resistance of a fluid.[64]

Continuous flow reactors offer greater control over the reaction conditions as there is typically a lower volume of the reaction medium undergoing a

reaction at any given time. This reduces the risk of the process by reducing the heated volume and also the energetic and economic costs of achieving the desired conditions.

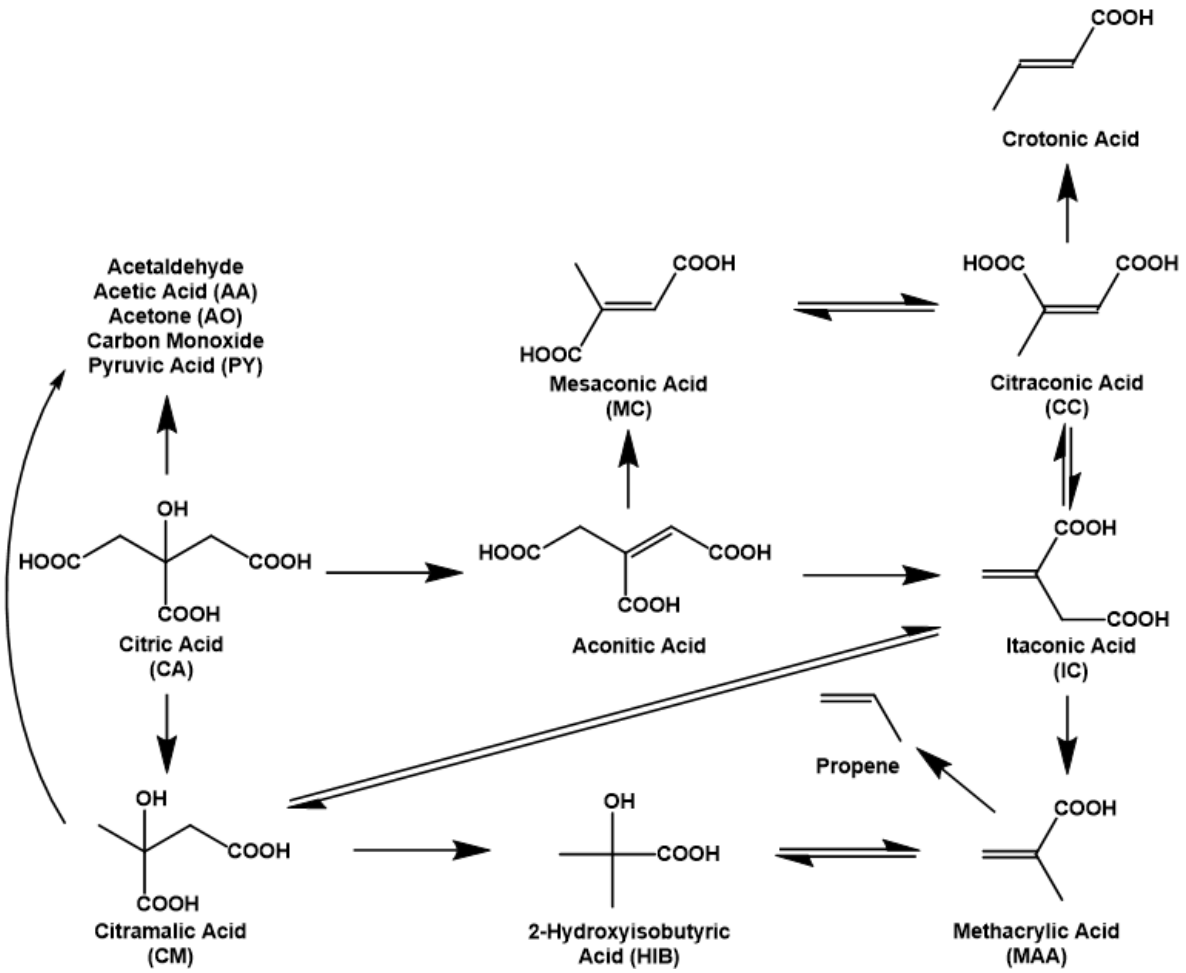
The production rates also differ greatly between batch and flow reactors. In batch, the rate is limited by the volume and the reaction times, which are usually in the order of hours or days. However, in flow reactions, the process can be kept running until the required amount of product has been collected and then the equipment can be shut down to reduce running costs.

Hydrothermal Production of MAA

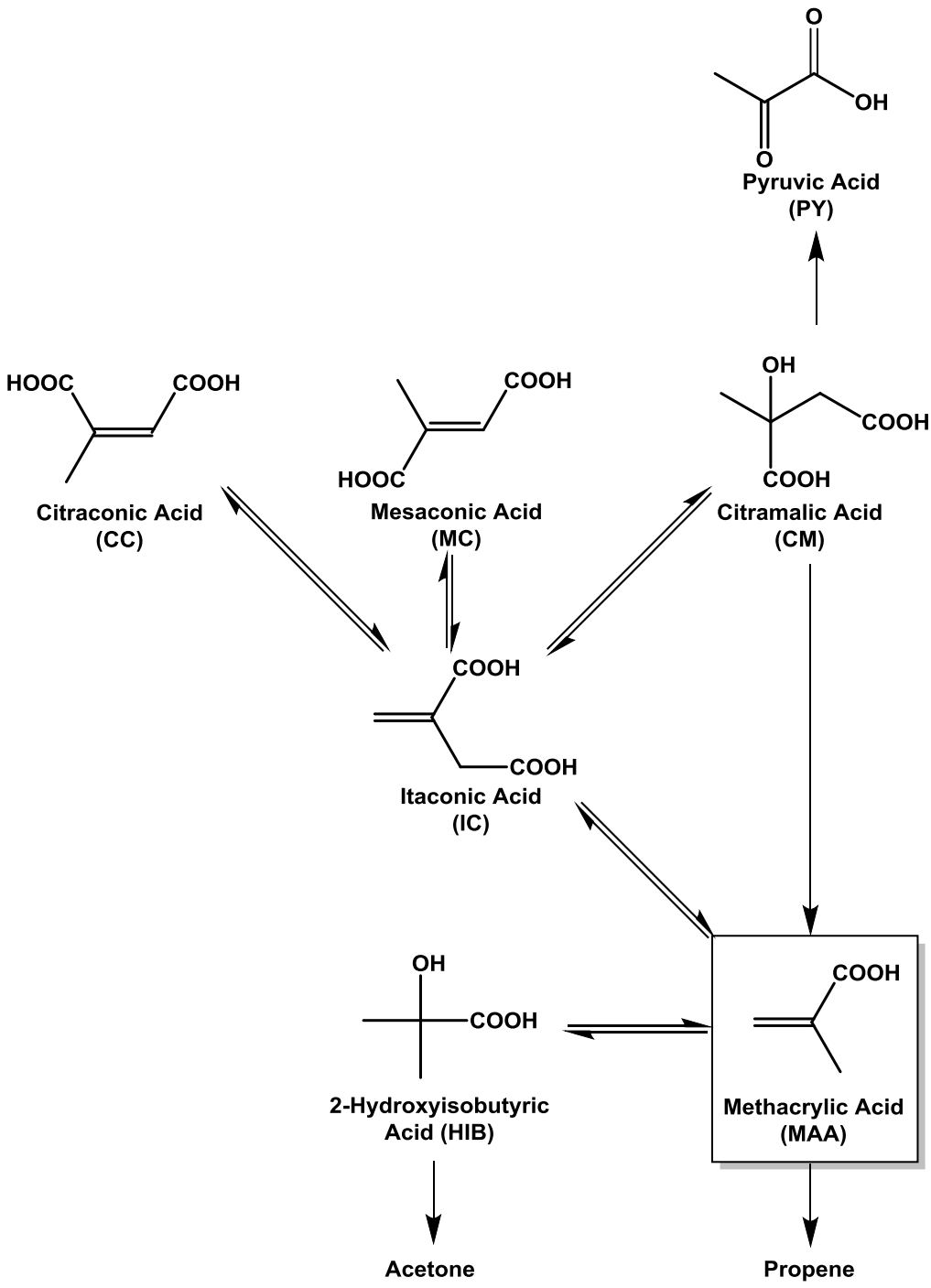
While direct biological routes to methacrylates remains impossible, research into a biological-synthetic route, combining both biological and more traditional synthesis seems promising. Fermentation of molasses using *Aspergillus niger* and *Aspergillus terreus* yields citric acid (CA) and itaconic acid (IC) respectively.[65, 66] Researchers have reported pathways from both CA and IC to MAA by various dehydration and decarboxylation steps as a potential route to bio-MAA.[67-76]

Carlsson *et al*. were the first to report this process and conducted their research in continuous flow reactors.[67] Investigating residence times of 1 - 10 s and 20 – 100 s, and temperatures of 220 – 400 °C at a constant pressure of 5000 psi, they found that at lower temperatures, CA was selectively decarboxylated at a slow rate. However, above 250 °C, unwanted byproducts were generated by parasitic reactions, lowering the selectivity of the reactions.

It was also reported that an MAA yield of up to 70 % could be achieved using IC as a precursor at 360 °C and 34.5 MPa with a short residence time



Scheme 1.7 A reaction scheme suggested by Carlsson *et al.* to show the various pathways to MAA from acidic precursors.[66]



Scheme 1.8 A revised scheme based on Huddle's work[72, 75, 76] drawn to emphasise the central role IC plays in the conversion of several di-carboxylic acids to MAA.

of 10 s with the addition of base. Carlsson *et* al. stated that a decreased pH, with the addition of H_2SO_4, favoured parasitic reactions, whereas the addition of a base, NaOH, increased the overall reaction rate without affecting the selectivity. Following this, they investigated the use of different bases and found that it was the pH, not the nature of the cation, which was a controlling factor. Through their various investigations, they developed the reaction scheme shown in Scheme 1.7.

The effect of pH was also reported by Li and Brill,[69] who were able to calculate rate constants of the decarboxylation of IC at different temperatures and found that pH_{25} = 3.75 gave the highest rate constants. This pH was achieved by adding NaOH to the starting solution which, in the absence of base had a pH of 2.31. Further research has shown that lower temperatures give a higher selectivity to MAA, and optimum conditions require equimolar amounts of IC and NaOH.[72]

Research carried out by Huddle[72, 75, 76] has led to the proposal of a modified scheme, Scheme 1.8, after several of the steps seen in Scheme 1.7 were shown to be improbable. For example, the route to MAA from CM is now shown as a single step reaction in Scheme 1.8, as opposed to the two step reaction *via* hydroxyisobutyric acid (HIB) that Carlsson *et al*. previously proposed. Another change to the scheme is the equilibria between IC, citraconic acid (CC) and mesaconic acid (MC), which are now shown to occur *via* IC. One can also see that a few of the original acids in Scheme 1.7 have been omitted. This is because their presence in the scheme has not yet been proved.

More recently, Le Nôtre *et al*. have investigated the effect of transition metal catalysts on the hydrothermal conversion of IC to MAA.[74] Unlike the prior art described above, Le Nôtre *et al*. studied the reactions in batch reactors. At a maximum, 80 % conversion of IC and up to 84 % selectivity

towards MAA was achieved with a Pt/Al_2O_3 catalyst. While this is a very promising result, the work by Huddle achieved moderate conversions and high selectivity without the use of an expensive transition metal catalyst. The work discussed later in this thesis builds on the results described by Huddle[72] and works towards an industrially viable route to MAA with a simple base catalyst.

Acrylic Acid

Properties and Uses

Acrylic acid is the simplest unsaturated carboxylic acid. It is a clear liquid at room temperature and releases an acrid smell. Glacial acrylic acid is sold as an intermediate for fine chemical reactions, but the crude acid is more commonly used for polymer production.

Akin to MAA, acrylic acid rapidly polymerises to poly(acrylic acid) and can be further neutralised to its sodium salt or functionalised to produce a range of poly(acrylates). Acrylic acid, its esters and their polymers are also used in acrylic paints, water-soluble coatings, resins, textile fibres and adhesives.[77-80]

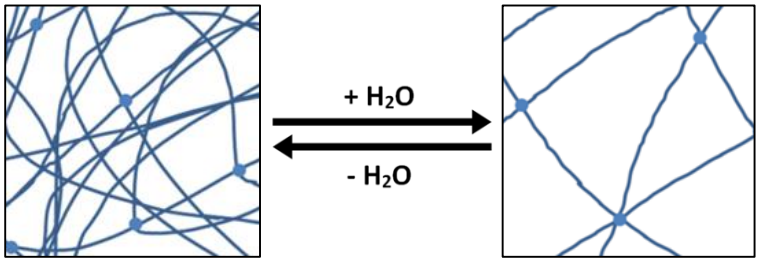


Figure 1.7 Showing the swelling of crosslinked polymeric chains in a superabsorbent polymer. The crosslinks (●) hold the polymeric chains (—) together and prevent infinite swelling as water is absorbed. Superabsorbent polymers form hydrogen bonds with water molecules to hold them tightly between chains.

Acrylic acid forms superabsorbent polymers (Figure 1.7), which when cross-linked are known as hydrogels. These superabsorbent polymers and hydrogels readily absorb water through hydrogen bonding. In fact, they can absorb up to 1000 times their own weight of deionised water,[81] although this is greatly reduced in the presence of ionic impurities. Their high absorbance lend themselves to use in disposable nappies,[82] fake snow[83] and FrogTape® (seen in Figure 1.8).[84]

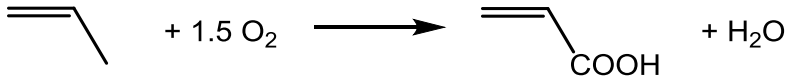


Figure 1.8 PaintBlock™ is a trademarked technology used in FrogTape® containing superabsorbent polymers, such as poly(acrylic acid). The tape includes strips of PaintBlock™ to prevent paint bleed and reveal clean lines when removed. The images above display the addition of water on PaintBlock™ to demonstrate this effect.[85]

Production of Acrylic Acid

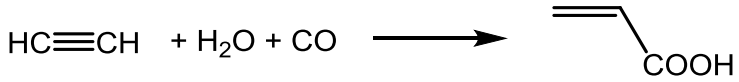
The market for acrylic acid and its derivatives was valued at $11.0 billion in 2013 and, due to rapid expansion, is predicted to be worth an estimated $18.8 billion by 2020.[86]

The main production route to acrylic acid involves the direct oxidation of propene, seen in Scheme 1.9. Not only does this process use a petrochemical based starting material, it is also energy intensive, using very high temperatures and pressures. The process usually occurs in two stages, each requiring an expensive mixed metal catalyst[87-90] *via* an acrolein intermediate.



Scheme 1.9 The oxidation of propene yields acrylic acid and water in stoichiometric quantities.

Another common route to the acid was developed by Walter Reppe.[91] Reppe showed the reaction between carbon monoxide, water and acetylene would yield acrylic acid without by-products (seen in Scheme 1.10).

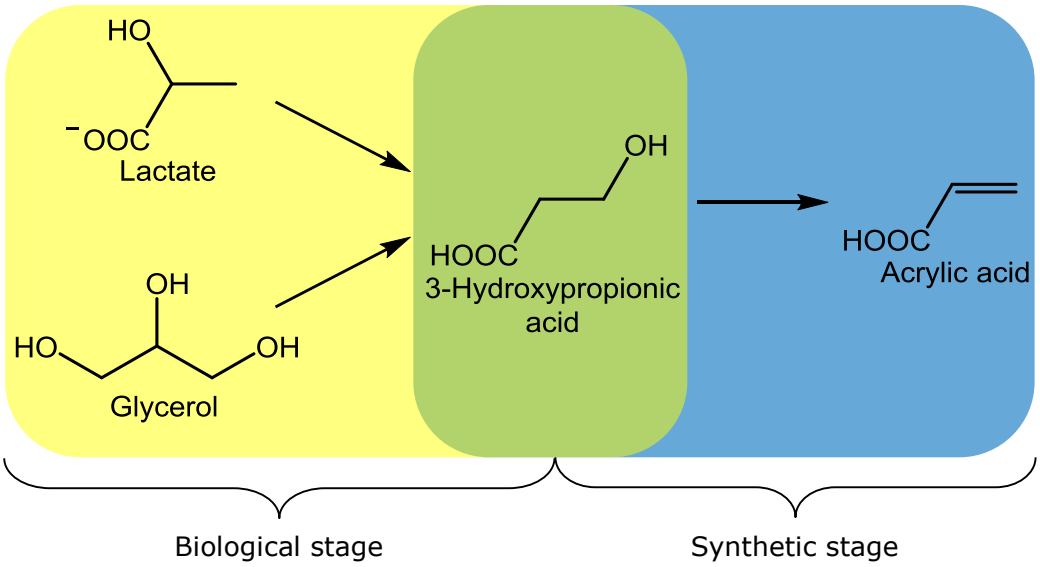


Scheme 1.10 The Reppe chemistry shown above can be used to produce acrylic acid with a perfect atom economy.

The Reppe method of acrylic acid production boasts perfect atom economy, while the oxidation of propene displays 80 % economy to acrylic acid. However, both methods require extreme conditions of high temperatures and pressures as well as using petrochemical feedstocks. More recent methods of acrylic acid production have focused on renewable and sustainable routes.

Renewable Processes to Acrylic Acid

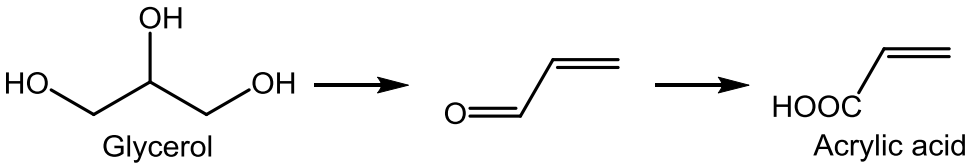
While there are currently no direct biological routes to acrylic acid, there are possible semi-synthetic routes. For example, 3-hydroxypropionic acid can be formed through several biological routes[92, 93] and can then be dehydrated with a phosphate or sulfate catalyst[94] to yield acrylic acid.[95] Purification of the crude acrylic acid has been shown to yield up to 99 wt % glacial acrylic acid[96] and has been successfully polymerised.[97]



Scheme 1.11 Acrylic acid can be made in a two-stage bio-synthetic process. Both Lactate ions and glycerol can be converted to 3-hydroxypropionic acid *via* biological steps before a simple dehydration reaction yields acrylic acid.

Companies such as Cargill and Novozymes are investing in such bio-synthetic routes. Cargill and Novozymes have chosen a preferred process and are currently testing the process in a pilot plant[95] despite BASF deeming the process as non-viable and leaving the partnership.[95, 98]

Glycerol is a by-product of biodiesel production.[99-101] As the production of biodiesel has increased, so too has the availability of glycerol and this has caused a glut for industry.[99] Hence, processes that use glycerol to make bulk chemicals are necessary and the production of acrylic acid is a great opportunity for industry to use this surplus.



Scheme 1.12 Glycerol can be collected as a by-product of biodiesel production and can be dehydrated and oxidised to produce acrylic acid.

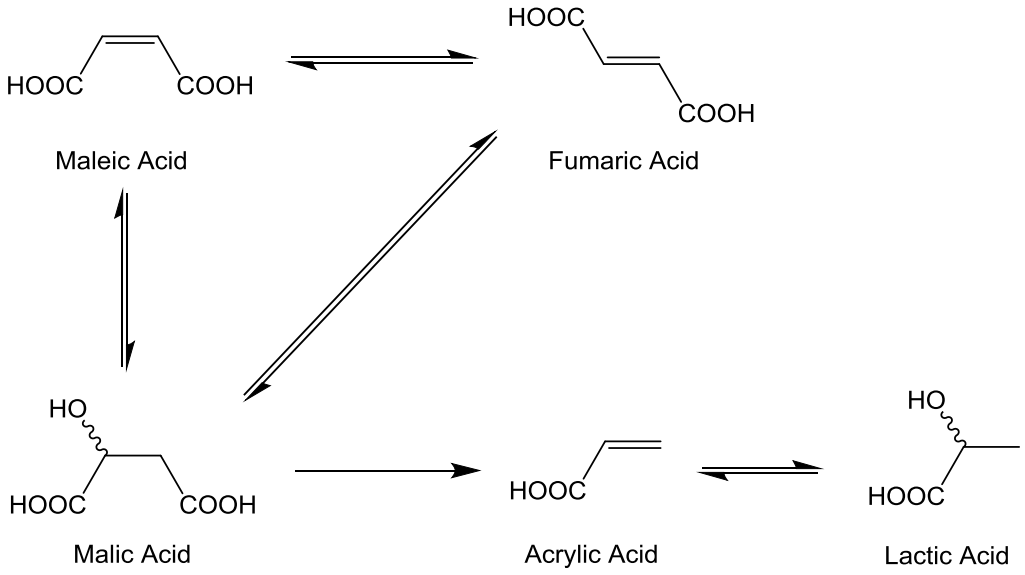
Non-biological routes include the conversion of glycerol to acrylic acid. A two-step dehydration and oxidation, seen in Scheme 1.12, can yield acrylic

acid;[102] although research has shown that a single step oxydehydration of glycerol is possible, the process is currently low yielding (28.4 %).[103]

Hydrothermal Production of Acrylic Acid

During his research into the production of MAA from CM, Huddle hypothesised that an analogous system, including malic acid and acrylic acid might be possible.[72, 75, 76]

Malic acid is used in the food industry and is predominantly made from maleic anhydride.[104] However, it is possible to make malic acid by fermentation with *Schizophyllum commune*[105] or modified *Escherichia coli*[106] making it suitable as an intermediate in a possible bio-synthetic route.



Scheme 1.13 This reaction scheme shows the production of acrylic acid from malic acid. The scheme shows expected by-products of the reaction, including lactic acid formed by the hydration of acrylic acid.

Scheme 1.13 shows the production of acrylic acid from malic acid, with expected by-products, including lactic acid formed by the hydration of acrylic acid. The acids seen in the scheme are analogous to some of those

seen for MAA in Scheme 1.8 and are produced through different combinations of decarboxylation, dehydration and hydration reactions.

Huddle began research into the reactions seen in Scheme 1.13,[72] but due to time constraints, he was unable to carry out more than a brief investigation. An aim of this thesis is to conduct a more detailed investigation using our understanding of MAA production, as shown in Scheme 1.8, to direct research into the hydrothermal production of acrylic acid.

Aims and Objectives

This CASE project is the second PhD at the University of Nottingham supported by Lucite International into the hydrothermal synthesis of MAA. The work of Huddle[72] made significant advances on the results of Carlsson *et al.* Perhaps most importantly, Huddle showed that Carlsson *et al*. had not fully disclosed results to support their scheme.[67] By investigating the conversion of IC to mesaconic acid (MC), Huddle found that equilibriation is not *via* citraconic acid (CC), but instead IC is in equilibrium with each of paraconic acid (PC), CC and MC. Primary research by Huddle had shown that the pathway from CM to MAA is probably direct; however, further research is needed to confirm this. Therefore, the main aim of my PhD project involves gathering data to underpin the larger scale development of high temperature and high pressure water reactions to make MAA and to follow on from the work of Huddle.

More specifically, the main aims of the project are:

1. Improvements are needed into the analysis of the complex mixture of acids produced. For example, data for HIB could not be obtained with the UV detection set up in Huddle's HPLC system. By utilising a refractive index detector (RID), a more detailed and reliable set of results for each experiment can be obtained.
2. Huddle's research will be used as a basis for a similar investigation into the production of acrylic acid. This is another monomer of interest to Lucite International and could lead to a second, independent chemical process.
3. Limited previous work has been carried out on the hydrothermal decomposition of MAA; thus the investigation into the stability of MAA at the conditions likely to be used in the process is imperative to the research. By determining the stability at a range of temperatures,

residence times and concentrations of both acid precursor and base, I should be able to suggest a viable working range for the process.

4. Preliminary studies by Huddle showed the possibility of recycling the sodium hydroxide and unreacted starting materials back through the rig after decarboxylation. In order to demonstrate this quantitatively, more data and more cycles are needed to show reproducibility. Recycling experiments will be run for a range of precursors to show the versatility of the process.
5. Finally, using a fermentation broth, it will be demonstrated that we have found a new bio-route to PMMA from biomass precursors. The process will be run from the fermentation step, through to the polymerisation of the esterified MAA to yield a pure sample of bio-PMMA.

Chapter 2 - Experimental Methods

At the heart of the project was a continuous flow rig that was based on the design used by Huddle.[72] This rig was inherited at the start of this project but was completely rebuilt and modified to reduce errors and better suit the aims of this thesis. The modifications included the removal of a quench pump, several different reactors and the removal of a post-processing dilution step.

Equipment

Reactors

A reactor is a container in which substances are made to undergo chemical reactions. In the case of high temperature water continuous flow reactions, this typically refers to that section of tubing which is heated to a temperature above that required for a reaction to occur. The efficiency of the heat transfer is dependent on the flow rate of the medium passing through the reactor and so it is difficult to measure the exact point along the tube where a reaction begins to take place. Once the tubing has extended out of the heated section, it is also difficult to quantify the cooling rate and hence quenching of the reaction. Early experiments in this project used a quench flow of water to speed up this cooling; however, this was removed for all experiments reported in this thesis in order to reduce experimental error, described later in this chapter.

During this research, reactors comprised of various lengths of 1/8” stainless steel 316 (SS316) tube or 1/8” hastelloy C276 tube coiled around an aluminium block with threaded grooves cut in to ensure better contact between the block and the tube. Into the centre of the aluminium block, a

400 W Watlow cartridge was placed to heat the coiled reactor. A second heating element was placed around the outside of the coiled tube. The element consisted of a 1000 W band heater with a layer of brass between the element and reactor coil to ensure even heat distribution. Four reactors were used during the research, two with volumes 2.4 ml and 7.7 ml made from SS316 and two more 8.6 ml and 10.0 ml coils made from Hastelloy C276 in order to achieve desired residence times (See Equation 2.2).

Corrosion

In 1993 Latanision and Shaw suggested that it would be "extremely unlikely" to find a "universal material that will perform in the preheater, reactor and cooldown sections of a supercritical water oxidation system".[107] Due to the harsh nature of the high temperatures and pressures used in the reactions detailed in this thesis, corrosion of the heated reactors became increasingly important.

The reactions shown in Chapter 4 made use of the two SS316 reactors described above. However, the harsh conditions seen in this research caused significant colouration of exit solutions in the reactions shown in Chapters 3 and 5.

In an attempt to reduce the level of corrosion in Chapters 3 and 5, a Hastelloy C276 reactor was used. However, during this research, it was noted that after continuous use of the 10.0 ml Hastelloy C276 reactor the exit solutions also gained colouration. After ICP analysis of a batch of product solution, seen in Table 2.1 it was found that the main components of the reactor walls had leached into the product solution.

Table 2.1 Concentrations of metal ions in an aqueous exit solution from the rig can be seen. The metals listed are the main components of Hastelloy C276, suggesting a leaching effect is taking place during reactions to cause the colouration of exit solutions.

Metal	Concentration / µg/L (normalised values)	Weight % Composition in Hastelloy C276[108]
Cr	2107.0 (41.7)	14.5 - 16.5
Fe	1232.5 (24.4)	4.0 – 7.0
Mn	50.5 (1.0)	1.0
Mo	660.5 (13.1)	15.0 – 17.0
Ni	8993.0 (178.1)	Balance
W	769.4 (15.2)	3.0 – 4.5

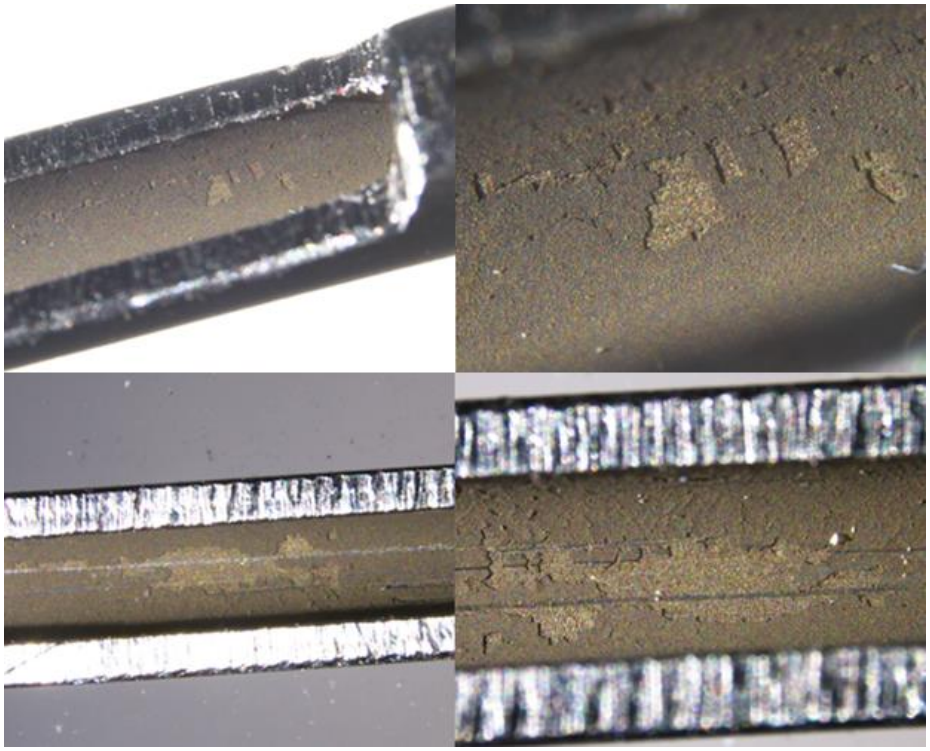


Figure 2.1 Magnified images of a section of reactor pipe (Hastelloy C276) to show the effects of surface corrosion on the inner wall of the tube. The surface appears brittle and shows clear signs of corrosion. Long, linear scratches seen in c) and d) were caused by the milling machine used to cut the section of tubing open.

Figure 2.1 shows a section of the 1/8" Hastelloy C276 reactor that has been cut open. Areas of general corrosion can be seen on the inner surface

of the tube. It would appear that the corrosion is surface corrosion due to the instability of a protecting oxide layer.

The Rig

The rig primarily consisted of stainless steel (SS316) Swagelok pipes and fittings designed for use under the harsh conditions of both high temperatures and pressures as well as a reactor, selected as previously described.

The acid precursor solution was introduced to the rig through a Gilson HPLC pump (model 305) fitted with a 10SC pump head and was flowed through lengths of 1/16" pipe to a Gilson 805 Manometric dampener module which relayed the system pressure to the Unipoint software, a needle down valve, pressure transducer, pressure relief valve (set to 5200 psi) and eventually passed into the reactor. The reactor was as described above, and included two thermocouples, T1 and T2; one of which fed to the Gefran 800P heat controller (T1) and another fed into a temperature monitor and the trip system (T2).

Immediately after leaving the reactor, T3 measured the outlet temperature, which was monitored and recorded using PicoLog™. The precursor flow could here be met with an optional quench flow (Figure 2.2), introduced via a second Gilson HPLC pump (model 305) fitted with a 5SC pump head, at a 90° angle to the reactor outlet in a T-piece. When the quench pump was not in use (Figure 2.3), this T-piece was replaced by an elbow joint. The flow was then passed through a heat exchanger and Tescom manual back-pressure regulator (BPR) at which point pressure was relieved and samples were released for analysis through a Gilson FC 203B fraction collector, seen in Figure 2.4.

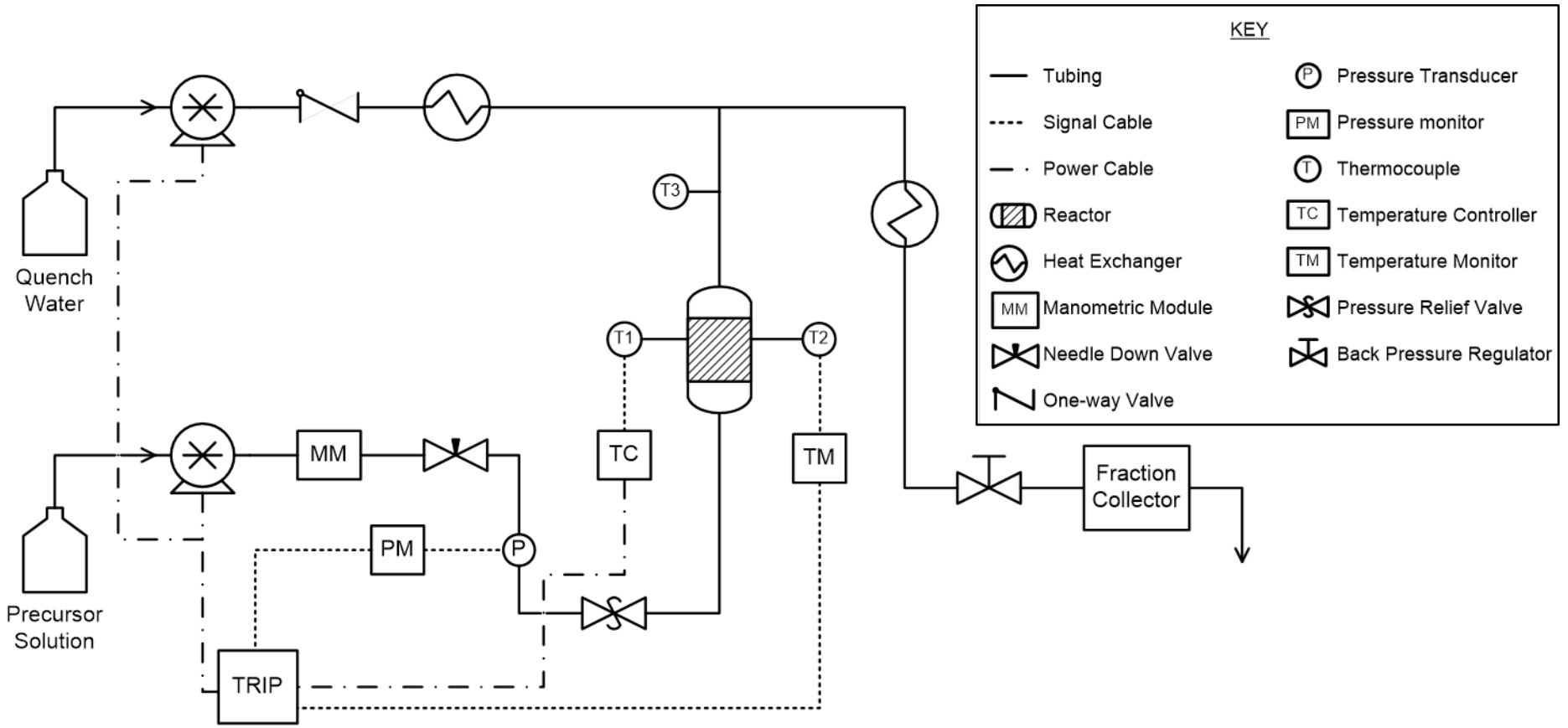


Figure 2.2 A rig diagram showing the inclusion of a quench pump. This configuration was used to calculate errors detailed in this chapter but was modified before experimental use.

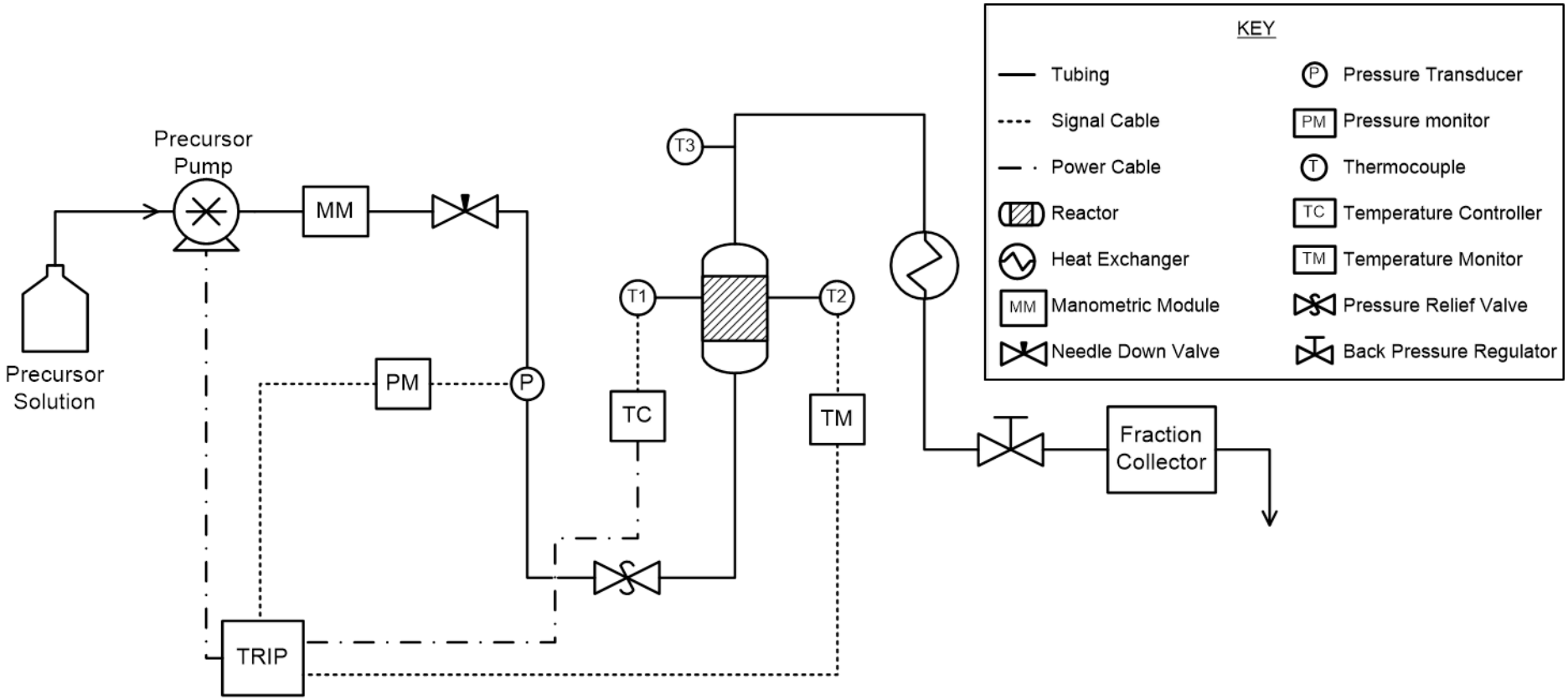


Figure 2.3 This rig diagram shows the configuration used in subsequent chapters. The precursor solution is introduced via a Gilson HPLC pump and passes through to a coiled reactor before being cooled and exiting the rig through a Tescom manual BPR and Gilson FC 203B fraction collector.



Figure 2.4 Diagram showing the Gilson FC 203B fraction collector used during this research.

The pressure in the rig was introduced by pumping and heating of the starting samples and was maintained by the BPR, which could be manually adjusted to set the required system pressure. The pressure was monitored via a pressure sensor with a digital output. A trip system was designed to cut power to the rig if the temperature at T2 exceeded 460 °C or the pressure measured by the pressure transducer exceeded 5000 psi.

The Fraction Collector

Once the sample flow reached the Gilson FC 230B fraction collector, it was directed either to bulk waste, or through the needle for sample collection. A Unipoint program was written to direct the flow to bulk waste during a predetermined equilibration period, which was calculated as a function of flow rate and reactor volume, seen in Equation 2.1. After equilibrium was reached, the position of the needle would be set and the injection valve would rotate to the needle position for sample collection.

$$Equilibration\ Period\ /\ min = \frac{Rig\ Volume\ /\ ml}{Flow\ Rate\ /\ ml.min^{-1}}$$

Equation 2.1 A calculation for the equilibration time of liquids inside the rig. The Rig Volume refers to the total internal volume of the entire rig.

The needle was positioned over a tray which was filled with collection vials. A plan of the tray can be seen in Figure 2.5. The initial position of the needle would be over vial 1 in Row B to collect a sacrificial sample. This would be collected in order to ensure the dead volume between the injector valve and the needle outlet was not contaminated by a previous sample. Once the sacrificial sample was collected, the needle would move to the corresponding vial in Row A to collect the sample to be analysed.

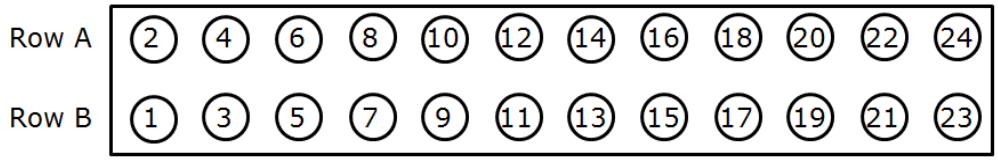


Figure 2.5 Diagram showing the numbered positions of the fraction collector tray.

During experiments that required larger volumes to be collected, larger vials were used instead of the tray and were replaced manually after collection.

HPLC Analysis

Previous work by Huddle[72, 75, 76] separated samples with a Phenomenex Rezex RHM monosaccharide H^+ (8 %) column, which was protected by a guard column. The compounds were then analysed and detected by an Agilent 1200 UV Multi-Wavelength Diode (MWD) detector, using a 210 nm wavelength.

During Huddle's work, citramalic acid was withdrawn from suppliers and so could not be used during HPLC calibration experiments. All other acids were calibrated once a month using five solutions of known concentrations of each acid. The peak areas were then plotted against concentration and the gradient was taken as the response factor of each acid. This was then used to calculate concentrations of these acids in reaction exit solutions from their peak areas.

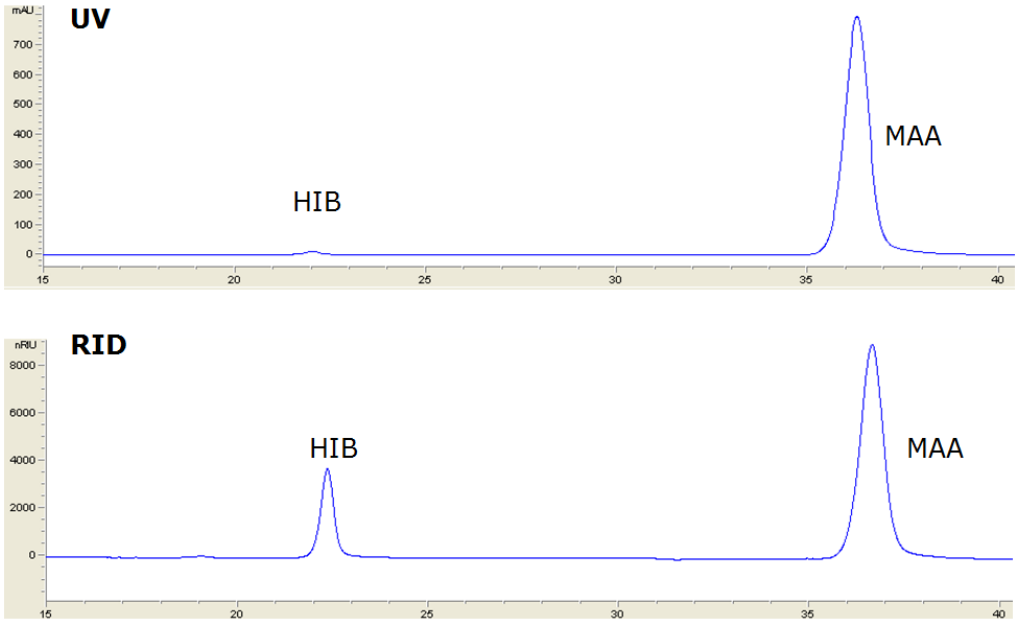


Figure 2.6 HPLC chromatograms of an MAA (0.025) and HIB (0.005) solution using simultaneously the UV detector and RID. A slight difference in elution time can be seen between the detection methods. This is due to the UV detector being upstream of the RID.

Highly conjugated or unsaturated systems, like MAA, are ideal for UV detection, but for fully saturated molecules, such as HIB, another detection method was required. Huddle calculated HIB concentrations by relative intensities of peaks in ^{1}H NMR spectra. However, a newly acquired refractive index detector (RID) allowed for more accurate analysis of compounds that could not be detected using UV, for example HIB. Figure

2.6 demonstrates the improved capability of HIB detection using RID rather than UV as the detection method.

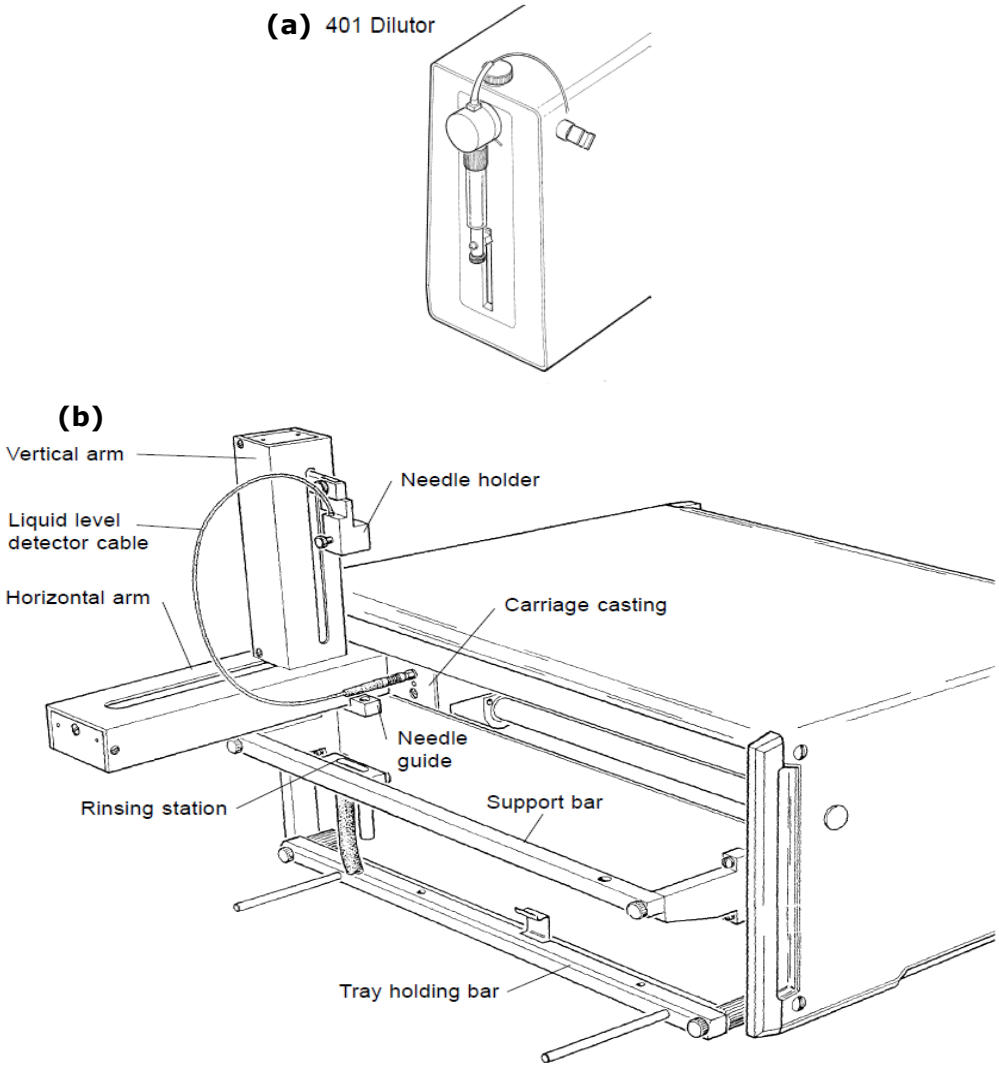


Figure 2.7 Sketch showing (a) the Gilson 401 Dilutor and (b) the Gilson 221 XL Liquid Handler and its components.[109]

The UV detector was easily overloaded by concentrated samples and so Huddle's exit samples from the rig required a dilution step before analysis. They were diluted by 1 in 100 using a Gilson 221 XL Liquid Handler and a Gilson 401 Dilutor, seen in Figure 2.7. The liquid handler was similar in set up to the Gilson FC 203B fraction collector used for sample collection in the rig; however, while the Gilson FC 203B fraction collector only dispensed samples, the Liquid Handler would draw small volumes of the sample, from

a vial, into the Dilutor and would dispense the sample (with a suitable volume of deionised water) into a second vial. This would then be repeated into a third vial to give the required 1 in 100 dilution. The liquid handler was then also used to dispense samples which would be diluted later by 1 in 5 with deuterium oxide for NMR analysis.

However, at the start of this project a new column and detection method were implemented. The RID was able to analyse much higher concentrations of organic acid than the previously used MWD detector and so no dilution steps were needed post-production. All samples, reported in this thesis, were analysed using an Agilent 1200 series with a Phenomenex Rezex ROA organic acid H^+ (8 %) column, protected by a guard column, and an Agilent 1260 infinity series RID without dilution. Using a similar method reported by Carlsson,[67] the method described in Table 2.2, was developed to give the optimum conditions for separation of the acids reported in Scheme 1.8 according to their pK_a values seen in Table 2.3. Each sample was analysed three times and average values have been quoted in this thesis.

Table 2.2 The method used to analyse all samples reported in this thesis is detailed here.

Standard HPLC Method Used	
Flow Rate	0.6 ml min^{-1}
Sample Injection Volume	10 µL
Mobile Phase	0.005 N H_2SO_4
Stationary Phase	Phenomenex Rezex ROA organic acid H^+ (8 %) column
Column Temperature	75 °C
Pressure	50 bar (±5 bar)
Total Method Time	45 mins
Detection Method	Refractive Index detection

Table 2.3 The pK_a values at 25 °C for the acids seen in Scheme 1.4.[110-112]

Acid	pK_a		
	pK_{a1}	pK_{a2}	pK_{a3}
Acetic Acid	4.75		
cis-Aconitic Acid	2.78	4.41	6.21
Trans-Aconitic Acid	2.91	4.33	6.16
Citraconic Acid	2.45	6.08	
Citramalic Acid	3.5	5.3	
Citric Acid	3.13	4.76	6.40
Crotonic Acid	4.69		
2-Hydroxyisobutyric Acid	3.98		
Itaconic Acid	3.90	5.56	
Mesaconic Acid	3.04	4.85	
Methacrylic Acid	4.68		
Pyruvic Acid	2.50		

NMR Spectroscopy, Mass Spectrometry and ICP-MS analysis

NMR spectroscopy was carried out at ambient temperatures using either a Bruker DPX300 spectrometer or a Bruker AV(III)400 spectrometer. The samples were diluted using deuterium oxide which was referenced according to literature.

Mass spectrometry data was obtained using a Bruker MicroTOF spectrometer which used electrospray ionisation.

Inductively coupled plasma - mass spectrometry (ICP-MS) was carried out on samples in 2 % nitric acid in ultra-pure water (18.2 MΩ.cm at 25°C, 2-5 ppb TOC, produced by a Millipore™ Milli-Q Advantage Ultrapure Water

System) using an iCAP™ Q ICP-MS.[113] The sample is converted into its corresponding ions by the ICP source and ions are separated by a Dionex ICS3000 HPLC system. The sample then passes through a 90° lens to remove neutral and negatively charged species from the sample and enters a quadrupole mass spectrometer for detection.

Materials

All chemicals were used as supplied and tested for purity with ^{1}H NMR. The reagents used for this thesis did not require any further purification. Deionised water (13-15 MΩ.cm at 25°C) was used for all experiments and was produced by an ELGA™ Purelab reservoir in the laboratory. Deuterium oxide (99.9 atom % D) and deuterated chloroform (99.9 atom % D) were used as NMR spectroscopy solvents and were obtained from Aldrich.

Precursors

Acidic precursors were sourced from various suppliers shown in Table 2.4 and the highest possible purity was selected in each case. Each precursor was made up with sodium hydroxide provided by Fisher Scientific (98 %).

Table 2.4 Purities and suppliers are listed for each acidic precursor used in calibrations and experiments.

Acid Precursor	Purity	Supplier
Acetic Acid	≥ 99 %	VWR Chemicals
Acetone	≥ 99 %	Fisher Scientific
Acrylic Acid	99 %	Alfa Aesar
Citraconic Acid	98 %	Aldrich Chemistry
Crotonic Acid	≥ 99 %	Merck Schuchardt OHG
Fumaric Acid	≥ 99 %	Aldrich Chemistry
2-Hydroxyisobutyric Acid	99 %	Alfa Aesar
Itaconic Acid	≥ 99 %	Aldrich Chemistry
Maleic Acid	99 %	Acros Organics
DL-Malic Acid	≥ 99 %	Aldrich Chemistry
Mesaconic Acid	99 %	Aldrich Chemistry
Methacrylic Acid	99 %	Aldrich Chemistry
Pyruvic Acid	98 %	Alfa Aesar
Sodium DL-Lactate	60 % (w/w)	Aldrich Chemistry

Organic Solvents

Several organic solvents were used during liquid-liquid extractions in this thesis. The purities and suppliers are listed in Table 2.5.

Table 2.5 Purities and suppliers are listed for each organic solvent used during the experiments in this thesis.

Organic Solvent	Purity	Supplier
Cyclohexane	99 %	Fisher Scientific
Dichloromethane	98 %	Aldrich Chemistry
1-Octanol	99 %	Acros Organics
Pentane	98 %	Aldrich Chemistry
Toluene	≥ 99 %	Fisher Scientific

HPLC

Ultra-pure water was used in the mobile phase of HPLC. The mobile phase was made up with concentrated sulfuric acid (95 - 98 %) from Fisher Scientific and Sigma Aldrich to a concentration of 0.005 N. Ultra-pure water was used to clean the Phenomenex Rezex ROA organic acid H^+ (8 %) column between uses and a 0.025 M solution of sulfuric acid as supplied above was used during regeneration of the column which took place quarterly.

Errors

As flow chemistry remains difficult to model perfectly, there are several areas that are susceptible to errors. While errors have been reduced, and where possible minimised, there are still some inaccuracies that were impossible to eradicate. Percentage analytical errors have been calculated for all results quoted in this thesis and are displayed as error bars on each plot.

Concentration – Stock solutions were made up using a Scaltec SBA-33 top loading balance and a 1000 ml volumetric flask. The error of the balance was quoted at ±0.0005 g and the volumetric error was ±0.40 ml. The error in stock solutions was minimised by measuring the HPLC-RI trace of all stock solutions as well as samples from the experiment. After calibration, this gave an accurate concentration for the stock solution that was used to calculate mass balances.

Inhomogeneous flow – The Gilson pumps used throughout this research produce pulses of fluid, which were reduced by the manometric module. However, the module was not able to eliminate the pulsing completely. The release of gaseous products, such as CO_2 also contributed

to the inhomogeneity of the stream. Perhaps the largest contributing factor was the flow of fluid through the tubes in the rig. Turbulent flow and a Reynolds number (Equation 1.4) exceeding 4000 are optimal in a flow system such as this to ensure proper mixing and a uniform flow; however, in this system it was not always possible to achieve a high Reynolds number with long residence times and relatively small reactor volumes. For example, the Reynolds number of the flow experiments discussed in Chapter 5 was calculated to be 125.

As the flow at the surface of the tube will be retarded, laminar flow allows a stream of fast moving fluid through the centre of a tube. This will lead to an inhomogeneous product stream and inconsistent residence times. In order to reduce the effect of an inhomogeneous flow, large sample volumes were collected. In most experiments, except the recycling experiments recorded in Chapter 4 where a much larger volume of 200 ml were collected, a volume of 15 ml was collected for each sample. In order to increase the Reynolds number of the flow, the smallest possible tube diameter was used.

Residence times – The residence times were calculated by Equation 2.2 using the flow rate, density and reactor volume where the reactor volume was defined as the internal volume of the section of tubing in direct contact with the heating elements. The density of the flow was estimated using the density of water at the reaction temperature, taken from data in the National Institute of Standard and Technology (NIST) database.[64]

The flow rate was set on the pump and the efficiency of the pump was calculated by mass flow over a 10 minute time period. The pump efficiency was measured once a week and the reactions were repeated if the efficiency was found to be less than 97 %. Another factor affecting the

residence time was the "reactor volume". This was measured as the volume of tube in contact with the heating elements; however, this assumes that the fluid inside passing through the reactor reaches the desired temperature instantly once it enters the "reactor" and cools instantly as soon as it leaves the "reactor". Due to the difficulty in modelling the heating and cooling of the tubing, this was assumed to be the most accurate way of measuring the reactor volume.

$$Residence\ Time\ /\ s = \frac{Reactor\ Volume\ /\ ml\ \times Density\ /\ g.ml^{-1}\ \times 60\ s}{Flow\ Rate\ /\ g.min^{-1}}$$

Equation 2.2 An equation is shown above for the calculations of residence time of liquids inside the reactor. The density of the flow was estimated using the density of water at the reaction temperature, taken from data in the National Institute of Standard and Technology (NIST) database.[64]

Pressure fluctuations – Pressure fluctuations due to the pulses produced by the Gilson pumps were found in each experiment. However, these fluctuations were found to be within a maximum range of ±100 psi, meaning all experiments were conducted at 2900 – 3100 psi. This is much higher than the vapour pressure of water (680.55 psi at 260 °C),

Temperature fluctuations – Due to the nature of the flow experiments, the temperature could be seen to oscillate slightly in some reactions due to the low residence times and thus high flow rates. This led to a change in heater controller which minimised these fluctuations to ±0.5 °C. The thermocouples used have an intrinsic error attached of ±1.5 °C, meaning the overall error associated with the temperature can be measured at ±2 °C.

Dilution – Dilution was required at the start of this project to analyse samples with the HPLC-UV. A standard program of 1-100 dilution had already been established by Huddle and was used without alteration.

This was seen to be one of the largest systematic errors in the process, measuring up to ±8.5 %. This large error was put down to the liquid handler drawing in air bubbles that were held in the water reservoir. In order to reduce this error, water in the reservoir was first sonicated before the handler was turned on. This reduced the error to ±2 %. After the RID had been implemented in the standard analysis, the dilution step could be removed as the samples no longer required dilution to fall within a linear response region for accurate analysis.

Detection – In order to find the area of peaks in HPLC traces, a baseline was drawn underneath each peak manually. The error in detection using HPLC-RI was calculated by repeat analysis of a single sample of known concentration MAA solution. The error was calculated at ±0.3 % and was attributed to human error during integration. All samples were analysed three times and an average of the three results quoted in this thesis.

Standard Operating Procedure

The standard operating procedure (SOP) for **Rig 27** (Figure 2.3) is below. Care must be taken when working with high temperature and high pressure water due to the high temperature, pressure and the potential for high temperature steam to be released potentially causing severe burns.

Start-up

1. A reaction solution should be prepared to include a dilute solution of organic acid and NaOH in water.
2. Using Equation 2.3, calculate flow rates required to achieve the desired residence times for the experiment, depending on the density of water (calculated as a function of temperature).
3. Turn pump on to begin pumping deionised water into the system.
4. While checking for leaks, adjust the back pressure regulator gradually to the required pressure (3000 psi).
5. If leaks are found, reduce pressure to ambient (1 atm, 14 psi) and tighten the fitting.
6. Once at required pressure, check pump operation efficiency (at 5 ml min^{-1}) by recording the time taken to collect a volume of 20 ml of water from system outlet (>95 % efficiency required).
7. Set pumps to flow rate required for first run.

Heating

8. The chiller for the heat exchanger should be set to 10 °C and turned on.
9. Turn on the heater (thermostat) and set the thermostat to the required temperature.

10. Once the temperature has been reached (as indicated by thermostat), monitor reactor outlet temperature until the value (accurate to 1 °C) is observed to remain static for a period of at least 5 minutes.

Reaction

11. The precursor pump is switched from the deionised water to the prepared precursor solution. Initial volume of reagent mixture is recorded.
12. Calculations including the flow rate and internal volume of the rig indicate the period before product solution will begin to emerge from the system outlet; however, this is confirmed by the visual and audible presence of gas bubbles exiting the apparatus (generated from the decomposition of reagents). Product collection is conducted after three times this period, to ensure the product is homogeneous.
13. If more than one flow rate or temperature is required, they can be changed and a sample taken after homogeneous flow is reached once again.
14. This process continues until all required samples have been collected.

Shutdown

15. The heater (thermostat) is turned off and the precursor pump is switched back to water.
16. The precursor pump is primed to flow at 10 mL min^{-1}.
17. Once the temperature inside the aluminium heating block has fallen below 60 °C, the pumps and cooling water are turned off.

Emergency shutdown

Turn off the power switch on the trip box. This will turn off power to the heater and pumps, while the temperature monitor, pressure monitor and heat exchanger will remain on.

Cleaning

The rig requires regular cleaning in order to prevent possible build-up of solid material. Typically nitric acid is used as this is able to dissolve any solid build up.

1. Prepare solution 0.5 mol dm^{-3} nitric acid.
2. Pump solution via precursor and quench pumps.
3. Swap feed to water.
4. Measure pH at regular intervals.
5. When neutral turn off pumps.

Experimental Procedure

Experiments in this thesis have been conducted using the following experimental procedures. Each procedure lists the corresponding experiment numbers. Where experiments were repeated, it has been specified in the reaction conditions before the results.

Decomposition reactions – Experiments 1-8 and 14-23

Modifications from the SOP described above are indicated in *italics*.

Start-up

1. A reaction solution should be prepared to include a dilute solution of organic acid and NaOH in water.
2. Using Equation 2.3, calculate flow rates required to achieve the desired residence times for the experiment, depending on the density of water (calculated as a function of temperature).
3. Turn pump on to begin pumping deionised water into the system.
4. While checking for leaks, adjust the back pressure regulator gradually to the required pressure (3000 psi).
5. If leaks are found, reduce pressure to ambient (1 atm, 14 psi) and tighten the fitting.
6. Once at required pressure, check pump operation efficiency (at 5 ml min^{-1}) by recording the time taken to collect a volume of 20 ml of water from system outlet (>95 % efficiency required).
7. Set pumps to flow rate required for first run.

Heating

8. The chiller for the heat exchanger should be set to 10 °C and turned on.
9. Turn on the heater (thermostat) and set the thermostat to the required temperature.
10. Once the temperature has been reached (as indicated by thermostat), monitor reactor outlet temperature until the value (accurate to 1 °C) is observed to remain static for a period of at least 5 minutes.

Reaction

11. The precursor pump is switched from the deionised water to the prepared precursor solution. Initial volume of reagent mixture is recorded.
12. Calculations including the flow rate and internal volume of the rig indicate the period before product solution will begin to emerge from the system outlet; however, this is confirmed by the visual and audible presence of gas bubbles exiting the apparatus (generated from the decomposition of reagents). Product collection is conducted three minutes after this time to ensure the product is homogeneous.
13. *A sample of 20 mL is collected and shaken for homogeneity before a smaller aliquot is taken for analysis.*
14. If more than one flow rate or temperature is required, they should be changed and a further sample taken after a stable temperature is reached and an equilibration period has passed once again.
15. This process continues until all required samples have been collected.

Shutdown

16. The heater (thermostat) is turned off and the precursor pump is switched back to water.
17. The precursor pump is primed to flow at 10 mL min^{-1}.
18. Once the temperature inside the aluminium heating block has fallen below 60 °C, the pumps and cooling water are turned off.

Analysis

19. *Aliquots of each of the samples collected during the experiment are analysed with HPLC-RID without dilution or neutralisation.*
20. *Smaller aliquots of each sample are diluted with D_2O and analysed with ^1H NMR.*

Liquid-liquid extraction reactions – Experiments 9-13, 16 and 24-30

1. An extraction solution should be prepared either by dissolving an organic acid and NaOH in water or by collecting the exit solution from the rig. A sample of this solution should be collected for HPLC-RID and ^1H NMR analysis.
2. The aqueous solution should then be shaken with an equal volume of organic solvent for 5 mins and be left to separate for 15 mins.
3. The layers should be separated and a sample of the aqueous solution should be collected for analysis.
4. If multiple extractions are required, the aqueous solution should be shaken with a second aliquot of organic solvent for 5 mins and left to separate. The process above can be repeated as many times as required.

5. After the extraction, the organic layers should be combined and solvent removed under reduced pressure to yield a crude sample of the desired product.

Recycling reactions – Experiments 25-30

Modifications from the SOP described earlier in this chapter are indicated in *italics*. Step 22 is included if pH balancing is required and should be passed over if the reaction does not require this step.

The aqueous solutions are labelled as follows:

RxSy where x denotes the cycle number and y denotes the step (1 = precursor, 2 = post decarboxylation, 3 = post acidification and 4 = post MAA extraction) *e.g.* R3S2 is the aqueous exit solution collected in the third cycle (R3) after decarboxylation (S2).

Start-up

- *Using Equation 2.2, the required flow rate to achieve a 300 second residence time for the experiment was calculated at 1.39 mL min^{-1}.*
- Turn pump on to begin pumping deionised water into the system.
- While checking for leaks, adjust the back pressure regulator gradually to the required pressure (3000 psi).
- If leaks are found, reduce pressure to ambient (1 atm, 14 psi) and tighten the fitting.
- Once at required pressure, check pump operation efficiency (at 5 ml min^{-1}) by recording the time taken to collect a volume of 20 ml of water from system outlet (>95 % efficiency required).
- Set pumps to *1.39 mL min^{-1}.*

Heating

- The chiller for the heat exchanger should be set to 10 °C and turned on.
- Turn on the heater (thermostat) and set the thermostat to the required temperature.
- Once the temperature has been reached (as indicated by thermostat), monitor reactor outlet temperature until the value (accurate to 1 °C) is observed to remain static for a period of at least 5 minutes.

Reaction

Step 1:

1. A *1 L* reaction solution should be prepared to include a dilute solution of organic acid, NaOH *and 250 ppm hydroquinone (if required)* in water *(R1S1). Take a sample for HPLC-RID and* ^{1}H *NMR analysis (with* D_2O*) and record the pH.*

Step 2:

2. The precursor pump is switched from the deionised water to the prepared precursor solution.
3. Calculations including the flow rate and internal volume of the rig indicate the period before product solution will begin to emerge from the system outlet; however, this is confirmed by the visual and audible presence of gas bubbles exiting the apparatus (generated from the decomposition of reagents). Product collection is conducted three minutes after this period, to ensure the product is homogeneous.

4. *Once all of the precursor solution has been pumped into the rig, the heater (thermostat) is turned off, the precursor pump is switched back to water and collection of RxS2 is stopped. A sample should be taken for HPLC-RID and ^{1}H NMR analysis and the pH of the exit solution recorded.*
5. The precursor pump is primed to flow at 10 mL min^{-1}.
6. Once the temperature inside the aluminium heating block has fallen below 60 °C, the pumps and cooling water are turned off.

Step 3:

16. *Calculate the total concentration of IC, CC and MC from the HPLC trace of RxS2 (i.e. [IC + CC + MC]).*
17. *Add an aliquot of IC so that the concentration of IC, CC and MC totals 0.5 M. The solution should then be stirred until all of the solid has dissolved.*
18. *Take a sample for HPLC-RID and ^{1}H NMR analysis (RxS3) and record the pH of the acidified solution.*

Step 4:

19. *Extract the MAA by running three serial liquid-liquid extractions, each with an equal volume of organic solvent.*
20. *Collect the organic layers and remove the organic solvent by evaporation under reduced pressure. A sample should be analysed by ^{1}H NMR to determine the purity of MAA extracted.*
21. *Take a sample of the aqueous layer (RxS4) for HPLC-RID and ^{1}H NMR analysis and record the pH of the solution.*
22. ***If required**, top up the volume of the solution with a second solution of precursor, as prepared in step 1 and the pH should be adjusted to 3.90 with NaOH or H_2SO_4 as required.*

23. *Take a sample for HPLC-RID and ^{1}H NMR analysis (Rx+1S1) and record the pH of the solution. This solution can be recycled into the rig as R(x+1)S1.*

Analysis

23. *Aliquots of each of the samples collected during the experiment should be analysed with HPLC without dilution or neutralisation.*
24. *Smaller aliquots of each sample were diluted with D_2O and analysed with ^{1}H NMR.*

Bio-PMMA Synthesis – Experiment 31

The collected MAA (1.0 mol) was refluxed with MeOH (1.0 mol) and Amberlyst 15H (10 g) for 18 hrs before filtration. The solution was distilled under reduced pressure to yield an orange-yellow mixture of MeOH, MMA and water, which was water washed and colourless MMA separated. MMA was dried over 3 molecular sieves and atmospherically distilled (the fraction boiling at 100 °C was collected).

Poly(methyl methacrylate) (PMMA) was formed by suspension polymerisation. A solution of MMA (2.00 mL) and toluene (0.50 mL) was added dropwise to a stirred solution of toluene (1.50 mL) and azobisisobutyronitrile (AIBN) (0.5 wt%) under an inert atmosphere. After 4 hours, PMMA was dissolved in tetrahydrofuran (THF) (50.0 mL) and precipitated in hexane (1.20 L) to yield pure PMMA (1.21 g).

Chapter 3 - A Novel Approach to Acrylic Acid Production

Much of the research conducted in this thesis was inspired by the publication by Carlsson *et al.* who described the aqueous high temperature and high pressure decarboxylations of citric and itaconic acids (IC) to methacrylic acid (MAA).[67] Their suggested scheme can be seen in Scheme 1.7 and details the pathways between a selection of related carboxylic acids and MAA. While the main focus of the paper was the decarboxylation of IC, Carlsson also suggested that citramalic acid (CM) could be decarboxylated to hydroxyisobutyric acid (HIB) before dehydration would yield MAA.

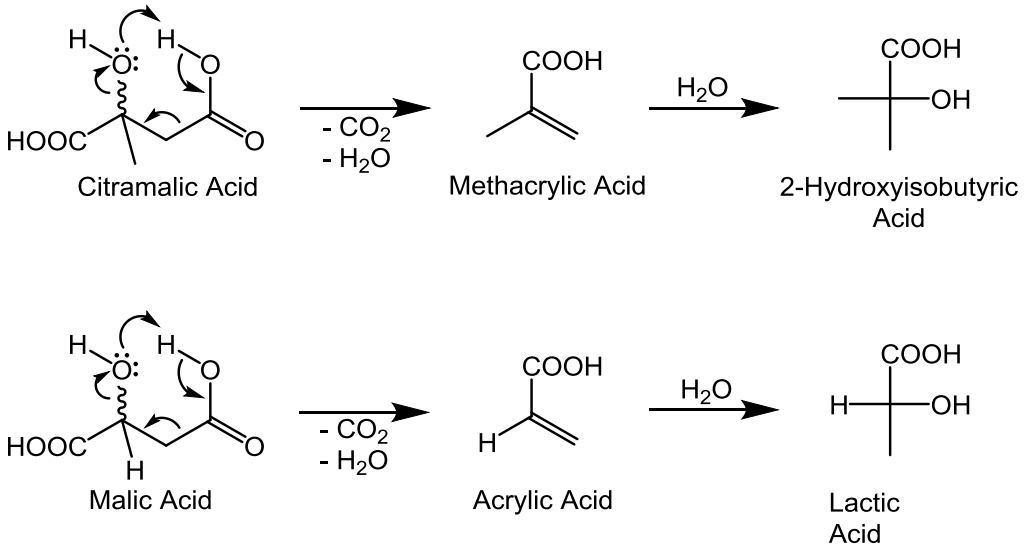


Figure 3.1 Showing the analogous mechanisms suggested by Huddle[72] for the dehydration and decarboxylation of CM to MAA and malic acid to acrylic acid.

Huddle studied this mechanism in detail and revealed that HIB was only formed in significant concentrations at longer residence times, where MAA

had already been formed and was hydrated to HIB. These results suggest that a single, concerted step, seen in Figure 3.1, was more likely.[72]

Huddle's research into CM suggested that, while high levels of MAA were produced, the overall selectivity of the process was unacceptable and the reaction yielded higher levels of by-products than seen from the decarboxylation of IC. However, the research into minimising these by-products was thwarted by the abrupt discontinuation of CM sales by all known suppliers.

It was noted that if the methyl group had no bearing on the concerted mechanism, an analogous system that did not include this pendant alkyl may be a suitable substitute for the investigation. The focus of this chapter is to follow up on Huddle's suggestion that the principles of the CM decarboxylation could be applied to an analogous system that includes malic acid and acrylic acid.[72]

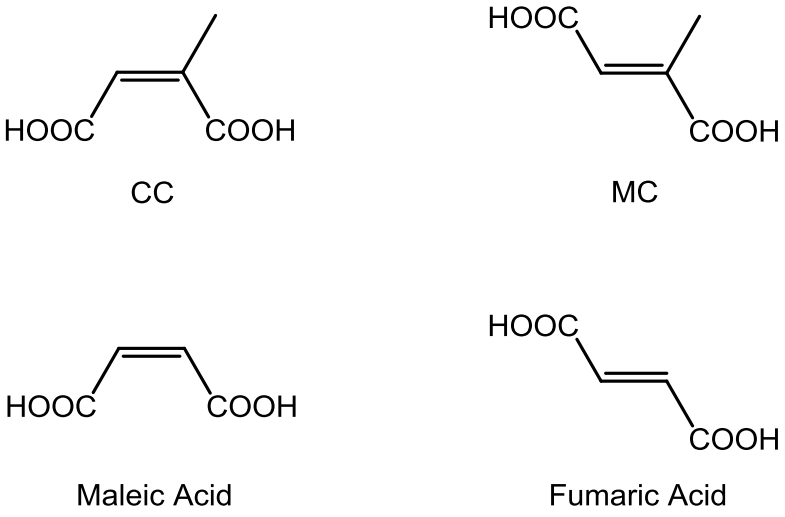
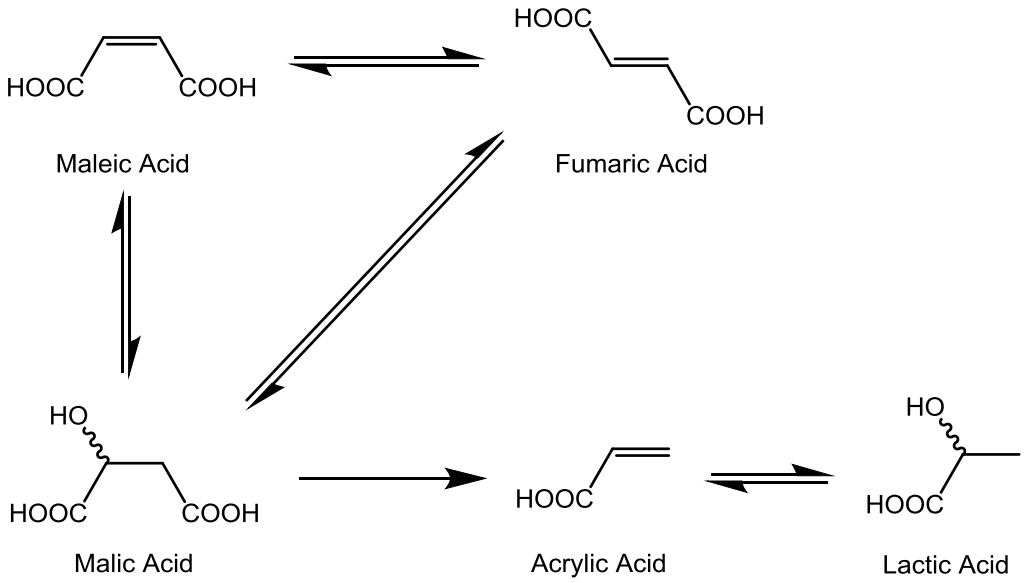


Figure 3.2 A comparison can be drawn between the structures of CC and maleic acid, and MC and fumaric acid. Huddle suggested that decarboxylation of these analogous acids would hence yield MAA and acrylic acid *via* similar pathways.

Huddle drew comparisons between the dehydration products of malic acid, maleic acid and fumaric acid, seen in Figure 3.2, with CC and MC, two

precursors to MAA. While both CC and MC must pass through IC before decarboxylation to MAA, maleic and fumaric acid must show different decarboxylation pathways as there is no terminal methyl group on IC that could be removed to form the corresponding isomer of maleic and fumaric acids. As it is impossible to directly compare IC with any isomers of maleic or fumaric acids, a new scheme must be drawn to show the conversion of these acids to acrylic acid.

Scheme 3.1 shows the pathways between various acidic precursors to acrylic acid. Here malic acid acts as a central molecule that both dehydrated isomers must pass through to yield acrylic acid. Malic acid can then undergo the concerted dehydration and decarboxylation to produce acrylic acid. As these processes occur in an aqueous environment and include the removal of water molecules, it is acknowledged that acrylic acid exists in equilibrium with its hydrated product, lactic acid.



Scheme 3.1 A scheme to describe the pathways between five carboxylic acids. The conversion of maleic and fumaric acids through malic acid is shown to produce acrylic acid, which exists in equilibrium with its hydrated counterpart, lactic acid.

After proposing the mechanism shown in Figure 3.1, Huddle investigated the conversion of malic acid to acrylic acid. He studied the reaction in both the absence of base and the presence of half equivalents of sodium hydroxide at various temperatures with a residence time of 100 s at 3500 psi.[72] Figure 3.3 shows the results from his first experiment with the conditions shown in Table 3.1.

Table 3.1 Showing the reaction conditions used by Huddle.

Malic Acid Decarboxylation	
Precursor	0.1 M Malic Acid
Base	N/A
Temperature	250 – 350 °C
Pressure	3500 psi
Residence Time	100 s

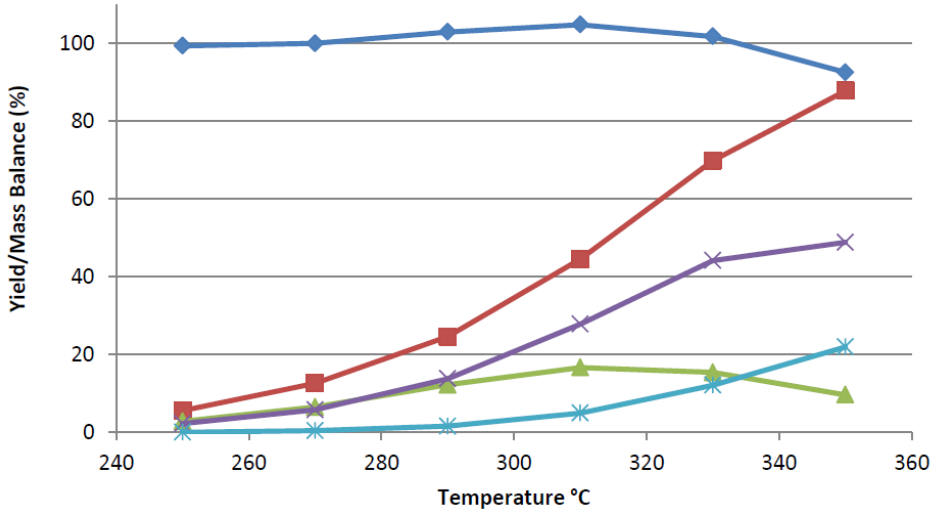


Figure 3.3 Taken from Huddle's thesis.[72] The percentage composition of exit solutions collected show the decomposition malic acid. The plot shows an increase in conversion of malic acid (—■—) and an increase in the concentrations of by-products, maleic (—▲—) and fumaric acids (—×—). Acrylic acid (—✳—) shows very low concentrations below 310 °C, but this rises to 22.0 % at 350 °C. Also shown is the total mass balance (—◆—) calculated.

Figure 3.3 displays the increased yield of acrylic acid in solution when malic acid is decarboxylated at higher temperatures. At 250 °C, acrylic acid is not detected in the exit solution. This increases slightly to 1.6 % at 290 °C and reaches a maximum of 22.0 % at 350 °C. The amounts of maleic and

fumaric acid also increase with increasing temperature, with maleic acid reaching 16.7 % of the total composition at 310 °C and fumaric acid reaching a maximum yield of 48.9 % at 350 °C.

It should be noted that the mass balance of this experiment lies between 92.6 and 104.9 %, hinting at a potential problem with the analytical techniques used in this experiment. Huddle put this down to problems with dilution, especially in sample preparation for HPLC analysis with a UV detector.

Huddle then investigated both the addition of base on the decarboxylation of malic acid and also the difference in acrylic acid yields when the precursor was switched to fumaric acid and then maleic acid. The conditions of these three reactions can be seen in Table 3.2.

Table 3.2 Showing the reaction conditions used by Huddle.

Malic Acid Decarboxylation	
Precursor	0.1 M Various Acids
Base	0.05 M NaOH
Temperature	250 – 350 °C
Pressure	3500 psi
Residence Time	100 s

With the addition of base to the malic acid, the concentration of acrylic acid can be seen to have significantly increased in each exit solution. At 350 °C, acrylic acid production reaches a maximum, yielding 53.7 % composition in the exit solution. This is a large improvement on 22.0 % achieved without base.

When the precursor was switched to maleic acid, there was a significant decrease in the amount of acrylic acid produced at each temperature. The same trend can be seen when fumaric acid was used, supporting the idea that these isomers must undergo hydration to malic acid before the concerted decomposition to acrylic acid and indicating that the hydration is a slow rate determining step. The conversion of the two isomers is much

lower than the conversion of malic acid at all temperatures except 350 °C, where the conversion lies between 86.0 and 88.3 % for each precursor.

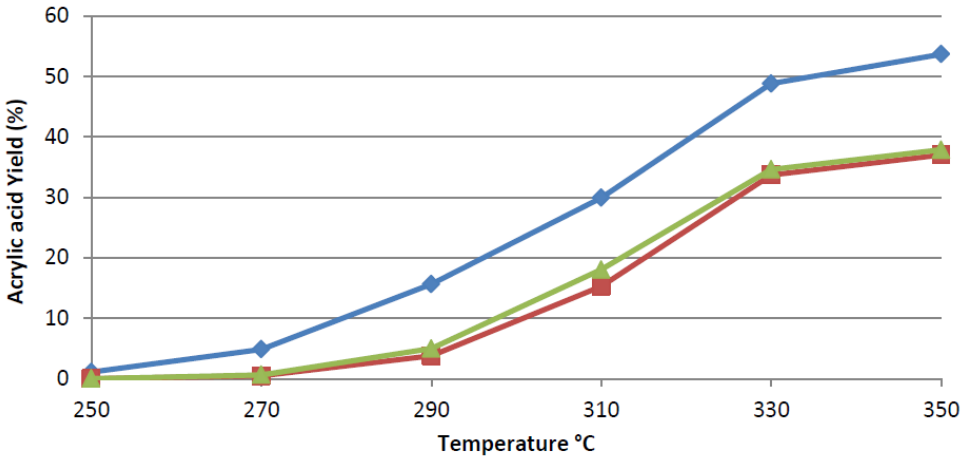


Figure 3.4 Taken from Huddle's thesis,[72] the effect of the nature of the precursor was examined with three different precursor acids – fumaric acid (▲), maleic acid (■) and malic acid (◆) – each in the presence of base. The plot shows the concentration of acrylic acid present in exit solutions collected at 20 °C intervals between 250 and 350 °C from three different precursors. In each experiment, the conversion to acrylic acid increases with increasing temperature, with the highest acrylic acid yields achieved with a malic acid precursor.

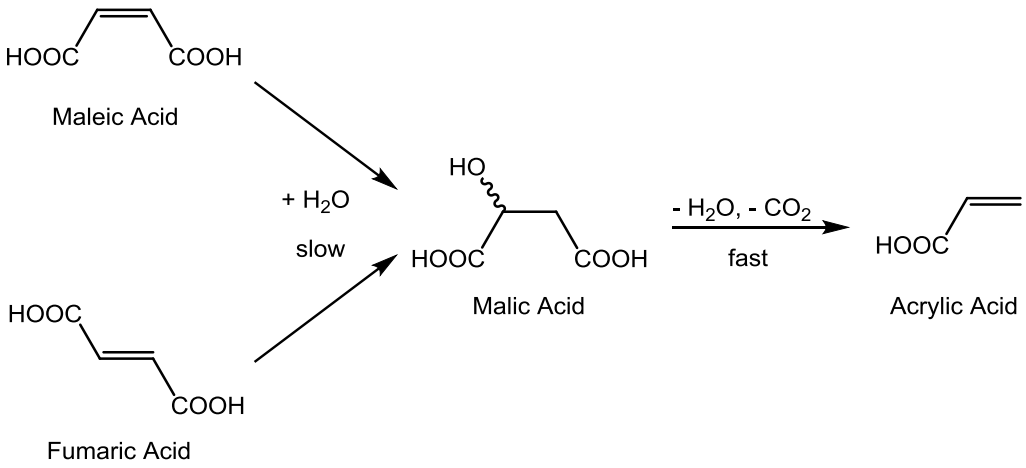


Figure 3.5 Initial reactions by Huddle indicate that the hydration to malic acid is the limiting step in the conversion of maleic and fumaric acids to yield acrylic acid.

The mass balances of these experiments were much lower than that of the previous experiment, shown in Figure 3.3. When malic acid was used with a base catalyst, the mass balance varied between 114.8 % at 290 °C and just 57.0 % at 350 °C. The mass balances were further decreased when maleic acid (45.2 – 101.0 %) and fumaric acid (44.4 – 98.7 %) were used as precursors, suggesting that dilution may not have been the only cause of such large discrepancies.

It is accepted that acrylic acid will exist in equilibrium with lactic acid under the conditions reported by Huddle; however, the use of HPLC-UV as the predominant analytical technique meant that lactic acid could not be detected in the aqueous samples collected because lactic acid is not UV active. Therefore, it would not be possible to calculate the yield of the hydrated product, which may go some way to explain the deficit in the mass balances shown.

With the introduction of a refractive index detector (RID) and the removal of dilution steps from the experimental procedure, the production of acrylic acid from malic acid was the focus of my new investigation and the assessment of the viability of this process as a whole was assessed.

Strategy

Aim - ***Previous research by Huddle was used as a basis for an investigation into the production of acrylic acid, AA. This is another monomer of interest to Lucite International and, if successful, could lead to a second, independent chemical process.***

This investigation was split into three distinct sections. First of all the effects of temperature and residence time were studied in order to better understand the conversion of malic acid to acrylic acid. Our first experiment was based on the second of Huddle's experiments described above and was used in the design of further experiments in this chapter.

Further to the decomposition of malic acid, the stability of acrylic acid was looked at. This work was partially conducted in collaboration with Miss Rossella Mascia as part of an ERASMUS funded Masters Research Project. The investigation was designed to aid the understanding of some unknown and low level products seen in the exit solutions of the malic acid studies.

The research concludes with the analysis of acrylic acid extraction into organic solvents. This work was conducted in collaboration with Miss Ailsa Suleman as part of a Masters Research Project. It has previously been shown that similar organic acids can be extracted in this way and the investigation will demonstrate the difficulties faced when the concept was used to design a method for selective acrylic acid extraction.

Finally an analysis of all the data provided in this chapter is used to discuss the possibility of this process being used in a novel route to acrylic acid.

Results and Discussion

Malic Acid Decomposition

Huddle reported low mass balances at high temperatures, which can be attributed to his use of HPLC-UV analysis. Figure 3.6 shows the difference RI detection can make to the analysis of an aqueous mixture containing a mixture of saturated and unsaturated organic molecules.

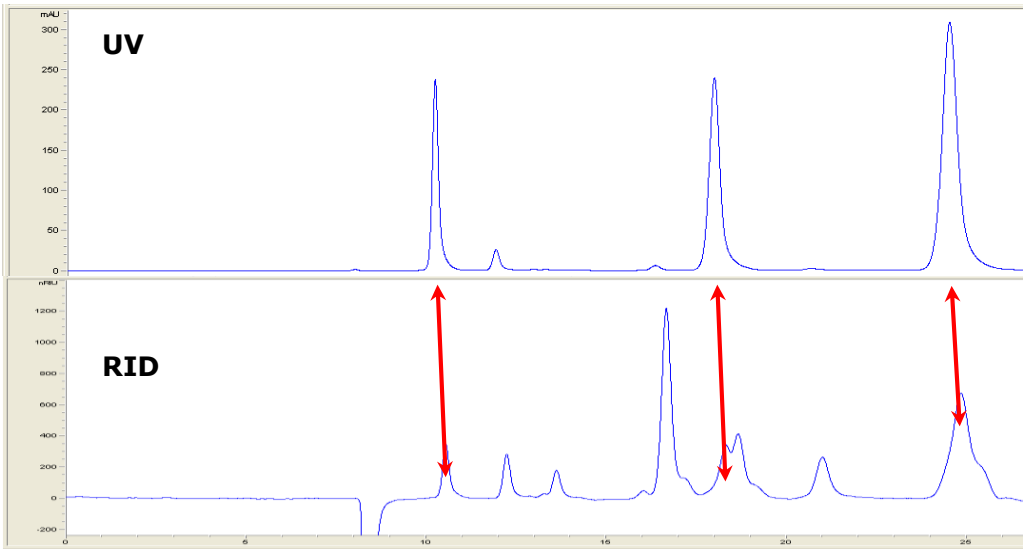


Figure 3.6 In a plot similar to that shown in Chapter 2, UV detection is again shown to be inadequate for systems containing saturated organic molecules. A trace collected by HPLC-UV is compared to a trace collected by HPLC-RID and the difference between the plots is clear. While the UV detection method shows five clear peaks, a further eight products are detected with a RID.

Consequently an experiment was designed to investigate the effect of temperature on the conversion of malic acid to acrylic acid between 190 °C and 350 °C at 3000 psi with a residence time of 100 s. With similar conditions to those reported by Huddle and shown in Table 3.2, it was expected that the experiment would yield a maximum concentration of *ca*. 0.05 M acrylic acid at 350 °C. It was also expected that the newly introduced detection methods would enable higher mass balances to be reached.

Experiment 1 - Decomposition of malic acid at various temperatures

Table 3.3 Showing the reaction conditions used in Experiment 1.

Experiment 1 Malic Acid Temperature Study	
Precursor	0.101 M Malic Acid
Base	0.050 M NaOH
Temperature	Varied
Pressure	3000 psi
Residence time	100 s
Number of repeats	3

While Figure 3.7 shows significant levels of conversion to acrylic acid, the repeated experiment shows much lower concentrations of acrylic acid at each temperature. In fact, the maximum concentration of the desired product is just 0.008 M (8 % conversion) at 330 °C.

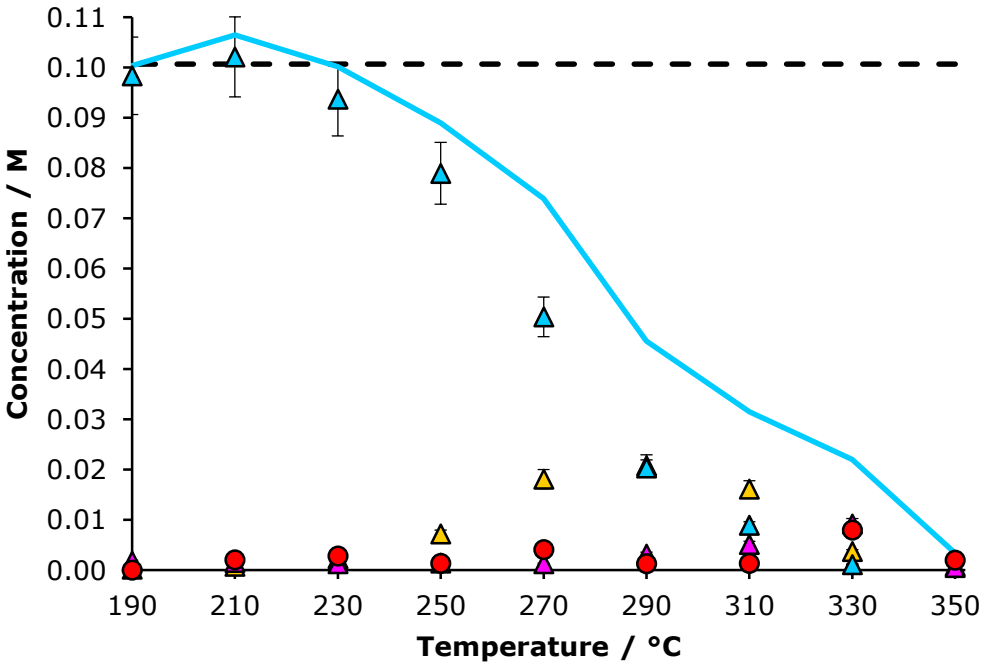
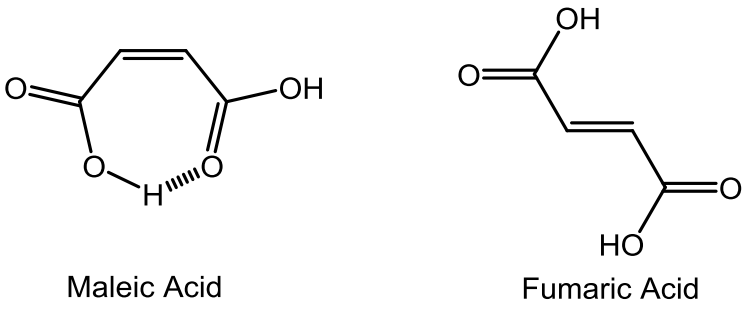


Figure 3.7 The decomposition of a 0.101 M malic acid (△) solution containing 0.050 M sodium hydroxide is shown at temperatures between 190 °C and 350 °C. The concentration of the precursor solution is shown (– – –) along with the mass balance (—). The concentration of maleic acid (△) rises up to 0.021 M at 290 °C, before decreasing. Fumaric acid (△) concentration peaks at 330 °C. Low concentrations of acrylic acid (●) can be seen in each exit solution, with a maximum concentration of 0.008 M collected at 330 °C. Each point is the average of 3 samples taken from repeated experiments.

The plot shows high levels of unconverted starting material below 250 °C but low selectivity above this temperature. While the mass balance lies close to 100 % up to 230 °C, it falls dramatically to 47 % at 290 °C and just 16 % at 350 °C, suggesting a trade-off between conversion and selectivity would be required for this process.

Above 250 °C dehydration of malic acid can be seen to yield maleic acid in small amounts. Fumaric acid was detected in much smaller concentrations in the aqueous exit solutions in this experiment, only showing a higher concentration than maleic acid at 330 °C. This suggests the activation energy to produce fumaric acid is higher than the energy required to produce the cis-isomer.



Maleic Acid Fumaric Acid

Figure 3.8 The cis-isomer, maleic acid, forms intramolecular hydrogen bonds (ıııı) between its two carboxylic acid groups. Due to restricted movement around the alkene double bond, the trans-isomer, fumaric acid, cannot rotate into an arrangement that can form such intramolecular hydrogen bonds. Hence, the entropy of fumaric acid is greater than that of maleic acid.

Figure 3.8 shows that while maleic acid can form internal hydrogen bonds, fumaric acid cannot. These intramolecular hydrogen bonds reduce the entropy of maleic acid. According to Equation 3.1, a larger entropy value will give a more negative value for the Gibbs free energy of a molecule. In other words, a larger entropy value results in a more stable molecule. Hence, once the activation energy is high enough to produce both maleic

acid and fumaric acid, the higher entropy of fumaric will favour its production.

$$\Delta G = \Delta H - T\Delta S$$

Equation 3.1 The Gibbs free energy (G) of a system is defined as the entropy (S) multiplied by the temperature of a system (T) and subtracted from the enthalpy (H).

As the experiment above involved a relatively short residence time of 100 s, a further experiment was designed to investigate the effect of lengthening the reaction time at 290 °C. This temperature was chosen because the presence of acrylic acid in samples collected at this temperature in Experiment 1 shows that there is enough energy in the system at this temperature both to dehydrate and to decarboxylate malic acid. It was hoped that by extending the residence time the conversion of malic acid would improve and allow an investigation into the selectivity to acrylic acid.

Experiment 2 - Decomposition of malic acid at various residence times

Similar precursor solutions were made for the following parts of the residence time study and were pumped into the rig at various flow rates to give comparable residence times.

Table 3.4 Showing the reaction conditions used in Experiment 2.

Experiment 2 Acrylic Acid Residence Time Study	
Precursor	0.089 M Malic Acid
Base	0.050 M NaOH
Temperature	290 °C
Pressure	3000 psi
Residence time	Varied
Number of repeats	3

A reactor temperature of 290 °C was chosen to produce a small amount of acrylic acid, while enabling a focus on the build-up of other by-products, especially fumaric acid.

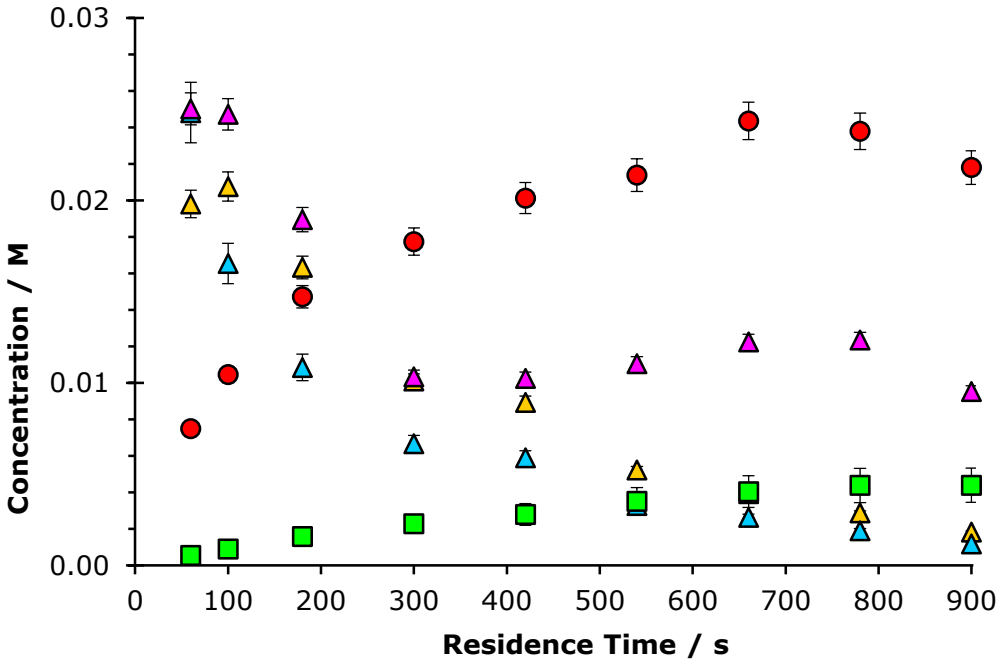


Figure 3.9 Malic acid (△) shows high levels of conversion in this experiment, leading to the formation of fumaric acid (△), maleic acid (△) and acrylic acid (●). However, there is a decrease in concentration of the dehydration products as the residence time increases, indicating further decomposition. Acrylic acid is hydrated to produce lactic acid (■) in all exit solutions, and this conversion appears to be dependent of the concentration of acrylic acid. Each point is the average of 3 samples taken from repeated experiments.

At 290 °C the conversion of malic acid is high, as seen by the low concentrations of unreacted precursor in the exit solutions. While the conversion is high, selectivity has improved slightly, with a maximum concentration of acrylic acid reaching 0.024 M at 660 s, a marked improvement on the 0.008 M formed in Experiment 1.

At this temperature, the concentration of maleic acid decreases with increasing residence time and is lower than the concentration of fumaric acid, supporting the earlier suggestion that fumaric acid is the thermodynamic product of the dehydration of malic acid.

The high temperature of this experiment has not improved the mass balance of the system (seen alongside results in Appendix 1), but has

shown an increase in the amount of acrylic acid produced with longer residence times. However, at 290 °C there remains a relatively low concentration of acrylic acid in solution. Hence, a follow up experiment was designed to investigate the effect of residence times at a lower temperature of 230 °C.

Experiment 3 - Decomposition of malic acid at various residence times

Table 3.5 Showing the reaction conditions used in Experiment 3.

Experiment 3 Malic Acid Residence Time Study	
Precursor	0.085 M Malic Acid
Base	0.050 M NaOH
Temperature	230 °C
Pressure	3000 psi
Residence Time	Varied
Number of repeats	3

Following the successful investigation into the effects of residence time at 290 °C, the experiment was repeated at 230 °C. It was expected that the concentration of acrylic acid would increase with longer residence times, as seen in the previous experiment. If our earlier suggestion that fumaric acid forms as a thermodynamic product, we should expect very little fumaric acid to be observed in the product solutions of this experiment.

At the lower reaction temperature, low levels of maleic acid were observed, reaching a maximum value of 0.013 M after 900 s. Due to the low temperature of the reactor, fumaric acid was not detected in any of the exit solutions, again supporting our suggestion that fumaric acid production follows a thermodynamic pathway.

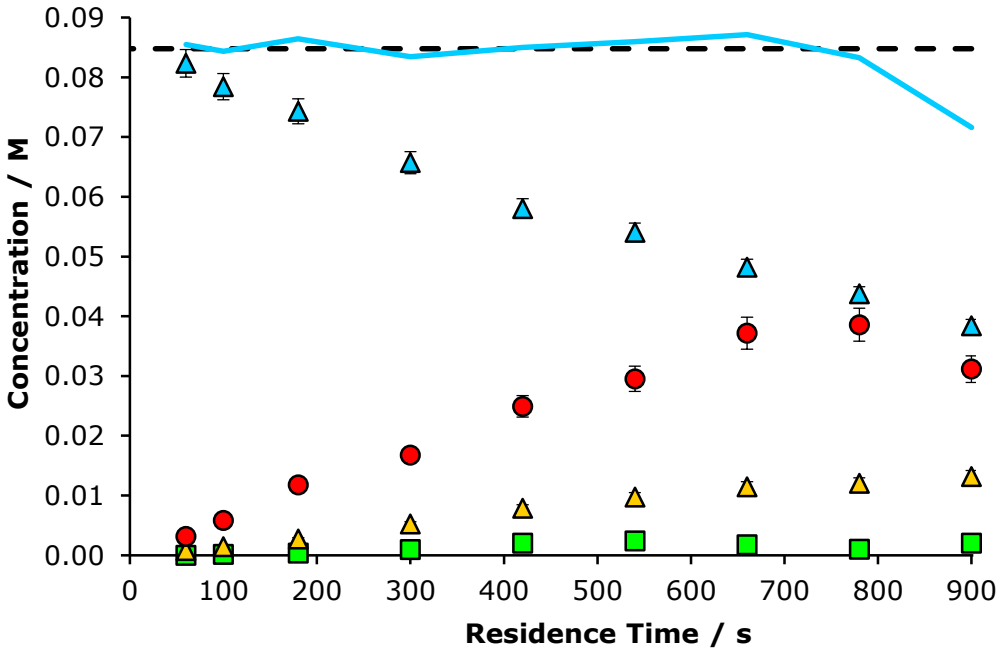


Figure 3.10 The original concentration of the malic acid (△) precursor solution is shown (– – –) and the overall mass balance (—) as the precursor is converted to maleic acid (△) and acrylic acid (●). Acrylic acid can be hydrated to lactic acid (■), shown by the low concentrations of the acid in each exit solution.

The conversion of malic acid has increased with longer residence times, as has the selectivity to acrylic acid. After 800 s, the reaction yields 0.039 M acrylic acid, much higher than the 0.008 M collected in Experiment 1. Low concentrations of lactic acid can be seen in the exit solutions; however, the concentration of this acid reaches a maximum at just 0.002 M.

The lower temperature has improved the mass balance, which remains close to 100 % at all residence times except 900 s. However, the decomposition of malic acid yields more than just the five major products that this chapter has identified so far. A number of unknown peaks remained in the HPLC traces and these peaks were investigated by ^{1}H NMR, but not characterised fully.

In order to help understand the system and ascertain which products are due to the decomposition of the acrylic acid product, a further set of

experiments were designed to investigate the nature of products collected after heating acrylic acid in the presence of base.

Acrylic Acid Stability

Experiment 4 - Decomposition of acrylic acid at various temperatures

The first experiment in this series pumped a solution of 0.098 M acrylic acid with 0.050 M sodium hydroxide through the rig and the effects of the temperature on the stability of acrylic acid were investigated.

Table 3.6 Showing the reaction conditions used in Experiment 4.

Experiment 4 Acrylic Acid Temperature Study	
Precursor	0.098 M Acrylic Acid
Base	0.050 M NaOH
Temperature	Varied
Pressure	3000 psi
Residence time	100 s
Number of repeats	3

It can be seen from Figure 3.11 that acrylic acid concentration remains high up to 250 °C, with only very low levels of hydration to lactic acid. However, when the system is heated above 250 °C the concentration of acrylic acid in the exit solutions drops off rapidly to just 0.048 M at 330 °C. The amount of lactic acid produced increases in each solution, reaching a maximum concentration of 0.022M at 290 °C, before falling away at temperatures above this. This indicates the presence of another decomposition pathway of acrylic acid as the mass balance of the results drops from 98.4 % at 270 °C to 57.2 % at 330 °C.

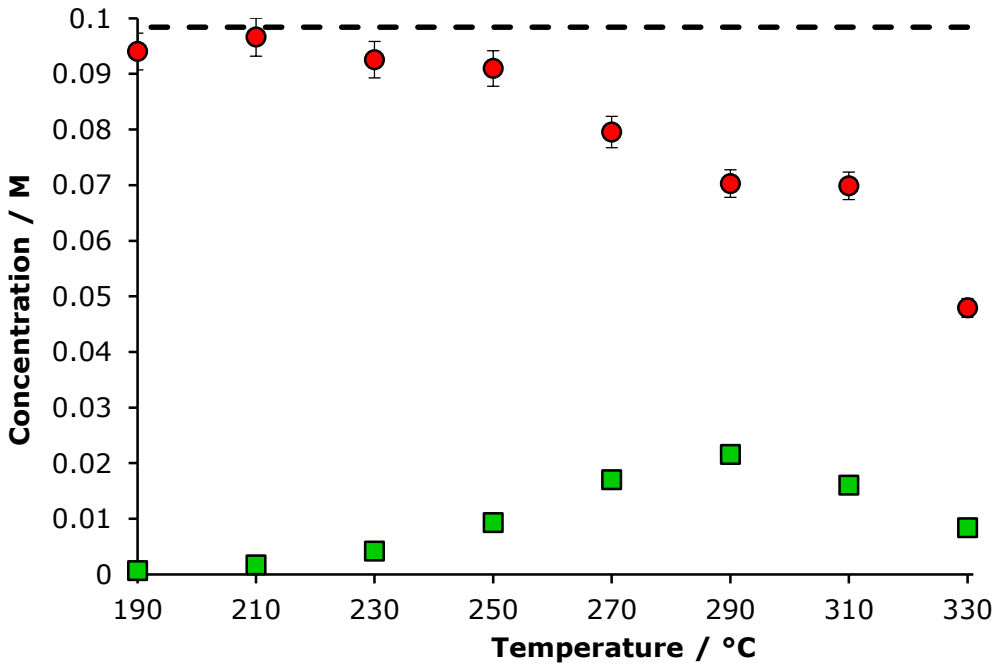


Figure 3.11 A plot to show the conversion of acrylic acid (●) to lactic acid (■) in high temperature conditions. The original concentration of acrylic acid is shown (**– – –**). Acrylic acid can be seen to be hydrated to lactic acid at elevated temperatures. The concentration of lactic acid in the aqueous solution increases with temperature, reaching a maximum concentration of 0.022 M at 290 °C. Above 290 °C the concentration decreases down to 0.008 M at 330 °C.

From the results of this temperature study, it appears that the decomposition of both acrylic and lactic acids above 300 °C goes some way to explain the substantial drop in mass balance shown in Experiment 1.

A subsequent study intended to mimic Experiments 2 and 3 was designed to investigate the effect of residence time on acrylic acid stability. It was decided that, because the concentration of lactic acid was low in Experiment 3, the temperatures studied should be 290 and 250 °C. As the conversion of malic acid to acrylic acid shown in Experiment 1 was increased slightly at 250 °C, it was hoped that this would provide a good basis for a reaction temperature and that by studying the stability of

acrylic acid under these conditions, a set of ideal reaction conditions could be decided upon.

Experiment 5 - Decomposition of acrylic acid at various residence times

Table 3.7 Showing the reaction conditions used in Experiment 5.

Experiment 5 Acrylic Acid	Residence Time Study
Precursor	0.111 M Acrylic Acid
Base	0.050 M NaOH
Temperature	290 °C
Pressure	3000 psi
Residence time	Varied
Number of repeats	3

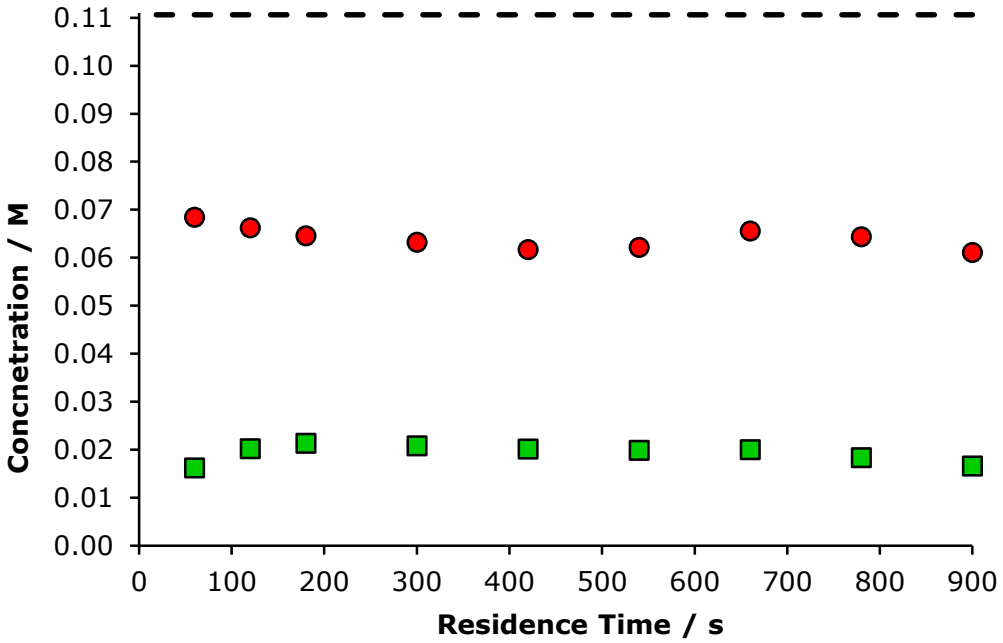


Figure 3.12 A plot to show the conversion of acrylic acid (●) to lactic acid (■) at various residence times. The conversion of acrylic acid to lactic acid appears consistent (0.016 – 0.021 M) at all residence times studied in this experiment.

It can be seen from Figure 3.12 that the reaction temperature was high enough to cause significant rate of hydration of acrylic acid, yielding 0.016 – 0.021 M lactic acid in each exit solution. There is also a consistent level of acrylic acid (0.062 – 0.068 M) remaining in each solution, suggesting the level of conversion had reached a maximum within the shortest

reaction time (60 s). However, there were very few other peaks present in the HPLC traces of these exit solutions, suggesting any lost mass balance was due to the formation of gaseous or volatile molecules that were lost before analysis.

It was thought that by lowering the temperature of the reactor to 250 °C, higher mass balances could be reached and a possible set of reaction conditions could be proposed for the reaction.

Experiment 6 - Decomposition of acrylic acid at various residence times

Table 3.8 Showing the reaction conditions used in Experiment 6.

Experiment 6 Acrylic Acid Residence Time Study	
Precursor	0.105 M Acrylic Acid
Base	0.050 M NaOH
Temperature	250 °C
Pressure	3000 psi
Residence time	Varied
Number of repeats	3

The concentration of acrylic acid seen in Figure 3.13 indicates that, as the residence time is increased, there is an increase in the amount of decomposition of the precursor. This increase is large between shorter residence times (60 – 300 s) but slows with residence times above 420 s with a much gentler gradient. This trend corresponds with the increase of lactic acid concentration shown between 60 and 300 s. The mass balance at these residence times lies above 90 %, suggesting only a small amount of decomposition of the acids.

However, the concentration of acrylic acid levels off at 0.028 – 0.032 M above 420 s and the mass balance falls to 73.9 % at the longest residence time shown. While this drop in mass balance is smaller than that shown at the higher temperature in the previous experiment, it is still deemed to be an unacceptable loss of mass. Hence, if the decomposition of malic acid were to be carried out at this temperature, close investigation of the

effects of the residence time on the stability of the product would indicate that flow rates that relate to a residence time below 300 s should be used.

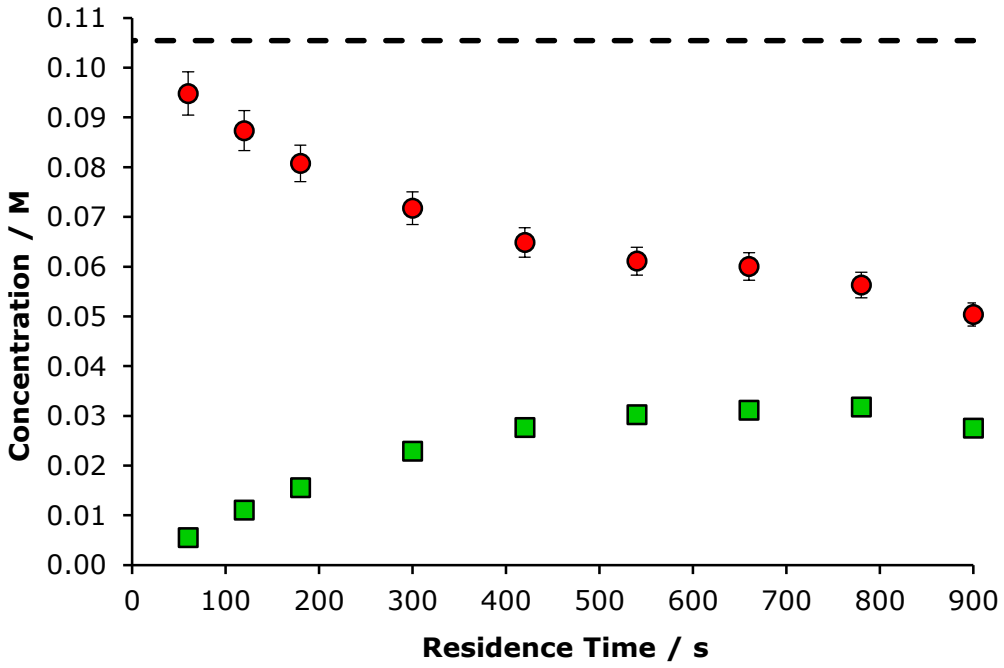


Figure 3.13 A plot to show the conversion of acrylic acid (●) to lactic acid (■) at varied residence times. The concentration of the original acrylic acid precursor is shown (**– – –**). Acrylic acid can be seen to be hydrated to lactic acid even at the shortest residence times investigated. The concentration of lactic acid in the aqueous solution increases with residence time, reaching a maximum concentration of 0.032 M at 780 s.

It was noted that the concentrations used so far in this study were lower than the concentrations used by Huddle in his related study of MAA production.[72] In Huddle's MAA experiments, he used precursor concentrations of 0.5 M, while these experiments were carried out using 0.1 M solutions. Thus, an experiment was designed to increase the concentration of acrylic acid to investigate the effects on the stability of the product. The conditions were kept identical to those seen in Experiment 4 to allow for comparison between the results of the two investigations.

Experiment 7 - Decomposition of acrylic acid at higher concentration

Table 3.9 Showing the reaction conditions used in Experiment 7.

Experiment 7 Acrylic Acid Residence Time Study	
Precursor	0.598 M Acrylic Acid
Base	0.250 M NaOH
Temperature	Varied
Pressure	3000 psi
Residence time	100 s
Number of repeats	3

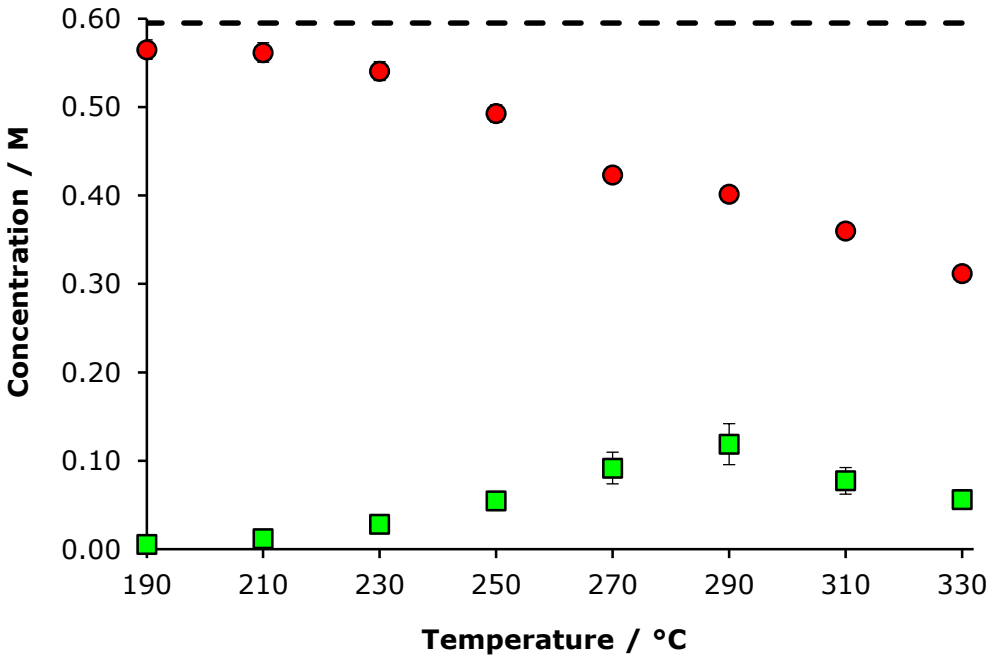


Figure 3.14 A plot to show the conversion of acrylic acid (●) to lactic acid (■) at various residence times. The concentration of the original acrylic acid precursor is shown (**– – –**). The concentration of acrylic acid decreases with increasing temperature from 0.565 M at 190 °C to 0.312 M at 330 °C. The decrease in acrylic acid concentration coincides with the conversion to lactic acid up to 290 °C before the concentration of lactic acid falls away.

When the results shown in Figure 3.14 are compared to those shown in Figure 3.11, the same general trends can be seen. There is a decrease in the amount of acrylic acid found in each exit solution as the temperature of the system is increased. In fact, the trends of both acrylic acid and lactic acid can be almost perfectly overlaid when the data is converted to

percentage composition of the original solution rather than absolute concentrations, as displayed in Figure 3.15.

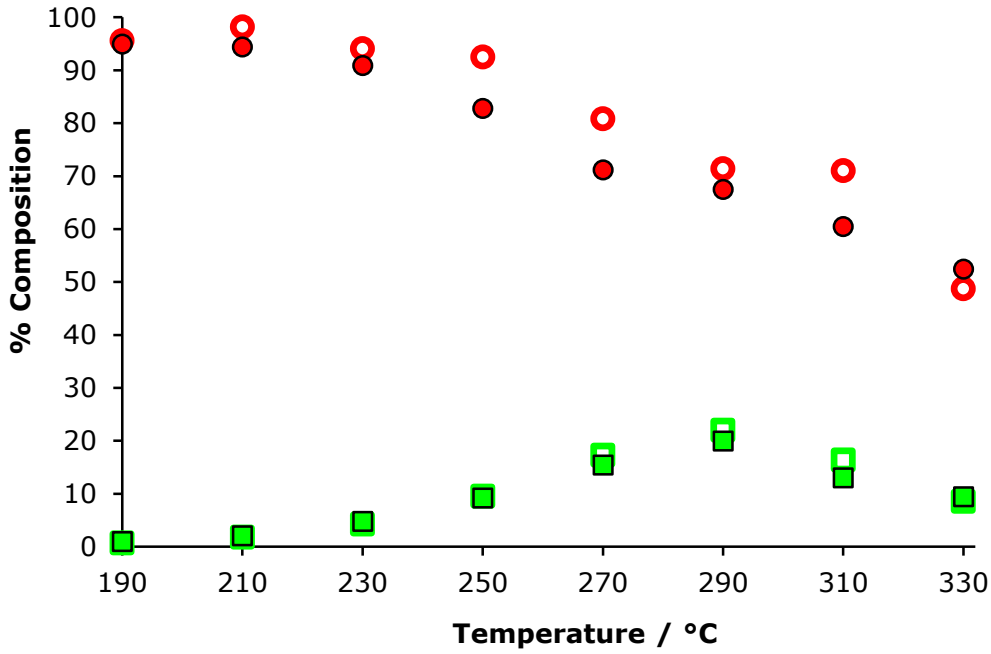


Figure 3.15 This plot demonstrates the similarities between the exit solutions from Experiments 4 and 7. The amount of acrylic acid in the exit solutions for Experiment 7 (●) shows a close correlation to the trend set by the acrylic acid in Experiment 4 (○). Similarly, the trends of lactic acid collected in Experiment 3 (□) and Experiment 7 (■) display a close likeness.

This result indicates that the concentration of the product does not influence the stability of the acid and so more concentrated malic acid precursor solutions may be implemented in this process to produce acrylic acid. It should be noted that with the increased concentration of precursor solution, each exit solution was coloured. Investigation of this colour has been previously described in Chapter 2 and suggests the more concentrated solutions strip the reactor of various metal salts. It would therefore be necessary to investigate different reactor materials for this process if it were to become industrially viable.

Once the concentration of the acid had been investigated, our attention turned to the relative concentration of base used. It should be noted that

previous research[67, 69, 72] into the decarboxylation of IC to MAA suggested that an equimolar amount of base should be used. So far in this research, the base has been in half molar quantities, so an investigation was designed to look at the effects of base concentration on the overall stability of the acrylic acid product.

Experiment 8 - Decomposition of acrylic acid with varied concentrations of base

Table 3.10 Showing the reaction conditions used in Experiment 8.

Experiment 8 Acrylic Acid Base Catalyst Study	
Precursor	Varied
Base	Varied
Temperature	Varied
Pressure	3000 psi
Residence time	100 s

Four different solutions were made up, each containing different amounts of base, and were pumped separately through the rig at a range of temperatures to allow comparison to previous experiments. Figure 3.16 shows each of the sets of results plotted as percentage composition so as to allow direct comparison between the data sets.

It can be seen from the above plot that when acrylic acid was pumped through the rig in the absence of sodium hydroxide, there was very little conversion of the acid. Low levels of the hydrated product account for some of the lost product, but the free acrylic acid showed much greater stability than the other solutions at higher temperatures.

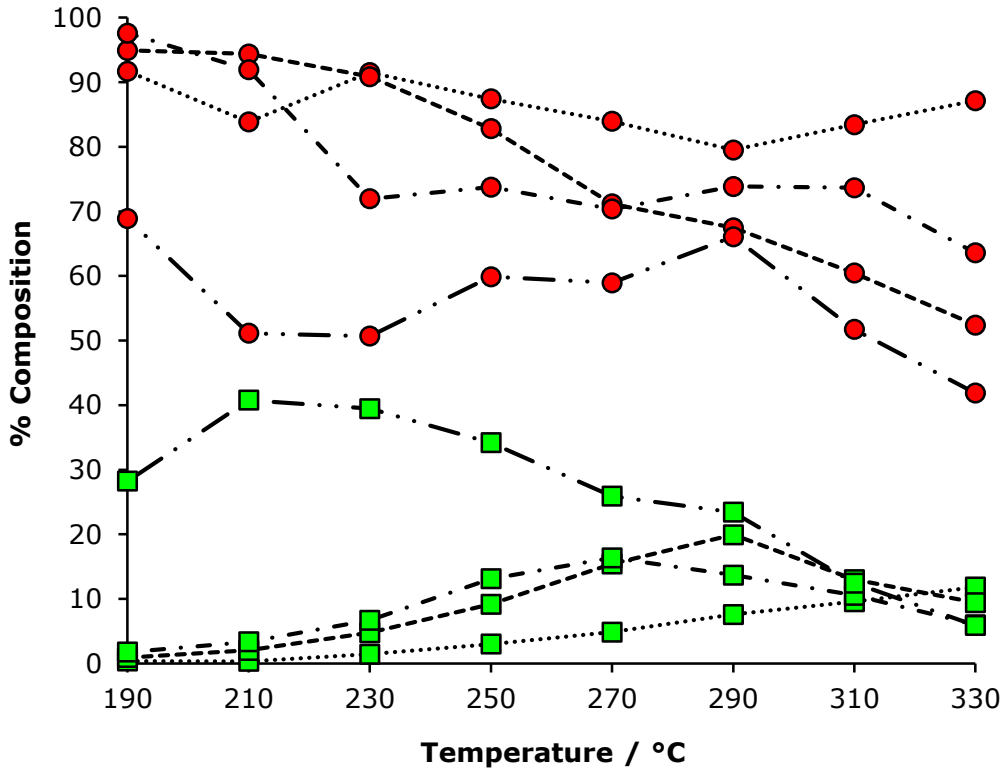


Figure 3.16 A plot to show the conversion of acrylic acid (●) to lactic acid (■) at various residence times. The plot shows the results of four different reactions when the amount of base catalyst used was varied. When 1.000 M base catalyst was used (—··), the level of conversion to lactic acid is greatest. Using equimolar quantities (0.50 M) of sodium hydroxide (—·—) yielded slightly higher concentrations of lactic acid below 270 °C, but at temperatures about 270 °C, the amount of lactic acid was greater when a half molar quantity (0.25 M) of sodium hydroxide was used (– – –). The lowest rate of conversion from acrylic acid to lactic acid was achieved in the absence of a base (····).

The results from half molar (0.25 M) and equimolar (0.50 M) equivalents of base appear to be similar at low temperatures (190 – 210 °C), before the equimolar results drop lower than their half molar counterparts. After this drop, the solutions containing equimolar base contain a constant concentration of acrylic acid at all remaining temperatures, while the acrylic acid concentration continues to fall in the half molar solutions,

dropping below the equimolar results at 270 °C. The production of lactic acid for each of these data sets is similar in every case.

When an excess of base is used, the concentration of acrylic acid in each exit solution is much lower than those shown by the other solutions, especially at temperatures below 270 °C. There is a large increase in the concentration of lactic acid in these exit solutions, suggesting that the hydration of the acrylate ion is more facile than that of the free acid. While the hydration of alkenes is traditionally acid catalysed, the presence of a strong deactivating group, such as –COOH, in the alpha position means that the resulting carbocation would not be stabilised and so would not form. By adding a base, such as sodium hydroxide, the deactivating power of the carboxylate ion is reduced and so the availability of electron density on the C=C bond is increased, enabling the electrophilic addition, seen in Figure 3.17.

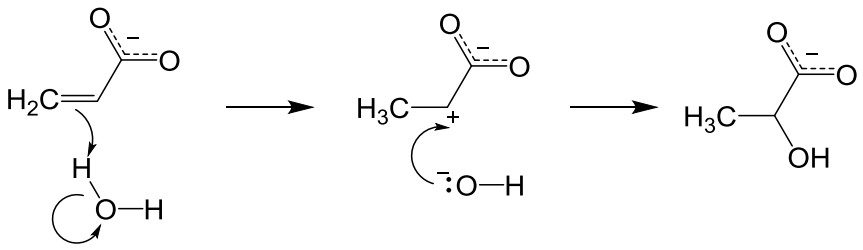


Figure 3.17 Showing the electrophilic addition of water to the acrylic acid ion across the carbon-carbon double bond to form a lactic acid ion.

These results support Huddle's use of half molar equivalents of base in his studies, repeated here in Experiments 1 – 6. The addition of half molar base increased the concentration of acrylic acid produced, while also limiting the hydration of acrylic acid to form lactic acid. Though it may be possible to extract and dehydrate lactic acid from the product stream of the reaction, it does add further expense and so minimising the amount of lactic acid should be a priority alongside achieving the maximum conversion and selectivity to acrylic acid.

It has been established that the production of acrylic acid from malic acid would require a compromise between high conversion and high selectivity since we have been unable to identify or recover lost mass. By using lower reaction temperatures (≤ 250 °C) with longer residence times (360 – 780 s), it may be possible to minimise this mass loss and find suitable conditions for the process. We have shown that the concentration of the precursor does not affect the production of acrylic acid, but may require careful consideration of reactor materials. Finally, it is important to consider the relative concentration of base to limit the hydration of the product, while enabling the decarboxylation and dehydration of the precursor.

At this point, a decision was made to re-focus the project on the possibility of extracting the acrylic acid product from the exit solutions. A series of experiments to assess the affinity of acrylic acid towards various organic solvents of varying polarities was conducted and is described in the next section.

Acrylic Acid Extraction

The selective extraction of carboxylic acids into organic solvents has been previously shown[72, 114-118] and the extraction of MAA has been discussed in detail by Huddle.[72] The extraction of carboxylic acids into an organic phase is facilitated by the formation of hydrogen bonds between two molecules, as shown in Figure 3.18. When the resulting dimers exhibit aliphatic pendant groups, such as MAA, the dimers will easily dissolve in organic solvents. Hence, while MAA exhibits good water solubility (89 g L^{-1} at 25 °C),[119] its ability to form such hydrophobic dimers allow for extraction into organic solvents.[120] Unlike the hydrogen bonded MAA molecules, unreacted precursors and other acids in the solutions, exhibit hydrophilic

pendant groups that allow for simple and selective extraction of MAA into a non-polar solvent, such as toluene.

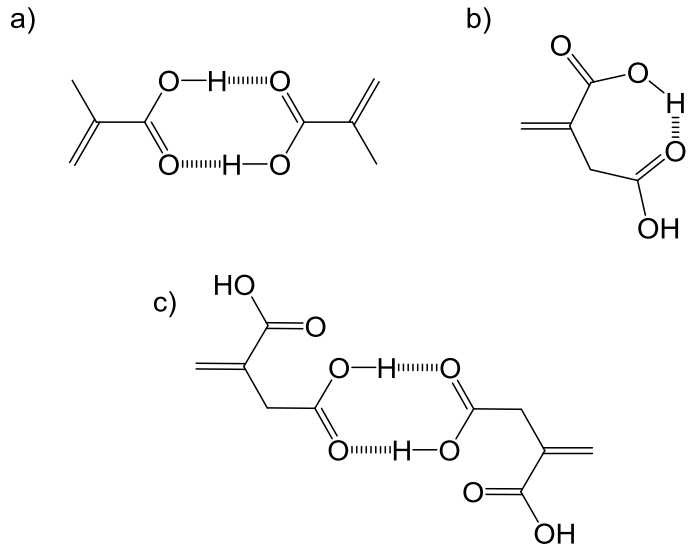


Figure 3.18 Showing the inter- and intramolecular hydrogen bonding between a) two molecules of MAA, b) a single IC molecule and c) two IC molecules. The MAA dimer exhibits aliphatic end groups, while the hydrogen bonded molecules of IC retain their hydrophilic pendant groups

It was therefore hypothesised that a similar effect may be seen with acrylic acid molecules. Although the removal of a methyl group may affect the affinity the molecule has towards an organic phase, by testing solvents with a variety of dielectric constants, it might be possible to achieve selective extraction of acrylic acid with simple liquid-liquid extraction. Hence, an initial experiment was designed to investigate the possibility of replicating Huddle's method for MAA extraction with an acrylic acid solution.

Experiments in this section were conducted by Miss Ailsa Suleman; however, all analysis and conclusions are original to this thesis.

Experiment 9 - Investigating the effect of concentration on the extraction of acrylic acid

Five solutions of varying concentrations were made up and shaken with an equal volume of toluene to simulate earlier extraction experiments conducted by Huddle.[72] The percentage of acrylic acid removed from each solution was calculated and is shown in Figure 3.19.

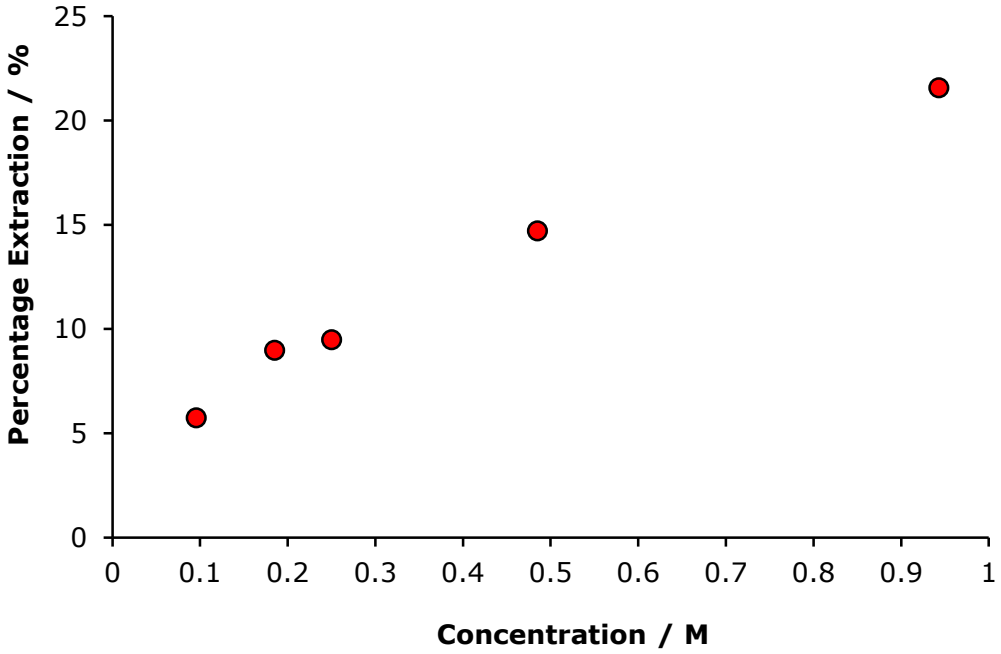


Figure 3.19 The percentage extractions of acrylic acid solutions of varying concentrations are shown. As the concentration of the aqueous acid increases, the amount of acrylic acid extracted into toluene after a single phase separation increases linearly.

A non-linear relationship can be seen between the initial concentration of acrylic acid and the percentage extracted with toluene. Huddle described a dependence of the percentage extraction on the initial concentration of MAA and results taken from Huddle's thesis, seen in Figure 3.20, show a curve, beginning to level off above 0.5 M.

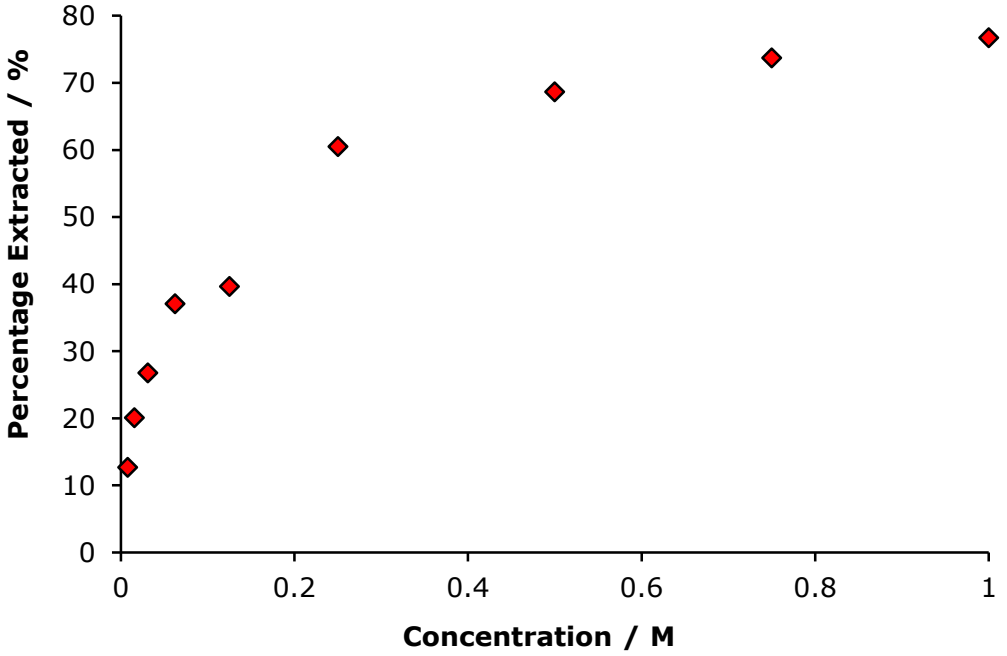


Figure 3.20 The percentage extractions of MAA solutions of varying concentrations were calculated by Huddle.[72] As the concentration of the aqueous MAA increases, the amount of the acid extracted into toluene after a single phase separation increases before levelling off above 0.5 M.

Huddle suggested that the extraction was proportional to the concentration of MAA squared, while our results show a linear relationship between the percentage extraction of acrylic acid and the concentration in aqueous solution. There is also a much lower percentage extraction achieved with acrylic acid than found for MAA by Huddle. The results clearly indicate that the loss of a terminal methyl group does affect the extraction of the acid into polar solvents. If the concentration of acrylic acid was increased above those used in our experiment, the linearity of the plot would be expected to give way to a plateau.

It was hypothesised that a higher percentage extraction could be achieved with multiple separations. Hence, an experiment was designed to test this by carrying out ten consecutive separations, using a new aliquot of toluene for each, on three aqueous solutions of varying acrylic acid concentrations.

Experiment 10 - Investigating the effect of multiple separations on the extraction of acrylic acid into toluene

Three solutions of acrylic acid (0.5 M, 0.25 M and 0.1 M) were used to investigate the effect of multiple extractions on the accumulative percentage extraction of the acid into toluene. After each separation an aliquot of the aqueous solution was collected for HPLC-RID analysis. The amount of fresh toluene used was adjusted with each extraction to ensure equal volumes of the two phases were mixed.

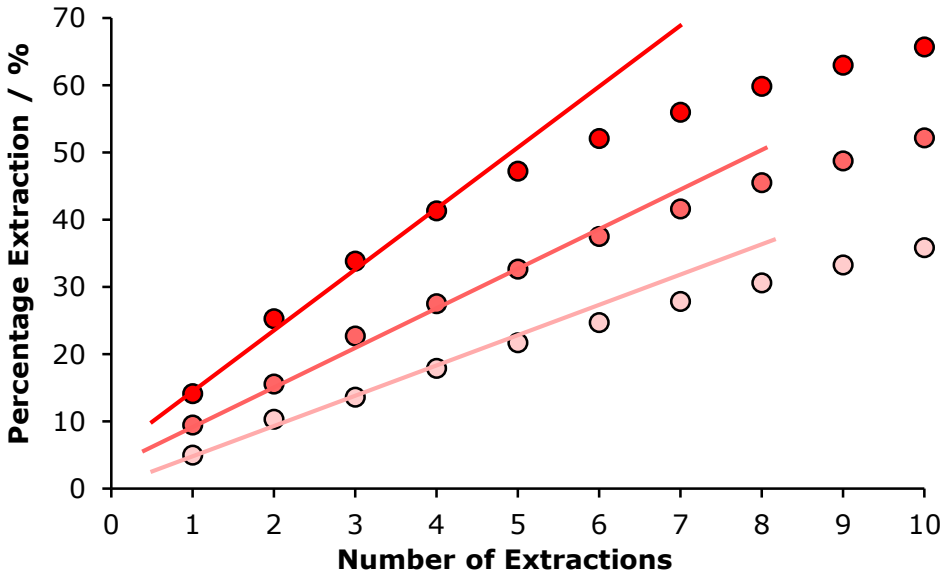


Figure 3.21 The amount of acrylic acid extracted from three different solutions with concentrations of 0.5 M (●), 0.25 M (●) and 0.1 M (●) is shown above. Each solution underwent ten consecutive extractions with toluene to show how increasing the number of separations can increase the yield of acrylic acid separated from an aqueous solution. Straight lines have been plotted to highlight the curves displayed by each concentration.

Figure 3.21 displays the results of this experiment, showing that, for each solution, the more extractions performed, the more acrylic acid was removed. In fact, 65.8 % of the acrylic acid could be removed from the most concentrated solution after 10 extractions. The plot shows greater amounts of acrylic acid were extracted from the most concentrated

solution and all three solutions present curves as the percentage of acrylic acid decreased with sequential extractions. As the partition coefficient is dependent on the concentration of the solute, it is expected that as more acrylic acid is removed from the aqueous solution, subsequent extractions will be reduced.

As the overall aim of this research is to explore the possibility of producing acrylic acid by the methods discussed in this chapter, it is important to consider the cost of multiple extractions in a process. While it may be possible to recycle the solvent after recovering the acid from the organic solution, increasing the number of extractions will increase the energetic and economic costs of the process. It may be possible to introduce a continuous flow counter-current extraction system to reduce the costs, but for the purposes of our research, a maximum of five batch extractions will be considered before the cost of further separations would outweigh the gain of further product recovery.

Once the extraction into toluene had proved successful but low yielding, it was decided that the focus should shift to finding a more effective solvent system. We chose a selection of organic solvents with varying dielectric constants that could be used in our batch extraction method.

Experiment 11 - Investigating the effect of solvent on the extraction of acrylic acid

Three different solvents were chosen to carry out single extractions from three aqueous solutions of acrylic acid (0.5 M, 0.25 M and 0.1 M). Figure 3.22 shows the results of the extractions with 1-octanol, dichloromethane (DCM) and cyclohexane alongside results taken from Figure 3.19 for reference.

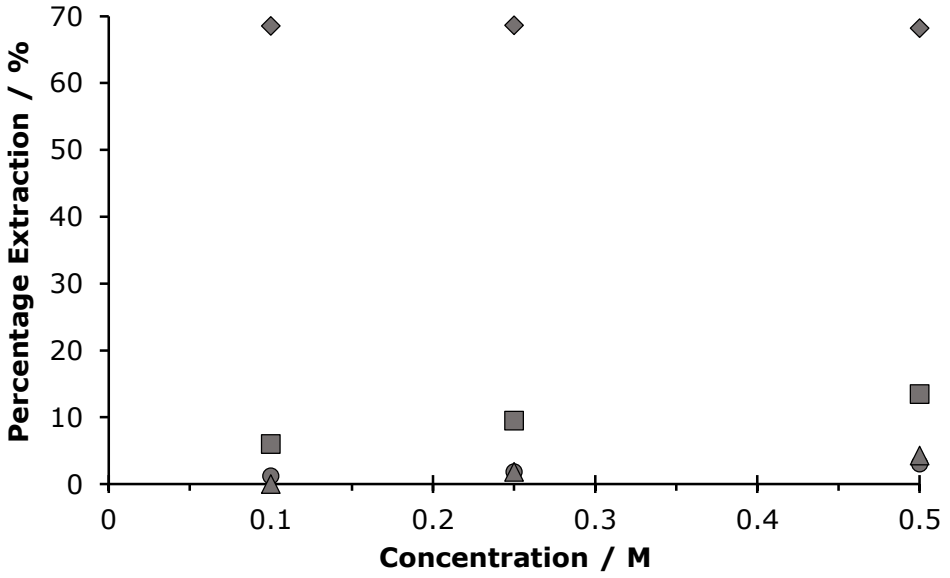


Figure 3.22 The percentage extraction of acrylic acid from three aqueous solutions is shown for three solvents, 1-octanol (◆), dichloromethane (DCM) (●) and cyclohexane (▲). The percentage extraction with toluene (■) has been plotted for reference.

The results show that while cyclohexane and DCM exhibit higher dielectric constants than toluene (Table 3.11) and so are more polar solvents than toluene, their ability to extract acrylic acid is in fact considerably lower. It may initially seem surprising then that 1-octanol, with a higher dielectric constant than the other solvents used, displayed a consistently high percentage extraction (68 %), independent of the acrylic acid concentration.

Table 3.11 The dielectric constants of the solvents used in acrylic acid extractions are compared to water.

Solvent	Dielectric constant[121]
Water	80.0
1-octanol	10.3
DCM	8.93
Cyclohexane	2.02
Toluene	2.38

However, research conducted by Wasewar *et al.* suggested that alcohols are very effective as extraction solvents for acids due to their ability to form hydrogen bonds to the acidic groups.[116] It should therefore be of no surprise that the extraction no longer relies on the concentration of acrylic acid as it does not depend solely on the formation of dimers and may extract the free acid monomers as well as dimers.

As 1-octanol showed such a high level of extraction for each aqueous solution after one separation, the next step was to investigate the maximum acrylic acid that could be removed with multiple serial extractions.

Experiment 12 - Investigating the effect of multiple separations on the extraction of acrylic acid into 1-octanol

This experiment was designed to show the percentage of acrylic acid that could be extracted into 1-octanol with ten successive separations. It was noted that after ten separations with toluene, a maximum 65.7 % was extracted, slightly lower than the amount removed with one separation using 1-octanol. Hence, it was expected that the serial extractions with 1-octanol could yield higher levels of extracted acrylic acid than had been achieved with toluene.

Figure 3.23 shows once more that the concentration of the original solution has no overall effect on the amount of acrylic acid. However, by

performing just four serial extractions, it is possible to extract 100 % of the acrylic acid in the aqueous solution. Each of the remaining aqueous solutions contained very little trace of acrylic acid (< 0.1 %) after four extractions.

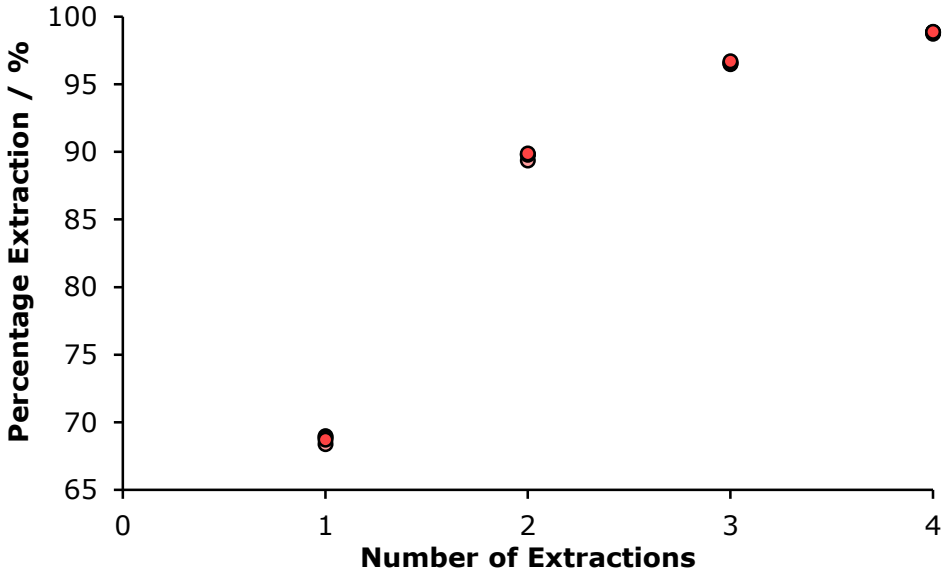


Figure 3.23 Five acrylic acid solutions were made up of concentrations equal to 0.5 M (●), 0.4 M (●), 0.3 M (●), 0.2 M (●) and 0.1 M (○). Individual points overlap on this plot, making it difficult to distinguish between the different concentrations. The plot shows the overall percentage extraction of acrylic acid after four serial extractions with 1-octanol, reaching 100 % after the fourth separation.

These results suggest that 1-octanol could be a very successful extraction solvent for acrylic acid. Therefore an experiment to test the selectivity of the extraction from an exit solution of the decarboxylation of malic acid was designed and is discussed below.

Experiment 13 - Investigating the selectivity of 1-octanol as an extraction solvent

A malic acid solution was run through the rig using the conditions specified in

Table 3.12. Table 3.13 displays the concentrations of various acidic components that were measured in the exit solution. Once this solution had been acidified with sulfuric acid to release the free acids, five serial extractions with 1-octanol were carried out.

Table 3.12 Showing the reaction conditions used in Experiment 13.

Experiment 13 Malic Acid Decarboxylation	
Precursor	0.514 M Malic Acid
Base	0.250 M NaOH
Temperature	250 °C
Pressure	3000 psi
Residence Time	300 s

Table 3.13 Showing the products of the decarboxylation of malic acid

Acid	Concentration / M
Acrylic Acid	0.095
Malic Acid	0.223
Maleic Acid	0.107
Fumaric Acid	0.071
Lactic Acid	0.018

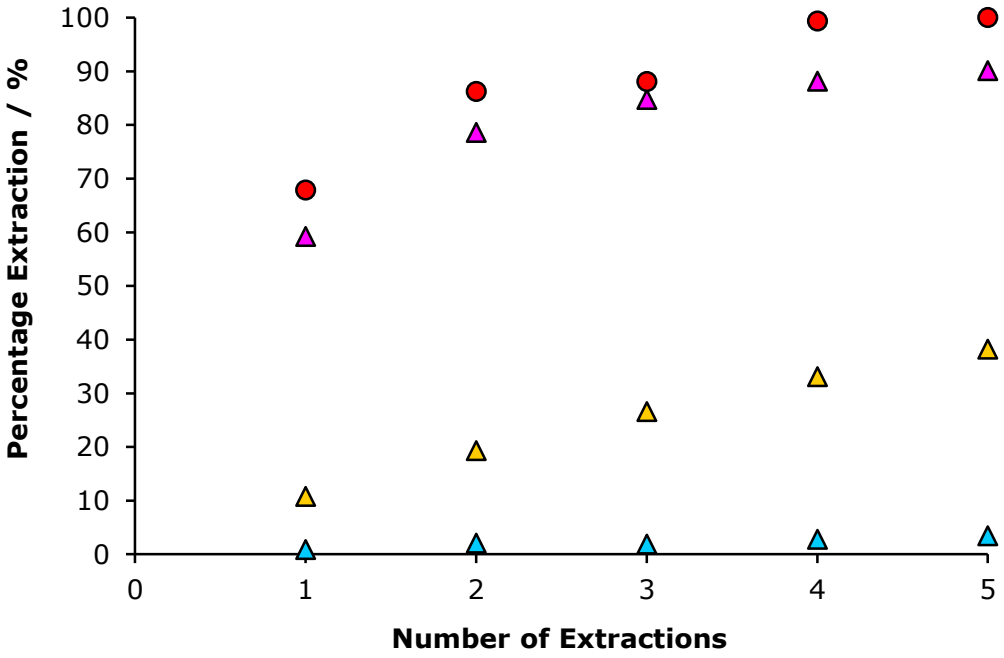


Figure 3.24 The plot shows that high levels of acrylic acid (●) are extracted with 1-octanol and after 4 serial extractions, 99.3 % of the acid has been removed from the aqueous solution. Fumaric acid (▲) is also extracted effectively, with 90.1 % extracted after 5 separations. Maleic acid (▲) shows less affinity for the solvent, while only a 3.4 % malic acid (▲) is extracted.

Although the long aliphatic tail allows 1-octanol to extract hydrophobic acrylic acid dimers, the hydroxyl group present can form hydrogen bonds with hydrophilic pendant groups (including –COOH) on each acid present. This enables 1-octanol to act as an extraction solvent for each of the acids shown in the plot. Although malic acid may be expected to be extracted into 1-octanol, the presence of an extra hydrogen bonding site means it retains its higher affinity for the aqueous phase.

Therefore, while 1-octanol provides a very efficient method for the extraction of acrylic acid, it has proved to be an unselective process. Other solvents may be more selective, but are not as efficient and so a new method for extraction would be required in the design of a process to separate acrylic acid from the aqueous mixtures.

Summary

The first part of this chapter showed that acrylic acid can be made from malic acid in high temperature, high pressure water. However, the selectivity of this process is similar to the analogous conversion of CM to MAA, which yields high levels of by-products. These large number of by-products found in exit solutions mean the process is lower yielding than the suggested decarboxylations of IC and its isomers shown by Antal[67] and Huddle[72] to yield MAA.

It was found that acrylic acid was reasonably stable under the conditions used to decarboxylate and dehydrate malic acid; but at high temperatures and long residence times, there is a drop in mass balance suggesting gaseous and volatile by-products are formed.

While 1-octanol offered an efficient route to extracting acrylic acid, it is unselective, extracting all other acidic components from aqueous solutions. We failed to identify a solvent that proved both selective and effective for acrylic acid extraction in this chapter and further work would be needed to find a new extraction method.

It has not been possible in this research to find a suitable, competitive method for the production and extraction of acrylic acid. The results in this chapter show the process had not been developed enough to be industrially competitive and with other routes to bio-acrylic acid already possible, it was decided that further work into this area should be halted and the focus of the project moved towards refining a route to continuous MAA production.

Chapter 4 - Methacrylic Acid Stability

As the focus of the project shifted towards refining the conditions for an industrially viable process for bio-MAA production, previous work by Huddle was examined. The work carried out by Huddle and associates had investigated the conversion of various di- and tri-carboxylic acids to MAA, but had not looked at the effects of these conditions on the MAA product.

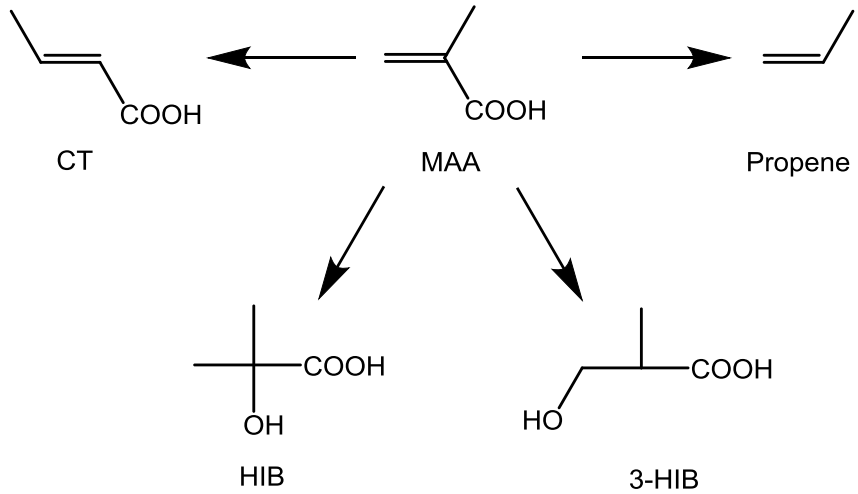


Figure 4.1 Showing the main decomposition routes of MAA, the decarboxylation to propene as suggested by Carlsson,[67] the methyl migration suggested by Huddle[72] and Chapman[70] and the hydration to both the Markovnikov (HIB) and anti-Markovnikov (3-HIB) products.

From Huddle's[72] and earlier work,[67] it is known that at elevated temperatures, MC, CC and IC reach equilibrium quickly and that these isomers decarboxylate to form MAA. It is also known that under such conditions MAA can easily be hydrated to form HIB. However, little is known about other routes of MAA decomposition. Carlsson *et al*. suggested a pathway for MAA to decompose to propene,[67] while other research has shown the possibility of a methyl migration step to form crotonic acid (CT).[70, 72] Later in this chapter, we will also discuss the formation of 3-hydroxyisobutyric acid (3-HIB) as the anti-Markovnikov product of MAA hydration.

Although it is possible to extract HIB and dehydrate the acid to form MAA, many other by-products of the reaction can be classed as carbon sinks. These by-products are not useful to the process and cannot be refined to yield MAA so must be disposed of.

Limited research into the stability of MAA has been previously reported within our research group.[70] Using a continuous flow rig, similar to the one seen in Figure 2.3, MAA was studied under a constant pressure of 5070 psi, temperatures of 250 – 400 °C and an MAA : NaOH ratio of 50 : 1.

Table 4.1 Showing the conditions used by Chapman in his first MAA decomposition study.[70]

MAA Decomposition	
Precursor	0.5 M MAA
Base	10 mM NaOH
Temperature	250 – 350 °C
Pressure	5070 psi
Residence Time	30 s

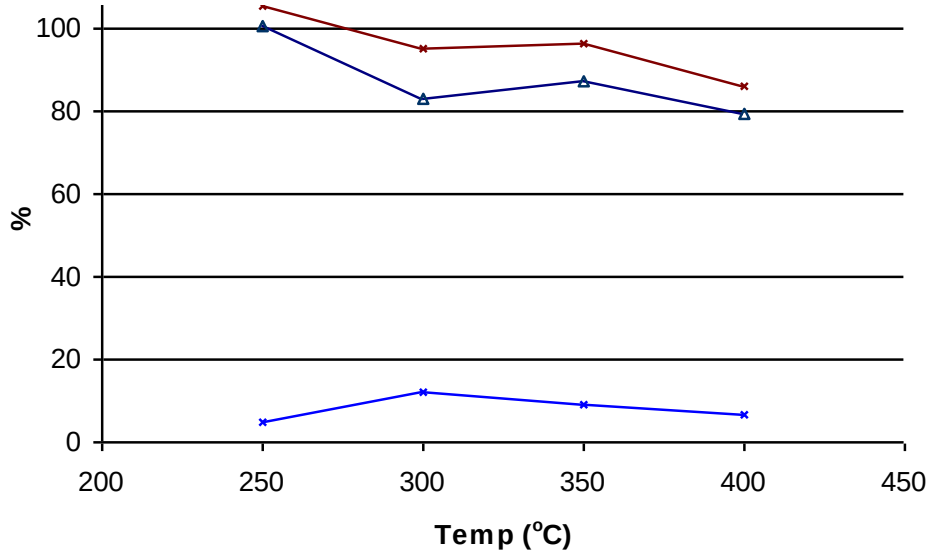


Figure 4.2 The plot shows the composition of the exit solutions collected by Chapman[70] at various temperatures (250 – 400 °C). As the temperature is increased, the concentration of MAA (—△—) shows a general decrease. The plot confirms the conversion of MAA to HIB (—×—) in the presence of NaOH and shows the decreases in mass balance (—×—) as the temperature is increased.

It was reported that at ambient temperature and a pressure of 5070 psi, there was no loss of mass balance, indicating MAA is not affected by pressure. However, Figure 4.2 shows that at elevated temperatures, there was a noticeable decrease in MAA yield. It was reported that conversion of MAA to HIB was occurring; however, the plot also shows a decrease in the overall mass balance, indicating the occurrence of unobserved parasitic reactions to unobserved by-products.

Chapman then investigated the effect of the residence time on the solution composition, after increasing the concentration of sodium hydroxide to 0.1 M. Figure 4.3 shows the results of this investigation and the conditions can be seen in Table 4.2.

Table 4.2 Showing the conditions used by Chapman in a further MAA decomposition study.[70]

MAA Decomposition	
Precursor	0.5 M MAA
Base	0.1 M NaOH
Temperature	360 °C
Pressure	5070 psi
Residence Time	Variable

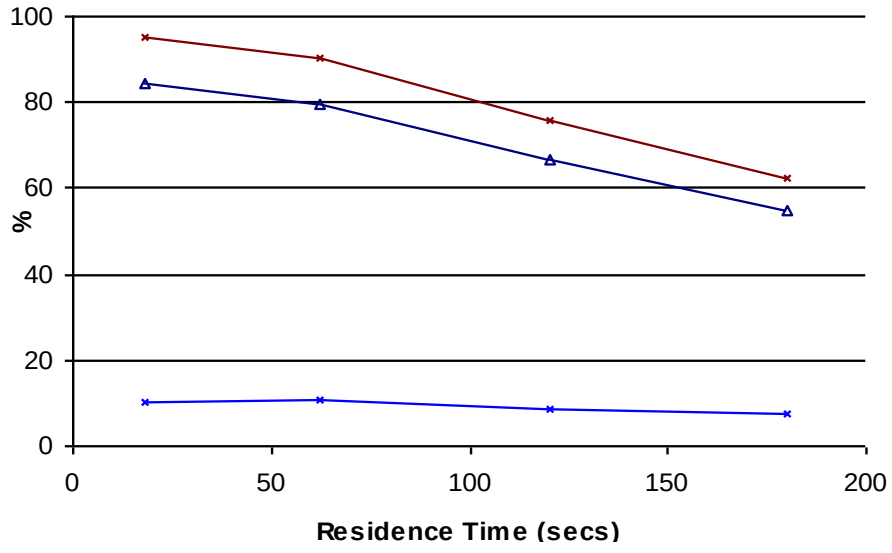


Figure 4.3 The decomposition of MAA (—△—) increases with residence time, while the mass balance (—×—) decreases. The conversion of MAA to HIB (—×—) does not appear to be affected by residence time.

It is difficult to understand the effects of the increased base concentration due to the different temperatures and residence times used in the two studies shown above. However, one can see that an increase in residence time correlates with a decrease in the MAA concentration. The plot shows the conversion of MAA to HIB remains reasonably consistent at all residence times. With the hydration yielding a steady level of HIB and a decrease in MAA concentration, the mass balance falls away at longer residence times.

While carrying out his investigation into the stability of MAA in high temperature and high pressure water, Chapman conducted a short experiment to look at the decomposition of CT. He noted that a potential cause of mass loss in IC decarboxylation reactions was the conversion of the CC isomer to CT and further decomposition of CT. In order to investigate decomposition pathways, Chapman replaced MAA with CT and used similar conditions to those reported above.

Table 4.3 Showing the conditions used by Chapman in a CT decomposition study.[70]

CT Decomposition	
Precursor	0.5 M CT
Base	0.1 M NaOH
Temperature	360 °C
Pressure	5070 psi
Residence Time	Variable

Rather interestingly, Chapman noted the presence of MAA in the exit streams by HPLC-UV. He reported that there was little chance for contamination during the reaction and there was no contamination in the starting material; however, the investigation was not taken further.

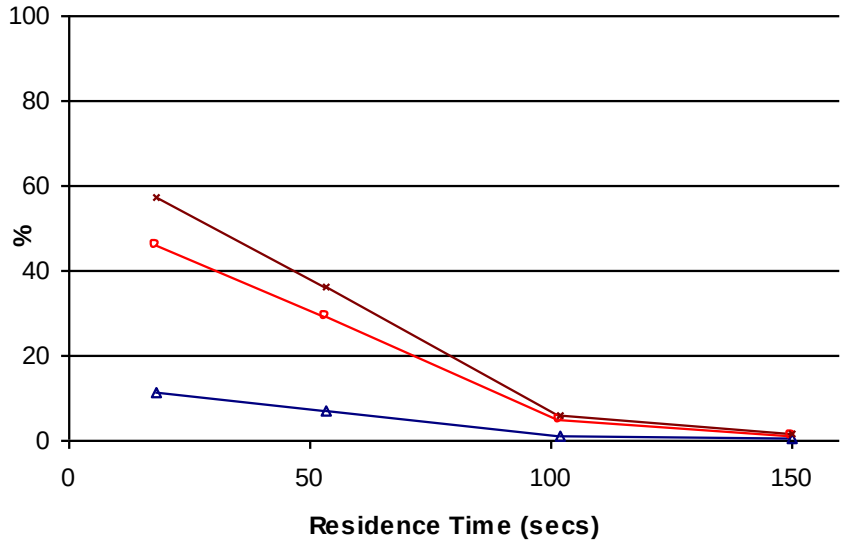


Figure 4.4 Work by Chapman[70] shows the decomposition of CT (—○—) increases with residence time, showing much greater levels of decomposition than MAA displayed in the previous investigation. The mass balance (—×—) is also much lower than shown in previous plots. Traces of MAA (—△—) were detected despite careful precautions to avoid contamination.

With only limited research into the stability of MAA at conditions recommended by Huddle[72] for the decarboxylation of IC, it was clear that a new study including our newly acquired analytical techniques was needed for a more complete investigation.

Strategy

Aim - ***Limited prior work has been carried out on the thermal decomposition of MAA; thus an investigation into the stability of MAA at the conditions likely to be used in the process is imperative to the research. By determining the stability of the product at a range of temperatures, residence times and concentrations of both acid precursor and base, I will be able to suggest a viable working range for the process.***

This investigation was split into three sections to investigate the effects of temperature, residence time and concentration on the stability of MAA. First of all the effect of the reactor temperature was studied. A range of 180 – 300 °C was selected to lie within the range of temperatures investigated by Huddle when looking into the decarboxylation of IC.[72]

Next, the effect of residence time was examined at both a high temperature (300 °C) and a mid-range temperature (260 °C) that was shown to cause little decomposition of MAA in the earlier temperature study. The full range of flow rates that could be achieved with the rig set up corresponded to a residence time range of 60 – 600 s. Further to this, the effect of concentration of both the acid and base were examined at a range of temperatures (200 - 300 °C).

During this research, the presence of an unknown peak in HPLC traces sparked a new investigation into the nature of this molecule. After a thorough investigation using ^{1}H and ^{13}C NMR techniques, the nature of this molecule has been confirmed as the anti-Markovnikov hydration product of MAA, 3-HIB.

Finally the stability of the Markovnikov hydration product, HIB, was examined at a range of temperatures and residence times and the data

collated in this chapter resulted in a clearly defined set of suggested conditions, which would limit the decomposition of MAA and HIB products.

Results and Discussion

MAA Stability

Experiment 14 - Investigating the Effect of Temperature

The first collection of experiments described in this chapter was designed to investigate the effect of temperature on the decomposition of MAA. Each experiment was designed to investigate the presence of decomposition products of MAA across a range of temperatures, previously used to study the formation of MAA from polycarboxylic acid precursors,[67, 69, 71-74] and was repeated three times to ensure reliability of the results. While the decarboxylation of these polycarboxylic acids has been studied widely by Huddle, it is important to also consider the decomposition of MAA at these conditions. Huddle noted a drop in mass balances at high temperatures which could be due to the decomposition of MAA into gaseous and other undetected products.

The conditions of Experiment 14 are shown below in Table 4.4. The flow rates were modified during three repeated experiments to maintain a constant residence time as the temperature of the reactor was changed (calculated using Equation 2.3).

Table 4.4 Conditions used during investigations into the effect of temperature on the stability of MAA molecules in a basic solution.

Experiment 14 MAA Temperature Study	
Precursor	0.510 M MAA
Base	0.500 M NaOH
Temperature	180 - 300 °C
Pressure	3000 psi
Residence time	300 s
Number of repeats	3

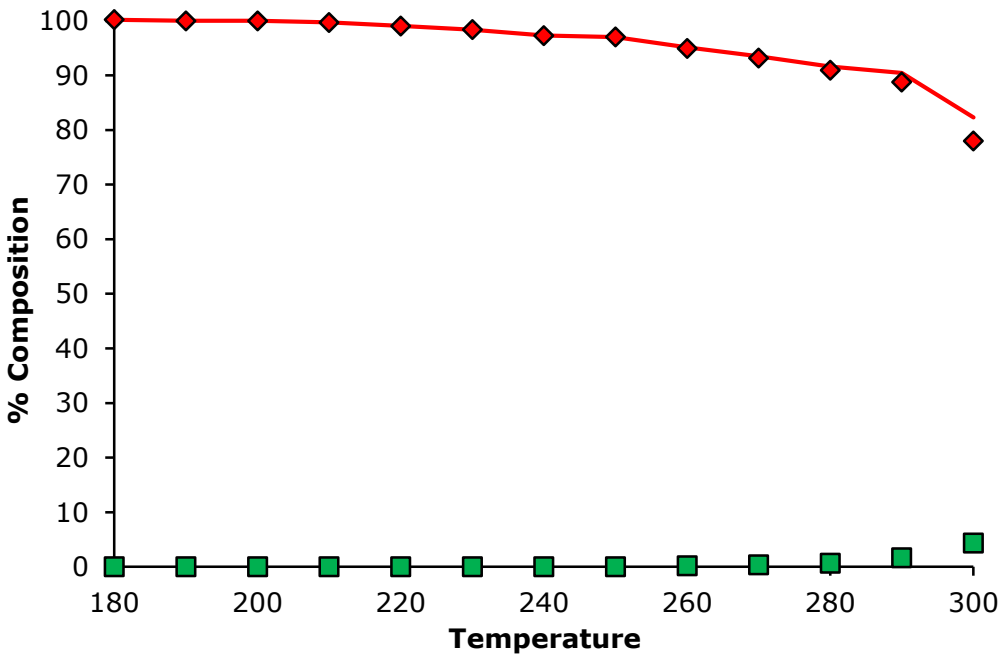


Figure 4.5 The percentage composition of both MAA (◆) and HIB (■) in the exit solutions are shown above. The mass balance (—) of these acids can be seen to have decreased at higher temperatures.

The results in Figure 4.5 show an increase in the decomposition of MAA with temperature. At temperatures above 250 °C, a hydration reaction of MAA yields low levels of HIB. The production of HIB increases with temperature up to 4.3 % at 300 °C. The results suggest that higher temperatures facilitate the conversion of MAA into HIB and other products in the continuous flow rig.

Colleagues at Lucite International indicated that below 5 % decomposition of MAA would be acceptable in an industrially viable process. With this in mind, closer inspection of Figure 4.5 indicates that a reaction temperature between 180 and 260 °C would fall within a suitable range and ensure less than the recommended level of decomposition of the final product.

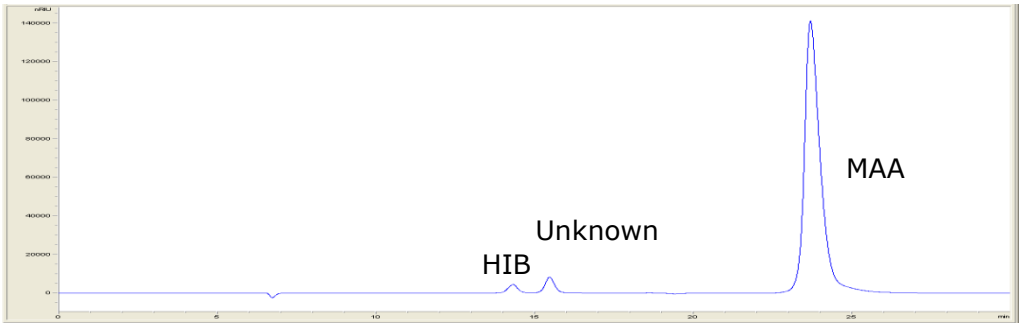


Figure 4.6 The HPLC-RID trace above shows the presence of three distinct peaks, HIB, MAA and a third, previously undiscovered peak.

While it is expected that this decomposition will yield some gaseous products that were not collected, a third peak can be seen in the HPLC-RID trace shown in Figure 4.6. This peak did not correspond to any of the acids that were known to be related to MAA and was not detectable in the HPLC-UV trace for the same sample. Hence, it would have gone unnoticed by Huddle and may count towards some of the apparent mass loss in some of Huddle's experiments.[72] The nature of this peak was investigated and will be discussed in detail later in this chapter.

Meanwhile, after exploring the effect of temperature on the stability of MAA, we focused on two temperatures, (300 and 260 °C). The higher of these temperatures was selected in order to enhance the level of decomposition of the MAA and aid in the investigation into the nature of a third peak in HPLC-RID traces.

Experiment 15 - Investigating the Effect of Residence Time

The previous experiment showed that the highest level of decomposition was reached at 300 °C and a third HPLC-RID peak appeared in the trace of this exit solution. In order to examine the effect of the residence time on MAA, a solution was made up and pumped into the rig according to the conditions shown in Table 4.5. It was hoped that at longer residence times,

the new peak would increase in area, indicating a greater concentration and aid in the identification of the new by-product.

Table 4.5 Conditions used during investigations into the effect of residence time on the stability of MAA molecules in a basic solution.

Experiment 15 MAA Residence Time Study	
Precursor	0.503 M MAA
Base	0.500 M NaOH
Temperature	300 °C
Pressure	3000 psi
Residence time	60 – 600 s
Number of repeats	3

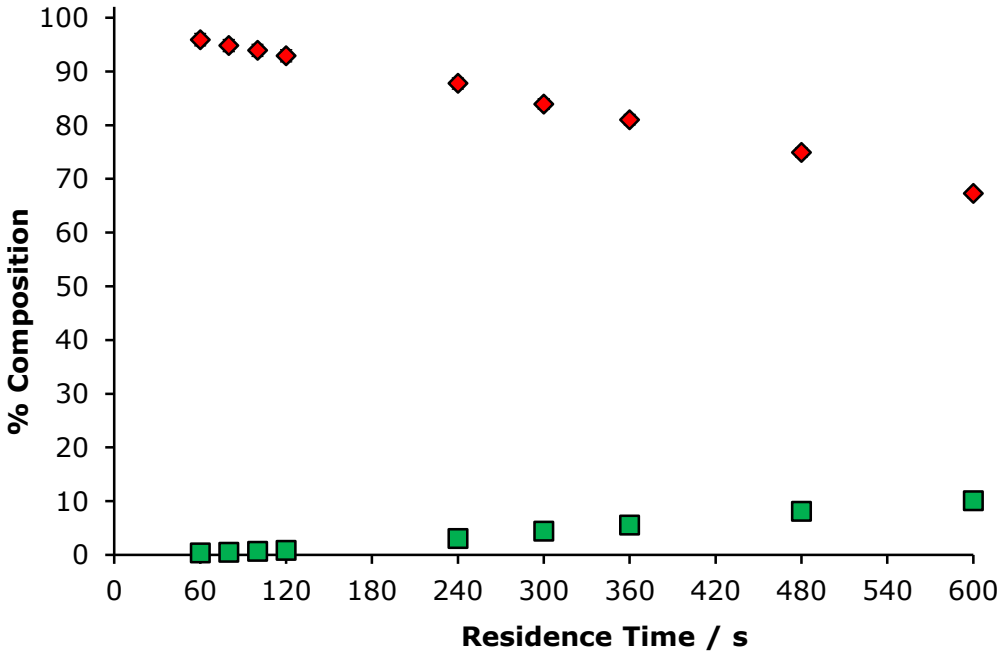


Figure 4.7 The percentage composition of both MAA (◆) and HIB (■) in the exit solutions are shown above. The mass balance of these acids can be seen to fall dramatically with increased residence time.

As can be seen from Figure 4.7, the level of MAA decomposition increases with increasing residence time. While the concentration of HIB also rises in progressive exit solutions, the concentration does not account for the amount of decomposed MAA. Hence, there must be other decomposition routes possible.

As already mentioned, a third peak was present in some HPLC-RID traces that corresponded to a previously unknown by-product of MAA

decomposition. The area of this peak did also increase with increased residence time. In order to understand the nature of this by-product, attempts were made to purify a sample and further analysis was carried out.

Experiment 16 - Investigating the Nature of a By-Product

The presence of a third peak in HPLC-RID traces indicated the presence of a previously unknown, non-volatile by-product of MAA decomposition. In order to carry out an investigation into the nature of this by-product, a solution was collected after a precursor solution was pumped through the rig under the conditions shown in Table 4.6.

Table 4.6 Conditions used during investigations into the nature of a decomposition by-product.

Experiment 16 By-product Investigation	
Precursor	0.500 M MAA
Base	0.500 M NaOH
Temperature	300 °C
Pressure	3000 psi
Residence time	300 s

The resulting solution was acidified with sulfuric acid (0.125 mol) and MAA was removed from the solution with toluene. Analysis of the remaining aqueous solution with ^{1}H NMR showed the following peaks: δ_H(300 MHz; D_2O, MeOH) 0.97 (3 H, d, *J* = 7.09, Me), 2.54 (1 H, m, CH) and 3.54 (2 H, d, *J* = 6.28, CH_2).

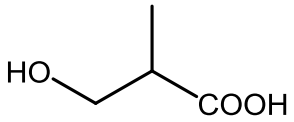


Figure 4.8 The anti-Markovnikov MAA hydration product is shown above.

It was hypothesised that the by-product might be the anti-Markovnikov hydration product of MAA, 3-HIB, seen in Figure 4.8. A sample of 3-HIB, synthesised by colleagues at Lucite International, was analysed with HPLC-

RID and eluted at the same time as the unknown peak in previous traces, increasing our confidence in the nature of the by-product as 3-HIB.

While a crude sample of 3-HIB was produced for the comparison of ^{1}H spectra and HPLC traces, it was not possible to purify the sample to an acceptable level to be used in the calibration of the HPLC. Hence, it was determined that the peak eluting at 15.5 min corresponded to the presence of 3-HIB qualitatively only.

Meanwhile, efforts to suggest a working limit on the temperatures and residence times used to produce MAA from IC and other carboxylic acid precursors continued with a further residence time study at the maximum suggested temperature, 260 °C.

Experiment 17 - Investigating the Effect of Residence Time

Table 4.7 Conditions used during investigations into the effect of residence time on the stability of MAA molecules in a basic solution.

Experiment 17 MAA Residence Time Study	
Precursor	0.515 M MAA
Base	0.500 M NaOH
Temperature	260 °C
Pressure	3000 psi
Residence time	60 – 600 s
Number of repeats	3

At this lower temperature, it was anticipated that there would be a lower rate of hydration to both products, HIB and 3-HIB. A starting solution was pumped through the rig at the conditions indicated in Table 4.7. We have previously shown in this thesis that acrylic acid can be hydrated in the presence of base, despite the more common hydration pathway requiring acidic conditions. During the decarboxylation of IC, MAA is produced in its ionic state along with other by-products of the reaction in the presence of a base. Hence it is important to understand the effect the base has on the stability of MAA.

Figure 4.9 shows that while there is still an increase in MAA decomposition with longer residence times, there is a much gentler gradient than displayed at the higher temperature seen in Figure 4.7. There is also a much lower concentration of HIB produced, with just 0.001 M (0.23 %) being observed after 600 s in the reactor.

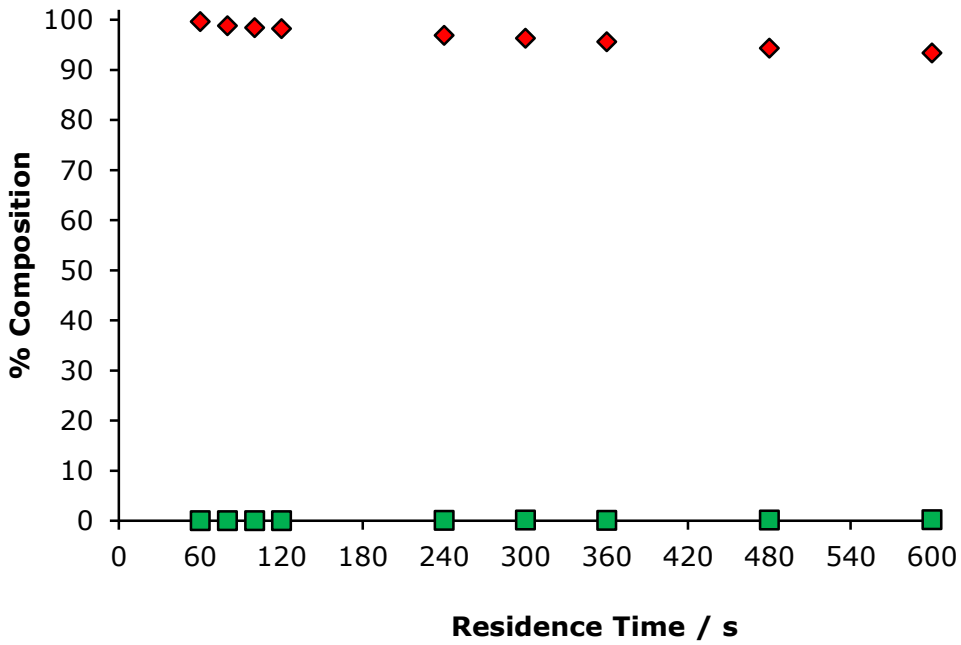


Figure 4.9 The percentage composition of both MAA (◆) and HIB (■) in the exit solutions are shown above. The mass balance of these acids remains above 90 % at all residence times investigated.

In fact, following the guidelines set by Lucite International, Figure 4.7 shows that at 300 °C only a residence time of 60 s would be suitable for decarboxylation reactions yielding MAA. However, by reducing the reactor temperature to 260 °C, residence times up to 360 s could be used.

Previous work indicated that the decarboxylation of IC was most efficient when equimolar amounts of sodium hydroxide were used and the mono-itaconate ion was present.[69, 72] However, little was known of the effect of base on the stability of MAA. In order to investigate these conditions on the decomposition of MAA, an experiment was designed to

vary first the concentration of MAA in solution and subsequently the concentration of base used.

Experiment 18 - Investigating the Effect of Relative Concentration of MAA

We have previously shown in this thesis that acrylic acid is hydrated in the presence of a base, despite the more common hydration pathway requiring acidic conditions. During the decarboxylation of IC, MAA is produced in its ionic state along with other by-products of the reaction in the presence of a base. Hence it is important to understand the effect of the presence of a base on the stability of MAA being produced.

Table 4.8 Conditions used during investigations into the effect of residence time on the stability of MAA molecules in a basic solution.

Experiment 18 MAA Concentration Study	
Precursor	Variable M MAA
Base	0.500 M NaOH
Temperature	Variable
Pressure	3000 psi
Residence time	300 s

Unlike acrylic acid, Figure 4.10 shows that MAA undergoes hydration to a greater extent when MAA is in excess over sodium hydroxide. Conversely, it can be seen that when 0.5 M and 0.25 M MAA solutions were used, hydration to HIB only occurs at temperatures above 260 °C and a maximum of 4.4 % HIB produced. This indicates that the presence of a base actually prevents the hydration of MAA to HIB.

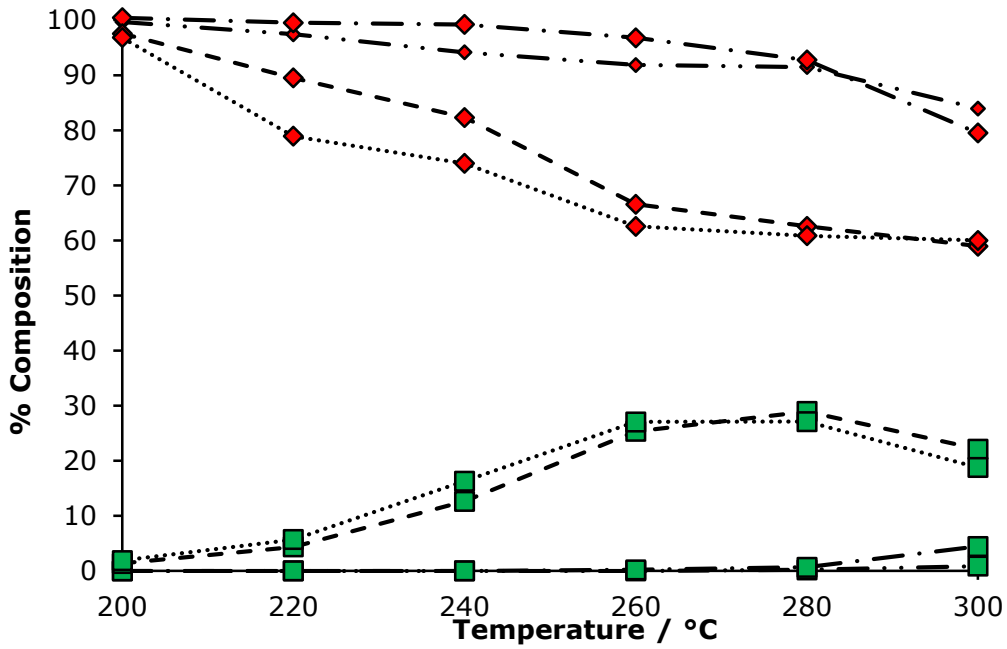


Figure 4.10 The percentage composition of both MAA (◆) and HIB (■) in the exit solutions are shown above. The plot shows the results of four different reactions when the amount of MAA used was varied but the amount of sodium hydroxide remained the same. When the amount of MAA exceeded the concentration of base (1.0 M (····) and 0.75 M (– – –)) the decomposition of MAA is high and the level of hydration yields high relative concentrations of HIB. However, when the concentration of MAA is decreased to 0.5M (— · —), HIB is only present above 240 °C and when the concentration of MAA is further decreased to 0.25 M (—— · ·) hydration only occurs at 280 and 300 °C.

The plot also shows a high level of decomposition to other products when MAA is in excess. Despite the presence of 3-HIB in these exit solutions, it was not possible to quantify this and so it is not clear how much of this decomposition was due to the production of volatile by-products, such as the decarboxylation product, propene.

Following on from these results, solutions were made to study the effect of varying the concentration of base while maintaining a constant concentration of MAA.

Experiment 19 - Investigating the Effect of Relative Concentration of Sodium Hydroxide

Experiment 19 was designed to vary the concentration of sodium hydroxide, while keeping the concentration of MAA constant. In doing so, it was possible to examine the effect of relative concentration of base on the stability of MAA, while maintaining a high concentration of MAA that would allow thorough investigation.

Table 4.9 Conditions used during investigations into the effect of residence time on the stability of MAA molecules in a basic solution.

Experiment 19 NaOH Concentration Study	
Precursor	0.502 M MAA
Base	Variable M NaOH
Temperature	Variable °C
Pressure	3000 psi
Residence time	300 s

Figure 4.11 shows a general trend of increasing MAA decomposition for each concentration of base studied. When an equimolar amount of base was used the level of decomposition remained below 3.2 % up to 280 °C whereupon it increased to 9.2 %.

When an excess of base was used, the percentage of MAA in solution did not follow a general trend and varied between 96.9 % at 200 °C and 83.0 % at 300 °C. As this result does not fit any overall trends shown by other solutions in this experiment, it would be recommended that this result be discounted from any conclusions made about the effect of base concentration on MAA stability before further investigations were conducted.

The solutions with 0.00 and 0.25 M sodium hydroxide show an increased level of decomposition, including high levels of hydration to HIB. While these results suggest that hydration of MAA is a more facile process at low pH, they seem to contradict the findings shown in the previous chapter about the hydration of acrylic acid.

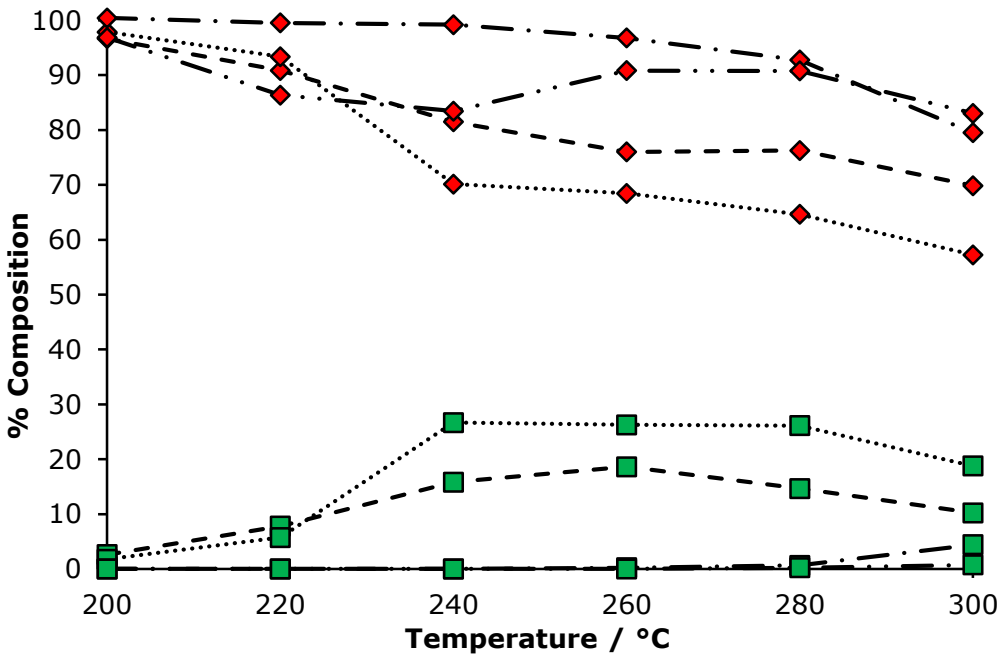


Figure 4.11 The percentage composition of both MAA (◆) and HIB (■) in various exit solutions are shown above. The plot shows the results of four different reactions when the amount of base catalyst used was varied. When an excess of base (1 M) was used (— · ·), the level of conversion to HIB is very low and HIB is only present at 280 and 300 °C. Using equimolar quantities of sodium hydroxide (— · —) yielded slightly higher concentrations of HIB but the amount of HIB was considerably greater when a half molar quantity of sodium hydroxide was used (– – –). The highest rate of conversion from MAA to HIB was achieved in the absence of a base (····) and correlated with the highest level of MAA decomposition.

Chapter 3 explains that the hydration of acrylic acid relies on basic conditions, while the results in this chapter suggest MAA relies on an acidic environment. This can be explained by looking closer at the mechanisms for each hydration, shown in Figure 4.12.

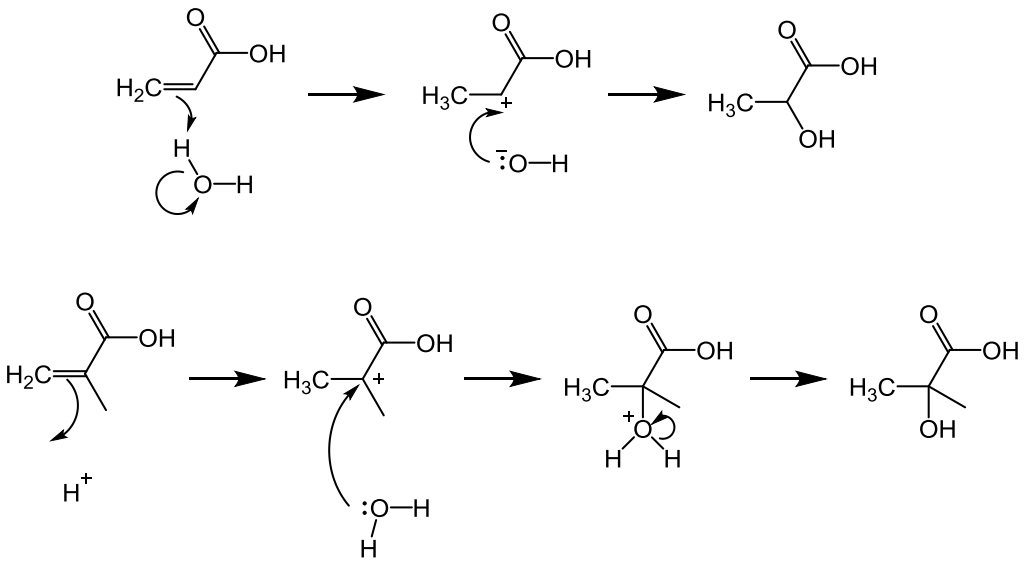


Figure 4.12 The two mechanisms showing the hydration of an acrylate ion and MAA are displayed above. It should be noted that the acrylate ion requires the presence of a base to activate the alkene, while MAA undergoes acid catalysed hydration.

The base catalysed hydration of acrylic acid, described in Chapter 3, occurs when the deactivating power of the –COOH group is dramatically reduced on addition of base. This allows the electrophilic addition to produce a stable carbocation. With the addition of a methyl group, the carbocation produced by MAA under acidic conditions is stabilised by the inductive effect from the methyl group and so MAA can undergo electrophilic addition as per the more traditional route of acid catalysed hydration in the absence of sodium hydroxide.

The results from these investigations suggest that equimolar or higher concentrations of sodium hydroxide offer the best conditions for MAA stability. Hence, it is our recommendation that **all decarboxylation reactions occur at temperatures below 260 °C and with residence times no longer than 360 s with equimolar sodium hydroxide.**

HIB Stability

It has been shown that the major decomposition product of MAA at elevated temperatures is the hydration to HIB and 3-HIB. While conditions have been suggested to reduce the formation of 3-HIB, HIB may still be formed (<5 %) within these guidelines. Hence, it is important to understand how to remove HIB and convert it to MAA.

The dehydration of tertiary alcohols is straight-forward through an E1 elimination mechanism, shown in Figure 4.13. With the use of a strong acid catalyst (commonly sulfuric acid) and gentle heating, the dehydration of HIB to MAA can easily be achieved.

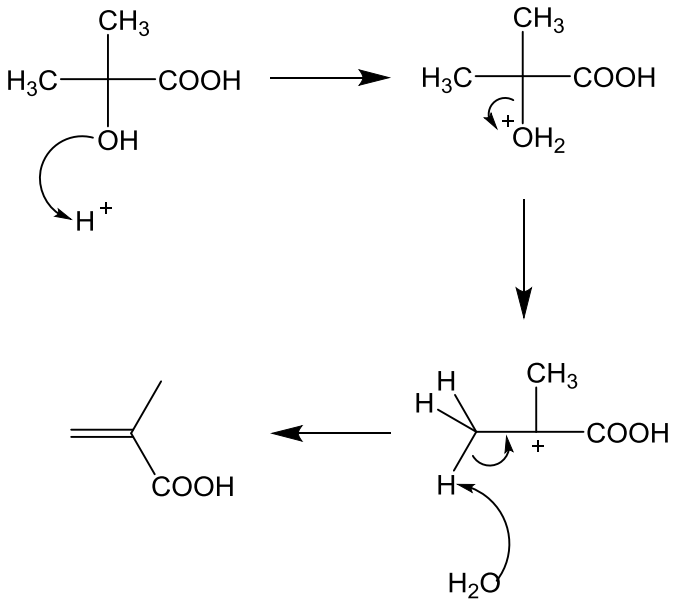


Figure 4.13 The dehydration of HIB to yield MAA is a straight forward E1 elimination using a strong acid catalyst.

The selective extraction of MAA will be discussed in depth in the next chapter and relies on the acidification of the exit solutions to free the desired acid from its ionic state. The use of strong acids to carry out this step could also aid the dehydration of HIB. Following the acidification, MAA can simply be removed with an organic solvent. By heating the acidified aqueous solution after extraction, a further crop of MAA could be achieved

with the dehydration of HIB. Once cooled, the aqueous solution could then be mixed with an organic solvent to remove this second crop. Since a higher yield of MAA depends on the stability of HIB under reaction conditions, a study into the effects of temperature, residence times and presence of base is also required.

During Huddle's experiments,[72] he found a maximum percentage composition of 30 % HIB in the exit solutions collected. Hence, in the following collection of experiments, a concentration of 0.150 M HIB was used under various conditions with equimolar base.

Experiment 20 - Investigating the Decomposition of HIB

The first experiment in this series investigated the effect of temperature on the stability of HIB. As we have previously described the new guidelines for decarboxylation reactions limiting the reactor temperature to 260 °C, the temperature range used in this experiment was 180 – 260 °C.

Table 4.10 Conditions used during investigations into the effect of temperature on the stability of HIB molecules in a basic solution.

Experiment 20 HIB Temperature Study	
Precursor	0.150 M MAA
Base	0.150 M NaOH
Temperature	Variable °C
Pressure	3000 psi
Residence time	300 s

Figure 4.14 shows the concentrations of HIB, MAA and acetone in the exit solutions collected. The plot shows a small amount of HIB decomposition at all temperatures, although very little conversion to MAA and acetone in each case. This suggests that the decomposition leads to volatile products that were not collected in this study.

When the temperature was increased above 260 °C, low levels of decarboxylation of HIB to acetone could be found, but only in trace

quantities. While acetone is considered a volatile compound, samples were collected in an ice bath during this study and were capped immediately after collection to limit the escape of volatile compounds.

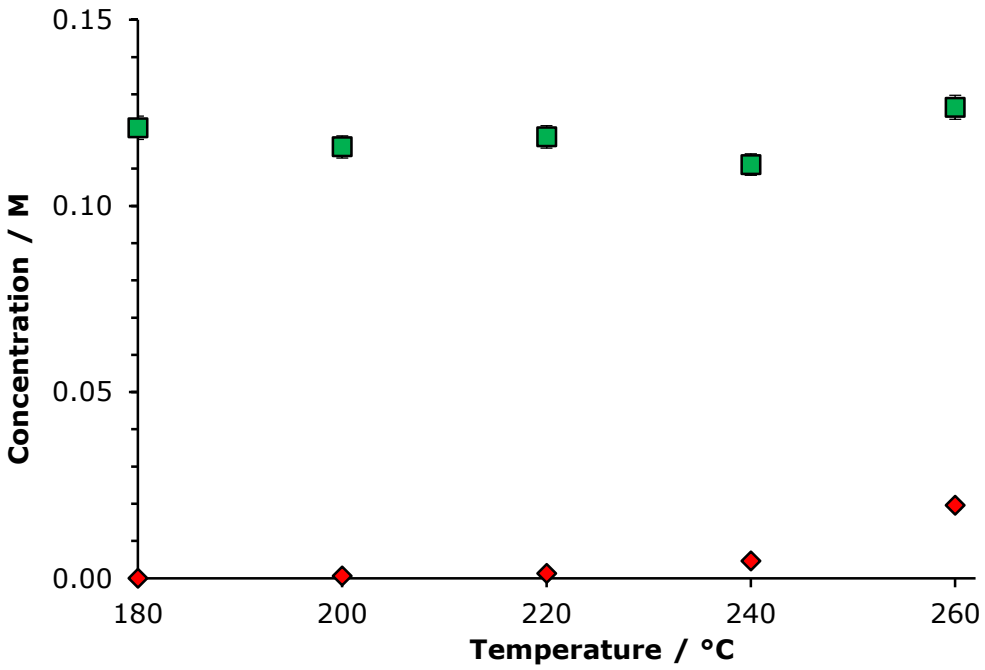


Figure 4.14 The concentration of HIB (■) and MAA (◆) in various exit solutions are shown above. The plot clearly shows the partial decomposition of HIB in each solution and the concentration of MAA increasing with reactor temperature. There was no trace of acetone found in these solutions.

Above 220 °C, there is an increase in the MAA concentration with increasing reactor temperature, up to 0.020 M at 260 °C. In contrast, the corresponding study into MAA stability (Experiment 14) showed HIB being produced at temperatures above 260 °C, suggesting that the dehydration reaction has a lower activation energy than the hydration of MAA to HIB.

The results here fit with the limits set earlier in this chapter, with limited HIB decomposition at temperatures up to 260 °C. Remaining within these boundaries, the effect of the residence time was subsequently investigated.

Experiment 21 - Investigating the Decomposition of HIB

Table 4.11 details the conditions used in this experiment into the effect of residence time on the stability of HIB. Flow rates were chosen to achieve residence times between 60 s (corresponding to the highest flow rate that could be achieved in the rig) and 360 s, the upper limit set earlier in this chapter.

Table 4.11 Conditions used during investigations into the effect of residence time on the stability of HIB molecules in a basic solution.

Experiment 21 HIB Residence Time Study	
Precursor	0.150 M HIB
Base	0.150 M NaOH
Temperature	260 °C
Pressure	3000 psi
Residence time	Variable

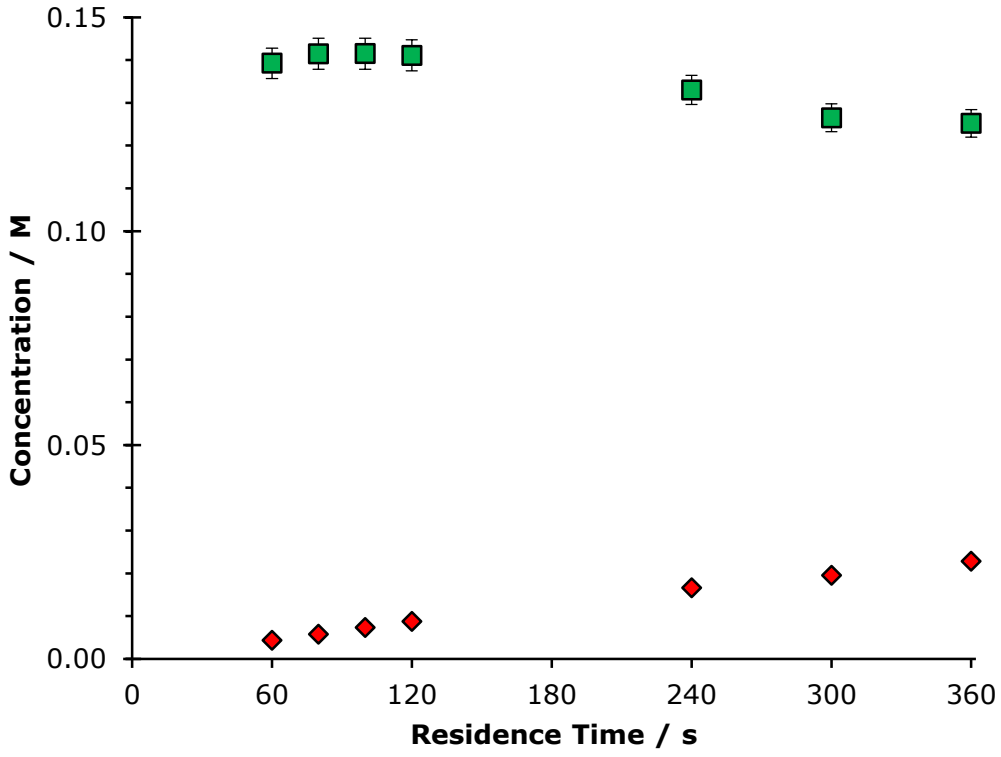


Figure 4.15 The concentrations of HIB (■) and MAA (◆) in various exit solutions are shown above. While acetone is not detected in any of the solutions, there is an increase in MAA production with increased residence time. This corresponds to an increase in HIB decomposition but does not account for the total HIB loss.

As expected, the plot shown in Figure 4.15 shows that as the residence time increases, so does the decomposition of HIB. At residence times below 120 s, there is a small amount of HIB decomposition and low levels of MAA appear in the exit solutions. At 240 s there is a greater increase in the decomposition of HIB and MAA continues to increase in a linear trend, which continues up to 360 s.

Once again no trace of acetone was found in the exit solutions recorded in Figure 4.15. In fact, when the residence time was extended up to 600 s, there remained no trace of acetone in solution, suggesting that the dehydration to MAA is a much more facile reaction than the decarboxylation of HIB, which requires a higher temperature than was used in this experiment.

The pKa values shown in Table 2.3 show that HIB is less acidic than IC and its isomers, meaning that if sodium hydroxide was used in less than equimolar quantities (compared to the dicarboxylic precursor acids) HIB would be present as its free acid, rather than its mono ion. As such, it is necessary to also consider the effect of temperature and residence time in the absence of base. The following experiment was designed to replicate Experiments 20 and 21 without the use of sodium hydroxide.

Experiment 22 - Investigating the Decomposition of HIB

In order to look at the effect of base on the stability of HIB, Experiment 20 was replicated but the addition of base was omitted. The temperatures and residence times were kept the same and Figure 4.16 details the results of the solutions collected between 180 and 260 °C.

Table 4.12 Conditions used during investigations into the effect of temperature on the stability of HIB molecules in a basic solution.

Experiment 22 HIB Temperature Study	
Precursor	0.145 M HIB
Base	N/A
Temperature	Variable °C
Pressure	3000 psi
Residence time	300 s

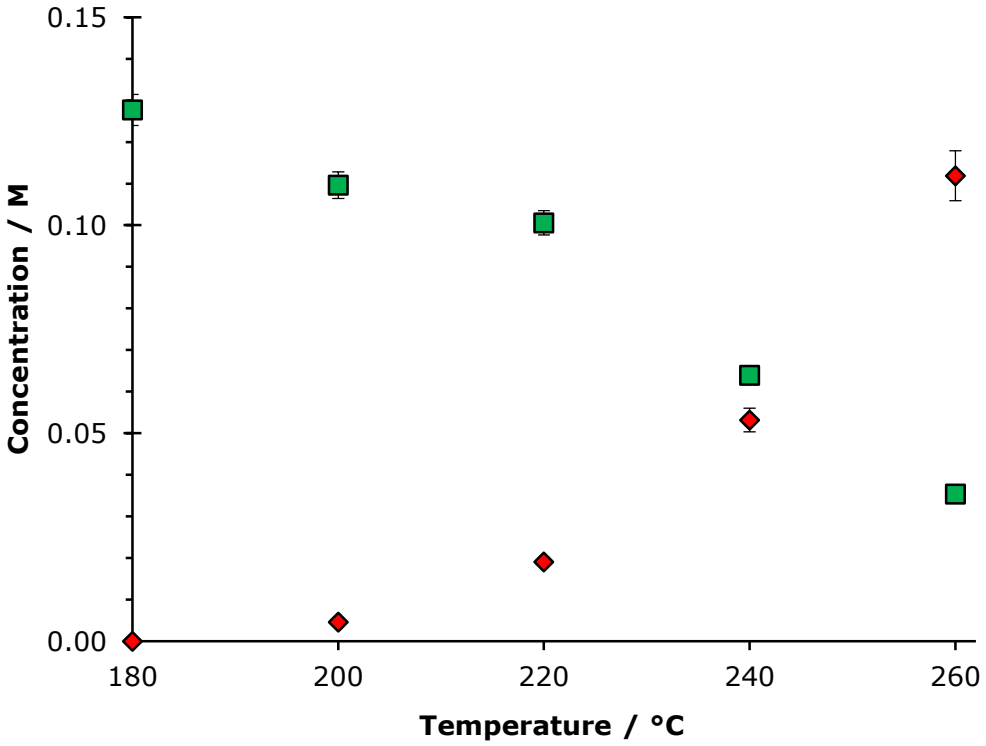


Figure 4.16 The plot shows the concentrations of HIB (■) and MAA (◆) in exit solutions collected in Experiment 22. The plot shows the level of HIB decomposition increased linearly with increased reactor temperature, corresponding to an increase in MAA production. The amount of MAA in the exit solution is greater than the concentration of HIB at 260 °C.

When comparing the above plot to the results displayed in Figure 4.14, it is clear to see that the presence of base impedes the decarboxylation of HIB to MAA. The above plot shows high levels of HIB decomposition and a steep linear correlation between decomposition and reactor temperature, while in the presence of base, there was no such trend.

There is a large amount (0.112 M) of MAA produced at 260 °C that was not achieved during the previous HIB stability experiments. This shows that the decarboxylation must rely on HIB being in its free acid state and can occur at temperatures as low as 200 °C. Once again, there was no trace of acetone found in the exit solutions displayed in Figure 4.16; however, when the experiment was extended beyond the working limits set earlier in this chapter, trace amounts of acetone were found at 280 °C (0.002 M) and 300 °C (0.003 M).

Finally, the effect of changing the residence time at the upper temperature limit in the absence of base was investigated. In order to do this, Experiment 21 was repeated without sodium hydroxide.

The findings of the HIB stability investigation described above suggests that the working limits set out earlier in this chapter are suitable for the reaction. While HIB will remain in its hydrated form, we have previously explained a potential method of dehydrating the product to yield MAA.

Experiment 23 - Investigating the Decomposition of HIB

Table 4.13 Conditions used during investigations into the effect of temperature on the stability of HIB molecules in a basic solution.

Experiment 23 HIB Temperature Study	
Precursor	0.145 M HIB
Base	N/A
Temperature	260 °C
Pressure	3000 psi
Residence time	Variable

The previous experiment showed that when base is omitted from the precursor solution, the level of HIB decomposition is much higher. The results in Figure 4.17 support this and show that at 260 °C, this decomposition is high even at the shortest residence time studied.

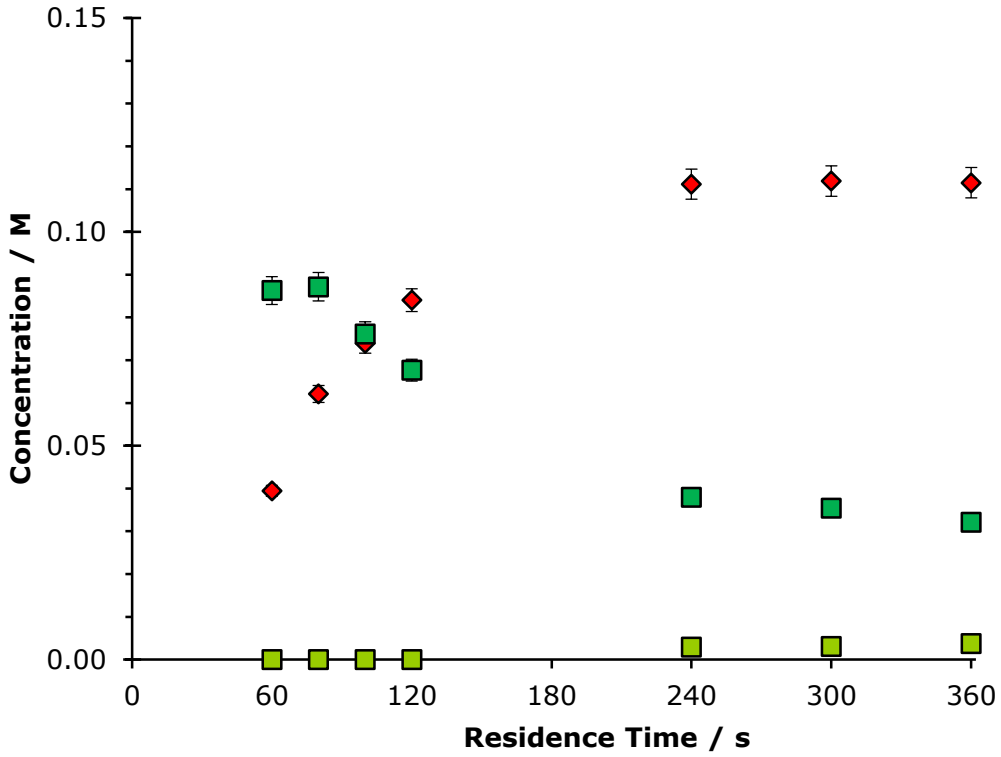


Figure 4.17 Above, the concentrations of HIB (■), MAA (◆) and acetone (■) are shown. It can be seen that at 260 °C, even with the shortest residence time, the level of HIB decomposition is high and a significant amount of MAA is produced. At longer residence times, acetone is also formed, showing the decarboxylation of HIB.

Previous experiments have shown that while MAA is produced as an HIB decomposition product, it remains in low concentrations (0.023 M) when a base is present. However, the plot above shows the concentration of MAA increasing with increased residence times to a maximum of 0.111 M at 240 s before the concentration levels off. This supports the suggestion in the previous experiment that the presence of a base hinders the dehydration of HIB to MAA.

Acetone has not been found in the solutions collected within the working limits in this study so far, suggesting that the presence of base may also hinder the decarboxylation of HIB to acetone. Hence, the presence of base should prove beneficial to achieving the highest second crop of MAA collected after a separate dehydration of HIB.

Summary

This chapter aimed to set out new working guidelines that would limit the amount of MAA decomposition and degradation during its production. The first part of this chapter suggested that a maximum temperature of 260 °C should be used in any MAA production. By limiting the temperature to 260 °C, the amount of thermal degradation of the desired product would be limited.

Using this temperature limit, the residence time was investigated and reactions of residence times of 360 s or less yielded less than 5 % decomposition of MAA. This limit was put together with the limiting temperature to offer a new guideline that sets the working conditions of any decarboxylation reactions yielding MAA to be below 260 °C and 360 s.

The acid : base ratio was also investigated and found that equimolar amounts were desirable to reduce the decomposition of MAA. This ratio does limit the amount of decomposition products in solution but also hinders the conversion of HIB back into MAA. However, we have suggested a way to yield a second crop of the desired acid from exit solutions after the first crop is extracted, hence increasing the overall yield of MAA in our reactions.

Finally we have suggested the collection of a second crop of MAA from the dehydration of HIB. Investigations into the stability of HIB show that while there was significant mass loss, there were only low amounts of MAA and acetone observed in the collected solutions. The presence of base prevents both the decarboxylation and dehydration of HIB, therefore increasing the amount that could be collected after experiments and converted to MAA.

Chapter 5 - A Recyclable Process

The use of sodium hydroxide as a driving force behind the decarboxylation of IC and other precursor acids has been discussed at length in previous chapters. The purpose of this chapter is to discuss and demonstrate how sodium hydroxide can be transformed from a reagent to a catalyst.

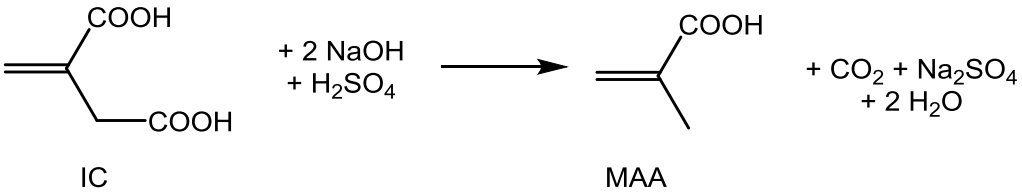


Figure 5.1 The overall decarboxylation of IC with sodium hydroxide yields free MAA when a strong acid is added at the end of the process.

Sulfuric acid is required because the sodium hydroxide used in the decarboxylation reactions means that MAA is produced in its ionised form (Na^+MAA^-), which cannot be easily extracted. The fact that the sodium hydroxide is neutralised at the end of the reaction in order to liberate free MAA means that for a single run it has to be considered as a reagent, as in Figure 5.1.

Huddle noted that the extraction of free MAA into an organic phase is highly selective because MAA molecules form a hydrophobic dimer when hydrogen bonded.[122] The presence of additional hydroxyl and carboxylic acid groups in both unreacted precursors and by-product acids in the exit solutions mean that when these dimerise (Figure 3.18), they retain their hydrophilicity and hence their affinity for the aqueous phase. Therefore, the effluent broth requires acidification with a strong acid, such as H_2SO_4, prior to extraction.

If this acidification and extraction are combined in a possible process, one can immediately see that there would be a problem with waste, Figure

5.2. By using inorganic acids to acidify the broth, an aqueous sodium salt waste product is formed.

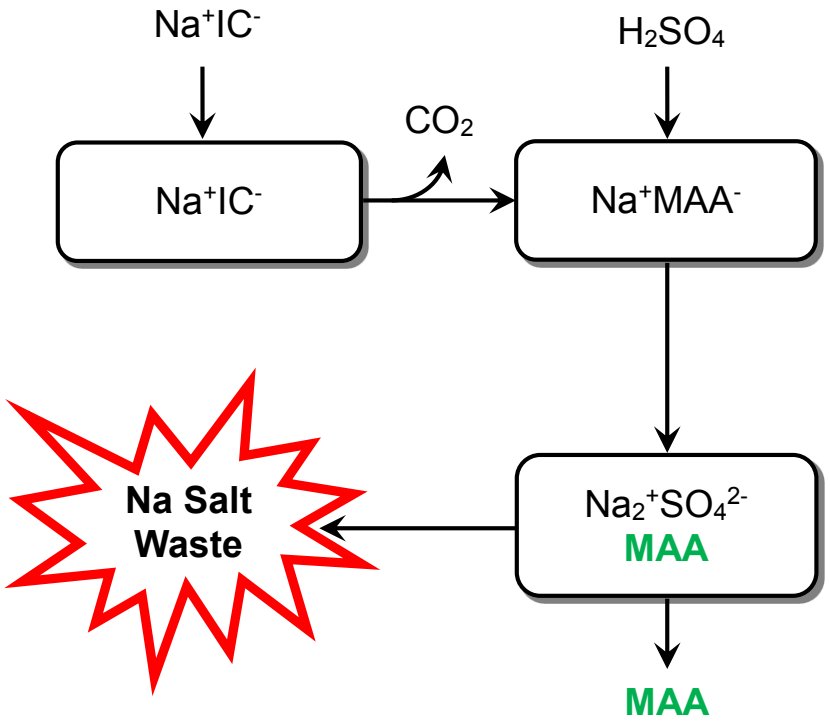


Figure 5.2 A simple process for MAA production from sodium itaconate. A strong acid, such as sulfuric acid, is added to the product of the decomposition to yield free MAA and sodium sulfate. The MAA is then separated but this releases unacceptable quantities of the aqueous salt for disposal.

As it is not possible to safely dispose of large quantities of contaminated aqueous waste, the water would have to be removed, adding further steps and significant extra energy costs to the process. Clearly a new process would make this route to MAA much more attractive.

This chapter develops some preliminary results from the end of Huddle's thesis into a new, efficient method recycling the sodium ions, thereby transforming the base into a *catalyst*. As explained below, his results were encouraging, but as the analytical techniques available were limited, the results need validating and developing further.

Table 5.1 The pK_a values at 25 °C for the acids seen in Scheme 1.4, compared to MAA.[110-112] This demonstrates that any of the precursor acids could be used in place of sulfuric acid to liberate MAA and aid the selective extraction of the free acid.

Acid	pK_a		
	pK_{a1}	**pK_{a2}**	**pK_{a3}**
Acetic Acid	4.75		
cis-Aconitic Acid	2.78	4.41	6.21
Trans-Aconitic Acid	2.91	4.33	6.16
Citraconic Acid	2.45	6.08	
Citramalic Acid	3.5	5.3	
Citric Acid	3.13	4.76	6.40
Crotonic Acid	4.69		
2-Hydroxyisobutyric Acid	3.98		
Itaconic Acid	3.90	5.56	
Mesaconic Acid	3.04	4.85	
Methacrylic Acid	4.68		
Pyruvic Acid	2.50		

The potential breakthrough in Huddle's research came with the realisation that the pK_as of IC and other precursor acids seen in Table 5.1 are *lower* than that of MAA. This means that any of these acids could be used in place of sulfuric acid to acidify the exit solution and liberate free MAA.

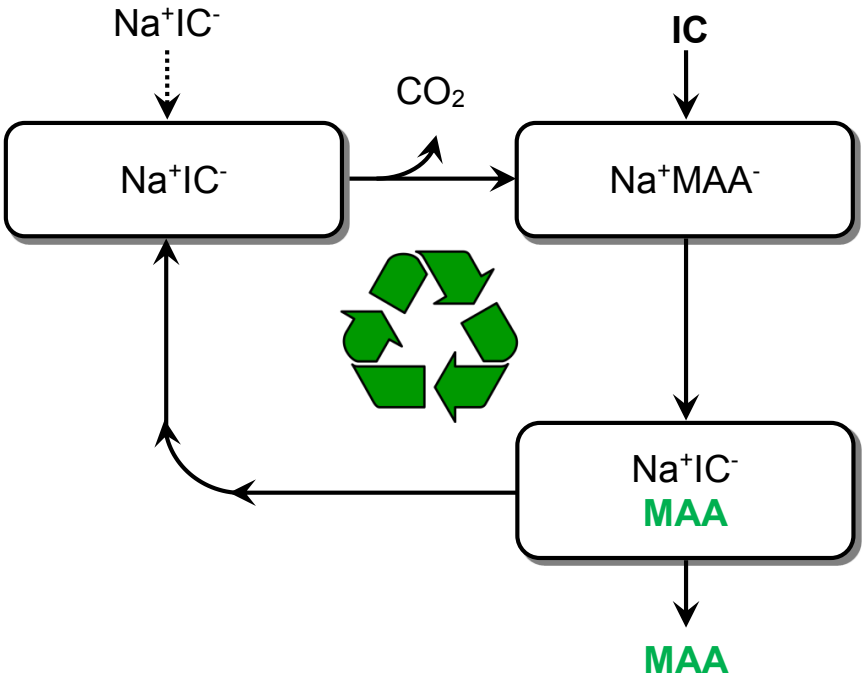


Figure 5.3 A proposed new process for MAA production to include the recycling of the NaOH catalyst. In place of a strong acid, IC is added to yield free MAA and sodium itaconate which can be separated in a simple phase separation. The sodium itaconate is then fed back into the reactor for further decomposition reactions.

After proposing this recycling process, Huddle then reported the results of a preliminary 4 cycle experiment;[72] the conditions of which are displayed in Table 5.2.

Table 5.2 Showing the reaction conditions used by Huddle.

Itaconic Acid Recycle	
Precursor	0.5 M Itaconic Acid
Base	0.5 M NaOH
Temperature	265 °C
Pressure	3000 psi
Residence Time	600 s

What was done was as follows. An initial solution was pumped through the heated rig. The solution was then acidified with IC so that the total concentration of the three isomers (IC, CC and MC) equalled 0.5 M once more. Aliquots of toluene were then used in four repeat extractions and the remaining aqueous solution was run back through the rig for another

decarboxylation cycle. The plot shown in Figure 5.4 displays the percentage composition of MAA in each exit solution after decarboxylation in each cycle and the concentration of MAA remaining in solution after each extraction.

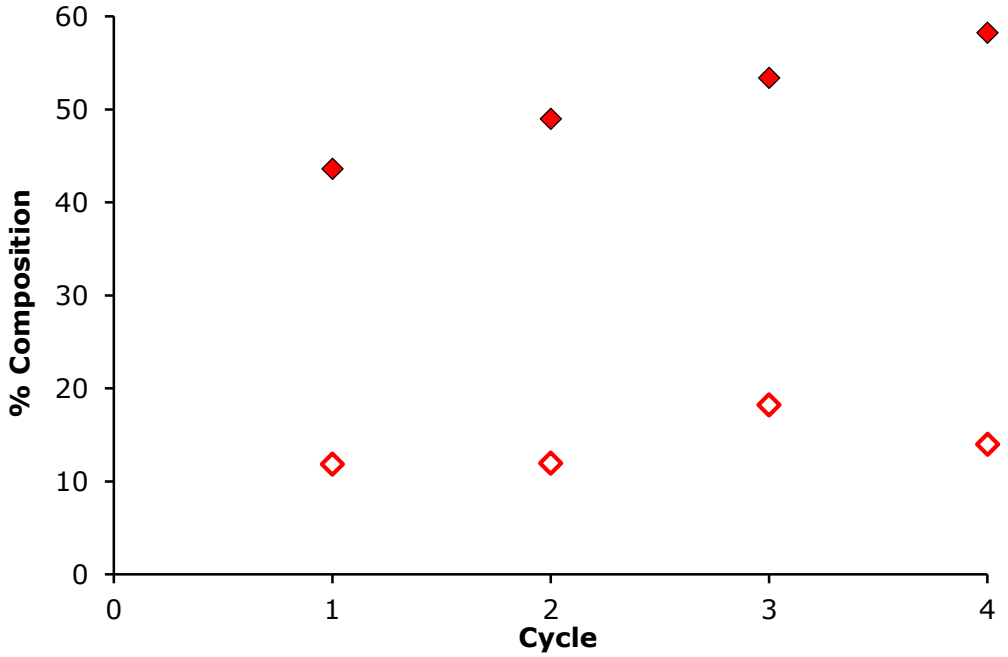


Figure 5.4 Results from Huddle's preliminary experiment[72] show the amount of MAA present in each decarboxylation exit solution (◆) and after four serial extractions with toluene (◇); see the text for discussion of potential problems.

It should be clear that there is a potential problem with Huddle's results. They indicate an increase in MAA concentration with every cycle. A step up between cycles one and two might be expected because of the small amount of MAA carried through after each set of extractions, although this was not mentioned by Huddle. No explanation was offered for the further increases in MAA production in subsequent cycles.

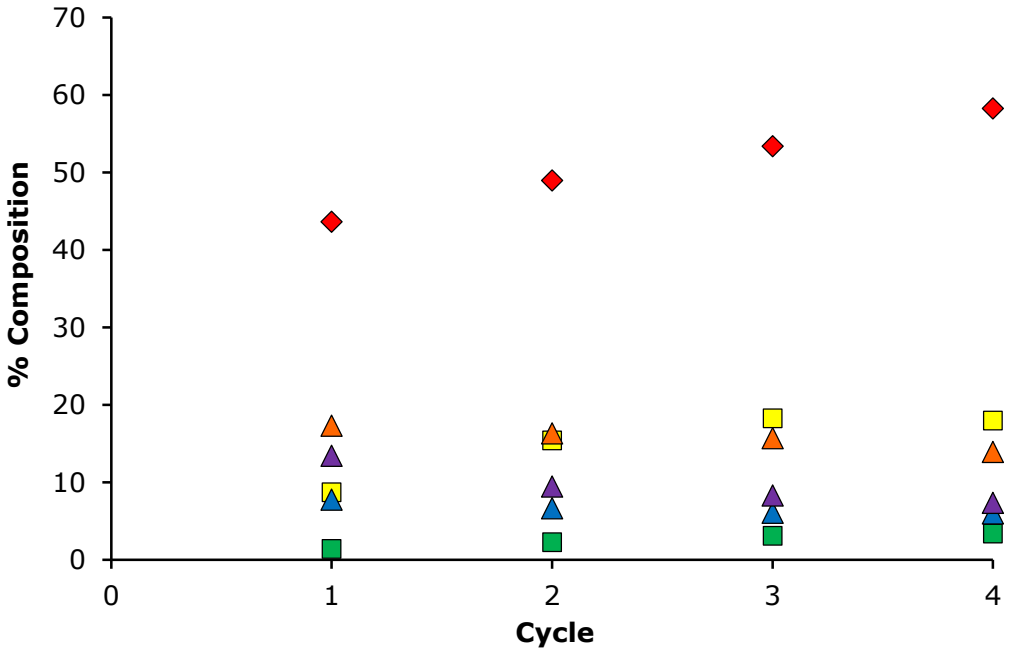


Figure 5.5 The progressive composition of exit solutions collected by Huddle after the decarboxylation of 0.5 M IC (▲) and 0.5 M NaOH are shown. The composition of MAA (◆) is plotted once more, showing a gradual increase in conversion of IC to MAA during decarboxylation reactions. Isomerism of IC forms CC (▲) and MC (▲) which show a slight decline over the four cycles. There is a slight increase in concentration of the hydrated version of MAA, HIB (■) and a build-up of the by-product PY (□) after each cycle.

If one looks at Huddle's full results in Figure 5.5, there is an initial build-up of MC and CC which both slowly decrease with each cycle. Huddle reported the build-up of PY over the first three cycles; however, after 3 cycles the concentration of PY does increase marginally from 3.12 % to 3.39 % and with a shortage of data, no firm conclusions about the build-up of PY could be drawn.

Although Huddle's results were extremely promising and were a key driver in the funding of my PhD project, it is clear that a more systematic investigation was needed to distinguish between real effects of recycling and artefacts of a rapid experiment.

Strategy

Aim – *A preliminary experiment by Huddle indicated there was a possibility of recycling the sodium hydroxide and unreacted starting materials back through the rig after the first decarboxylation. In order to demonstrate the feasibility of recycling in a real process, more data and more cycles are needed.*

An initial study was carried out with solutions of MAA to determine the optimum number of extractions and to balance the amount of MAA extracted with the amount of solvent and energy required.

As illustrated in Chapter 3, the analytical techniques used by Huddle were not comprehensive and overlooked the presence of saturated by-products present in the aqueous mixtures. With this in mind, a series of experiments was designed to re-examine the products of short recycle experiments, similar to the one conducted by Huddle (see above).

Then, in order to demonstrate the potential of the process in industry, further recycling experiments were carried out with alternative precursors. At present, IC is the cheapest of the precursors available on the market and the only precursor available via fermentation. However, if CC or MC become available through fermentation and present a cheaper alternative to IC, it would be useful to know if one could simply swap the precursors or whether new conditions would be required.

Following this, the length of the recycling experiment was increased and efforts to extend the duration were considered to improve the viability of the reaction, leading to a scaled up experiment taking place in collaboration with colleagues from Lucite International.

Results and Discussion

Experiment 24 - Optimising the Extraction Method

Before the recycling was considered, the extraction of MAA was revisited in order to fully understand the process and also to look at the efficiency and ensure nothing was missed in previous studies.

A preliminary experiment to determine the optimum number of extractions with toluene was conducted. The method is described in detail in the Experimental Chapter of this thesis (Chapter 2) and consisted of an aqueous solution of MAA undergoing ten serial separations with toluene in order to calculate the total percentage of MAA extracted after each of the serial extractions. The results are reported in Table 5.3 and Figure 5.6 below.

Table 5.3 Showing the amount of MAA extracted from an aqueous solution after serial extractions with equal volumes of toluene.

Number of Extractions	Concentration of Aqueous MAA / M	Percentage of Remaining MAA Removed / %	Overall Percentage of MAA Removed / %
0	0.25	0	0
1	0.10	60.7	60.7
2	0.052	48.1	79.6
3	0.032	38.7	87.5
4	0.021	33.3	91.7
5	0.015	29.3	94.1
6	0.011	25.0	95.6
7	0.0087	22.9	96.6
8	0.0068	21.6	97.3
9	0.0054	20.1	97.9
10	0.0045	17.3	98.2

Table 5.3 shows that as MAA is removed, a lower percentage is extracted at each subsequent step. In the first separation 60.7 % of MAA is removed, but in the tenth separation only 17.3 % of the remaining MAA is

removed. It can be seen in Figure 5.6 that the amount of MAA extracted by toluene decreases with each extraction and in the final six extractions (5 – 10) less than 4.2 % of the initial concentration of MAA is removed. This reduced efficiency is due to the lower concentration of MAA in the aqueous sample. As this concentration decreases, the amount of MAA found in the organic phase will decrease accordingly due to the partition coefficient.

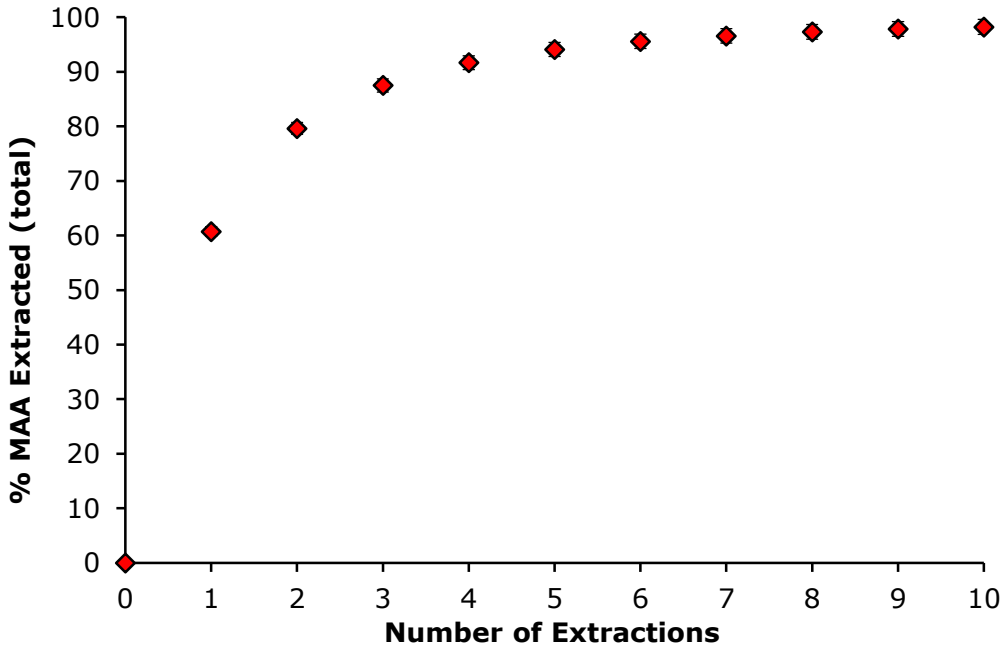


Figure 5.6 Showing the total amount of MAA extracted from a 0.25 M aqueous solution after serial extractions with toluene.

When considering the number of extractions required in a process, the amount of the desired product which can be recovered is important, but it is not the only factor. With each subsequent step the volume of solvent required increases and thus the potential waste is increased. On the basis of this experiment, we redesigned Huddle's method to use just three serial extractions with toluene to remove a large percentage of MAA from aqueous solutions (87.5 %) while keeping the volume of organic solvent used to a minimum.

The next experiment was designed to repeat Huddle's experiment over 5 cycles with improved conditions and analytical techniques. It was clear that Huddle did not consider the stability of MAA in designing his experiment. The results in Chapter 4 indicate that the temperature of his recycling experiment was slightly higher than recommended (265 °C was used instead of below 260 °C) and the residence time was far too long (600 s rather than 300 s, which we have now set as an upper limit).

As a result of these limits, the recycling experiments reported in this chapter have been conducted at the lower temperature of 260 °C, a pressure of 3000 psi and a residence time of 300 secs. For each of these experiments, the hastelloy reactor with the smaller internal volume of 8.6 mL was used and so a flow rate of 1.39 mL min^{-1} was set.

Experiment 25 - Recycling Itaconic Acid : 5 Cycles

Table 5.4 Showing the reaction conditions used in Experiment 25.

Experiment 25 Itaconic Acid Recycle	
Precursor	0.5 M Itaconic Acid
Base	0.5 M NaOH
Temperature	260 °C
Pressure	3000 psi
Precursor flow rate	1.39 ml min^{-1}
Residence time	300 s
Number of repeats	3

Table 5.4 displays the conditions selected for our preliminary recycling experiment, using IC as a precursor acid. Five cycles were run in this experiment, and aqueous samples were analysed by HPLC-RID. The results of Experiment 25 are summarised in Figure 5.7.

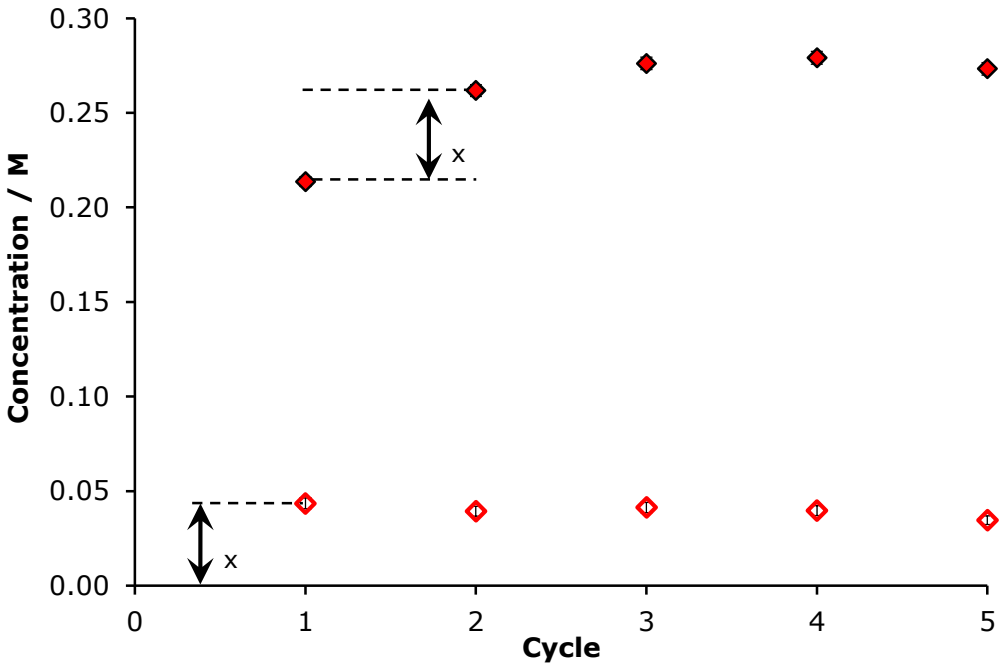


Figure 5.7 A plot to show the amount of MAA present in each decarboxylation exit solution (◆) and after three serial extractions with toluene (◇). There is a small amount (x = 0.043 M) of MAA carried through after the first set of extractions, which can be seen on the plot. This concentration is similar to the difference in levels of MAA in the exit solutions of cycles 1 and 2.

A significant increase in MAA concentration can be seen between cycle 1 and cycle 2 (0.214 M to 0.262 M) and a smaller increase between cycle 2 and cycle 3 (0.262 M to 0.276 M). A small amount of MAA (0.042 M) remained in the aqueous solution after extraction with toluene, which boosts the concentration seen in the exit solution of cycle 2 and can partially explain the increased concentration of MAA in the exit solution. In fact, Figure 5.7 shows the amount of MAA carried through as a value of "x". When "x" (0.042 M) is compared to the stepped increase in MAA in the exit solution of cycle 2 (0.048 M), it can be seen to only fall slightly short of this amount. After cycle 2, the maximum conversion and selectivity have been reached and the concentration of MAA in the exit solutions appears to reach a maximum and level off at 0.279 M.

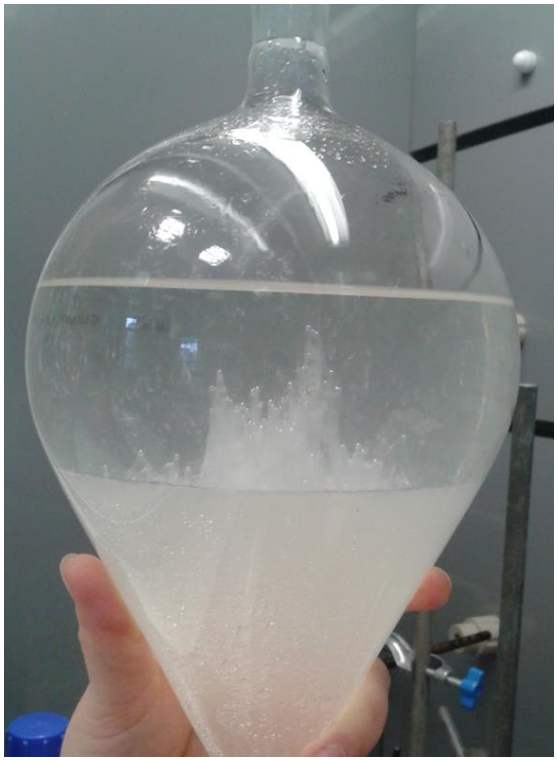


Figure 5.8 One of the major issues faced during the recycling experiments was the formation of strands of suspected polymerised MAA at the solvent interface during extraction. Here the strands can be seen lifted into the organic phase by small air bubbles during separation. The strands dissolved into the aqueous phase and were not isolated. In later experiments, the addition of a stabiliser to the starting solution (described in Experiment 28) removed all visible signs of this formation.

The serial extractions of MAA removed between 80 % and 87 % from the acidified exit solutions, closely agreeing with the 87.5 % extraction obtained in the previous experiment. However, upon mixing the aqueous phase with toluene, strands of solid were observed, possibly polymer or oligomer at the interface between the two phases, see Figure 5.8. The strands were water soluble and were not isolated during this project.

In order to isolate the crude MAA (42.49 g, 0.494 mol), toluene was removed under reduced pressure after each cycle. Analysis of the removed toluene with ^{1}H NMR showed the purity to be of high enough quality to be

recycled in subsequent cycles and so a minimum volume of toluene was used in this experiment.

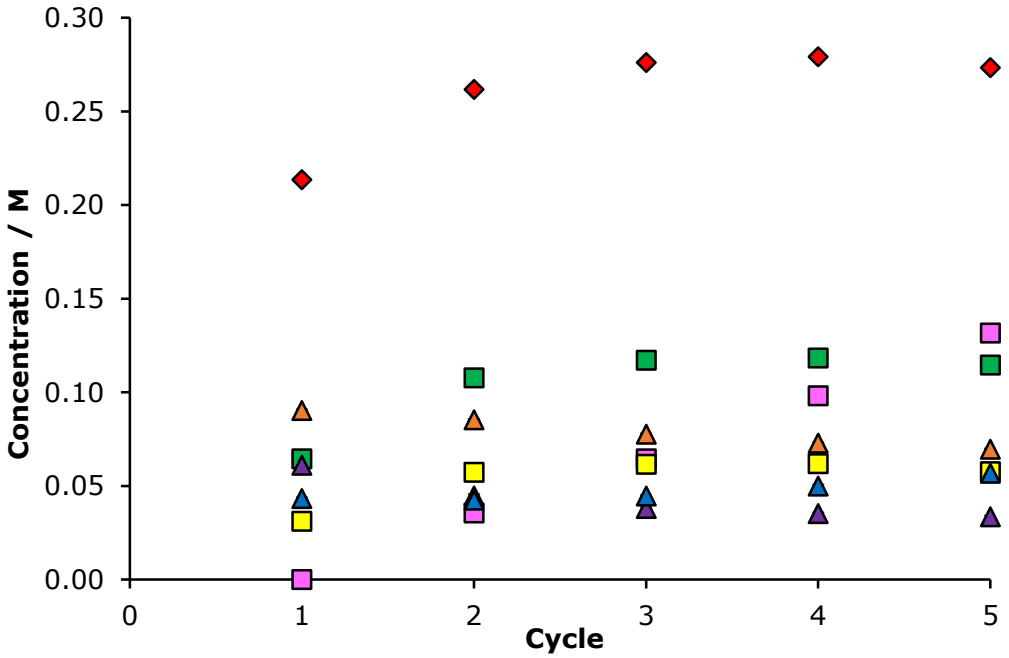


Figure 5.9 A plot to show the progressive composition of exit solutions collected after decarboxylation of IC (▲). The results show a gradual increase in concentration of MAA (◆) and the hydrated version of MAA, HIB (■), during decarboxylation reactions. Isomerism of IC forms CC (▲) and MC (▲) which show a slight decline over the five cycles. There is an increase in concentration of AA (□) and a build-up of the by-product PY (□) after each cycle.

Figure 5.9 shows the results from the decarboxylation of IC over five cycles. The concentration of the precursor acid in the exit solutions can be seen to slowly increase from 0.043 M in cycle 1 to 0.057 M in cycle 5. As discussed earlier in this thesis, IC is known to isomerise to CC and MC and the presence of these acids in the exit solutions supports this. While the concentration of IC increases over the five cycles, both CC and MC decrease, suggesting that the isomers have not reached equilibrium or that the equilibrium is shifting over the course of the experiment. The total conversion of the isomers increases over the five cycles as the

concentration of the three acids decreases from 0.195 M in cycle 1 to 0.160 M in cycle 5.

As explained in Chapter 2, citramalic acid (CM) has not been quantified in this thesis due to difficulties in synthesising or purchasing a pure product for HPLC calibration. However, it has been possible to measure the concentration of two of the decomposition products of CM, acetic acid (AA) and pyruvic acid (PY).

The proposed mechanism for the decomposition of CM to AA and PY is shown in Figure 5.10. The concentration of AA in the exit solutions builds up with each cycle to 0.131 M. However, the concentration of PY appears to level off at 0.057 – 0.062 M after two cycles. Analysis of the combined organic phases showed no trace of PY or AA, suggesting PY has a decomposition route at high temperature and pressure that is not shown by AA.

The concentration of HIB increases over the first three cycles from 0.062 M in cycle 1 to 0.117 M in cycle 3 and reaches a steady level at 0.115 – 0.118 M. This increase in HIB concentration appears to correlate to an increase in MAA concentration over these three cycles.

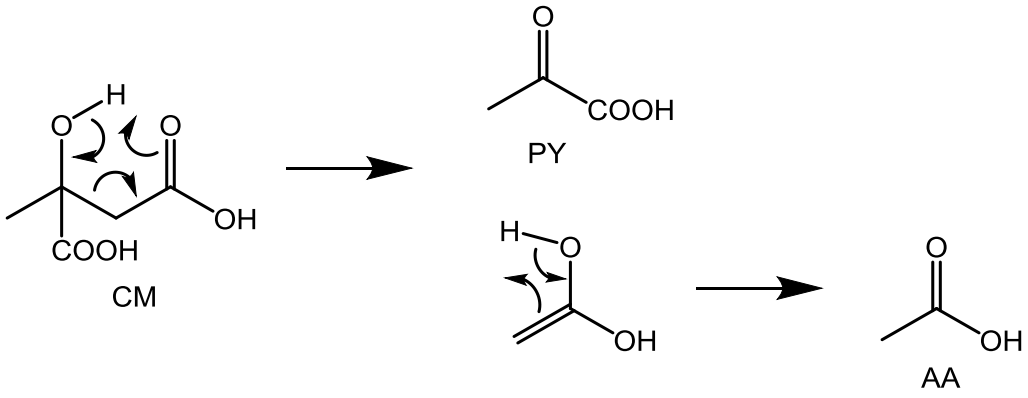


Figure 5.10 A suggested mechanism for the decomposition of CM to produce equimolar quantities of AA and PY.

With the improved analysis and a careful look at the results of the recycle, the anomaly of the increasing concentration of MAA shown in Huddle's results disappears after the third cycle. When we analysed the other materials present in the exit solutions, it can be seen that while Huddle did not quantify AA, he did not miss any other components of the solutions.

The success of this experiment led to questions being asked about the nature of the precursor. As suggested earlier in this chapter, both CC (pK_{a1} = 2.45) and MC (pK_{a1} = 3.04) are strong enough acids to free MAA^- ions for extraction. On the basis of this experiment, Experiments 26 and 27 were designed to show the flexibility of the process by utilising these isomers of IC instead of IC itself as precursors for the recycling.

Experiment 26 - Recycling Citraconic Acid : 5 Cycles

Table 5.5 Showing the reaction conditions used in Experiment 26.

Experiment 26 Citraconic Acid Recycle	
Precursor	0.5 M Citraconic Acid
Base	0.5 M NaOH
Temperature	260 °C
Pressure	3000 psi
Precursor flow rate	1.39 ml min^{-1}
Residence time	300 s
Number of repeats	3

Figure 5.11 shows the concentration of MAA before and after three serial extractions with toluene. It should be noted that the concentration of MAA over the first three cycles follows the same pattern set by the previous experiment. However, the concentration of MAA in the fourth cycle also increases slightly, showing a similarity to the results described by Huddle. The errors are shown on the plot and cannot explain this apparent increase in the fourth cycle, so it can be assumed that the conversion and selectivity to MAA has increased on each cycle. This could be due to changes in pH as the build-up of by-products affects the solution.

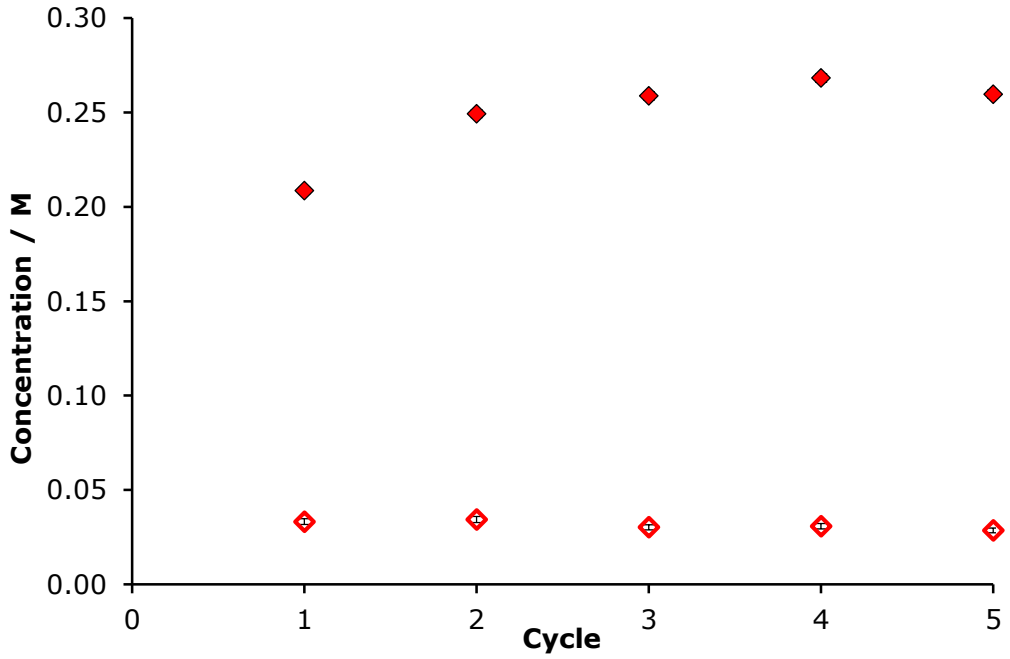


Figure 5.11 A plot to show the amount of MAA present in each decarboxylation exit solution (◆) after CC was put through the rig and after three serial extractions with toluene (◇).

The serial extractions remove between 84 % and 89 % of MAA in the exit solution during each cycle. This value is similar to that shown in Table 5.3 (87.5 %), showing the reliability of the extraction process and is not affected by the recycling of toluene once removed from the crude MAA product. Once again, white strands of suspected polymer were seen on the interface between the aqueous and organic phases during extraction, which dissolved into the aqueous phase upon separation.

Figure 5.12 shows the concentrations of the various components of exit solutions when CC was decarboxylated in the rig. The plot shows similar trends in the concentration of the three isomers in the aqueous mixture, with a decrease in concentration of CC (0.092 – 0.067 M) and MC (0.063 – 0.031 M) while IC slowly increases throughout the five cycles to 0.055 M.

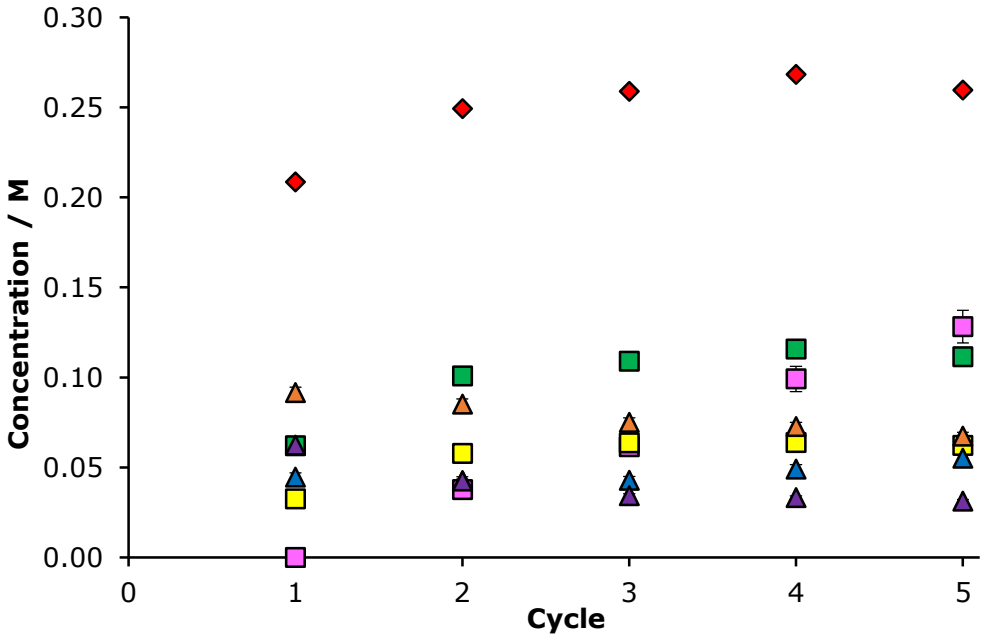


Figure 5.12 A plot to show the progressive composition of exit solutions collected after decarboxylation of CC (▲). The results show a gradual increase in concentration of MAA (◆) and HIB (■) during decarboxylation reactions. Isomerism of CC forms IC (▲) and MC (▲) which show a slight change in concentration over the five cycles. There is an increase in concentration of AA (■) and a build-up of the by-product PY (■).

The concentration of AA builds up over the five cycles to 0.128 M, while PY plateaus after three cycles at 0.062 – 0.064 M. The hydration of MAA to form HIB appears dependent on the concentration of MAA, as the concentration of HIB increases with the concentration of MAA, both of which can be seen to level off after three cycles.

Experiment 27 - Recycling Mesaconic Acid : 5 Cycles

Table 5.6 Showing the reaction conditions used in Experiment 27.

Experiment 27 Mesaconic Acid Recycle	
Precursor	0.5 M Mesaconic Acid
Base	0.5 M NaOH
Temperature	260 °C
Pressure	3000 psi
Precursor flow rate	1.39 ml min^{-1}
Residence time	300 s
Number of repeats	3

When the same experiment was carried out with MC as a precursor acid, similar results to those seen in Experiment 24 were seen once more. The conversion to MAA shows similar results to those seen in Figure 5.7 and Figure 5.11 with the concentration stepping between cycles 1 and 2. Figure 5.14 again shows a small amount of MAA being carried through in the aqueous solution to the next cycle, which appears to boost the concentration in cycle 2. After cycle 2, there is another small increase in the concentration of MAA from 0.239 M to 0.250 M before extraction, but no further increase after this cycle.

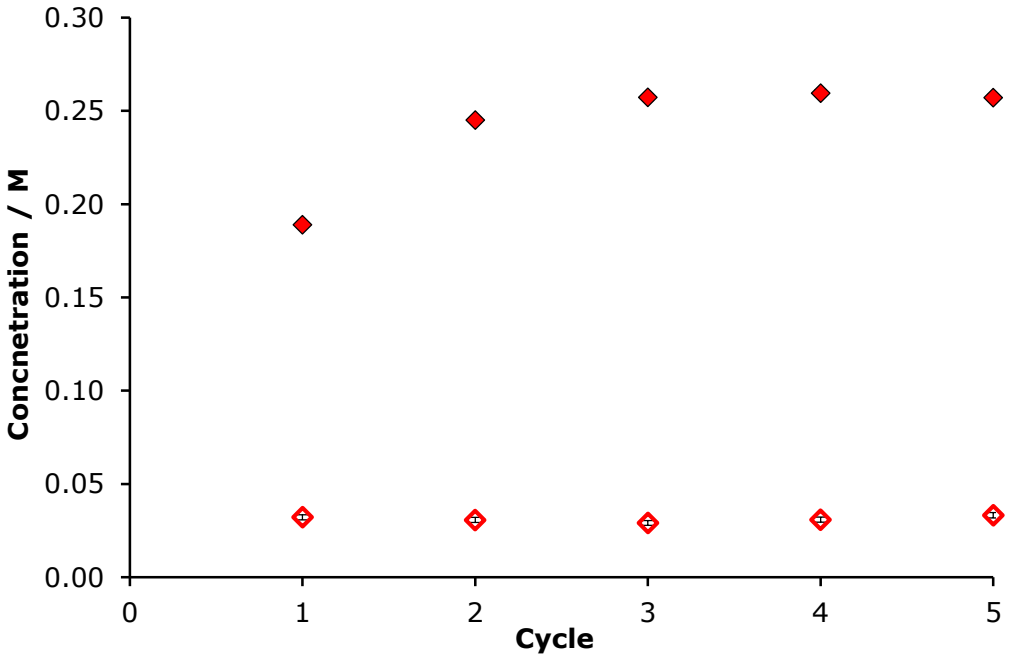


Figure 5.13 A plot to show how much MAA is produced after decarboxylation of MC (◆) and after three serial extractions with toluene (◇).

When the acidified aqueous solution was mixed with toluene, a similar level of suspected polymer formed on the interface, dissolving into the aqueous phase when disturbed. The concentration of MAA remaining in the aqueous solution lies between 0.028 M and 0.032 M. This corresponds to between 83 % and 89 % of MAA extraction in each cycle.

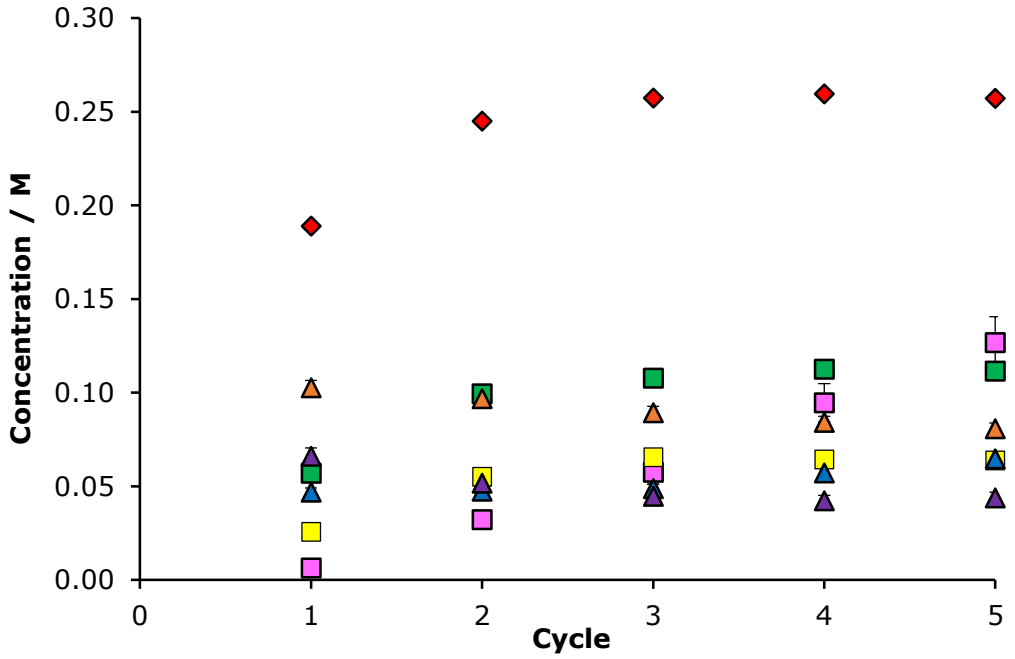


Figure 5.14 A plot to show the progressive composition of exit solutions collected after decarboxylation of MC (▲). The results show a gradual increase in concentration of MAA (◆) and HIB (■) during decarboxylation reactions. Isomerism of CC forms CC (▲) and IC (▲) which show a slight change in concentration over the five cycles. There is an increase in concentration of AA (■) and an initial build-up of the by-product PY (■).

Figure 5.14 shows the decrease in concentration of CC (0.103 – 0.081 M) and MC (0.066 – 0.044 M) over the five cycles, while IC slowly builds up to a maximum in the fifth cycle of 0.065 M. The concentration of AA continues to rise through the five cycles, to a maximum at 0.127 M. The concentration of PY increases through the first three cycles and then plateaus at 0.064 – 0.065 M. HIB also increases over the first three cycles but the concentration levels off at 0.108 M and remains steady at 0.112 M during the final two cycles.

Comparison of Isomeric Precursors

When comparing the results of the three recycle experiments, Table 5.7 shows that the nature of the precursor isomer does not have a significant effect on the decarboxylation. As IC is the central molecule in Scheme 1.8, CC and MC must pass through it in order to decarboxylate to MAA. The fast isomerisation between the three isomers allows the starting solution to be interchangeable between these molecules. The concentration of MAA present in the exit solution of cycle 5 in Experiment 24 was slightly higher at 0.265 M while the concentrations in Experiments 25 and 26 were 0.253 M and 0.251 M respectively. This supports the observation of IC as a central molecule while CC and MC must undergo isomeric transformations prior to decarboxylation, meaning a lower conversion of CC and MC to MAA.

Table 5.7 A display of the concentrations at three points during the previous experiments to show the similarities between the results.

	IC Precursor			**CC Precursor**			**MC Precursor**		
	Cycle 1	Cycle 3	Cycle 5	Cycle 1	Cycle 3	Cycle 5	Cycle 1	Cycle 3	Cycle 5
MAA / M	0.214	0.276	0.273	0.209	0.259	0.260	0.189	0.257	0.257
CC / M	0.090	0.078	0.069	0.092	0.075	0.067	0.103	0.089	0.081
IC / M	0.043	0.045	0.057	0.045	0.034	0.055	0.047	0.049	0.065
MC / M	0.061	0.038	0.034	0.062	0.034	0.031	0.066	0.045	0.044
AA / M	0.000	0.065	0.132	0.000	0.062	0.128	0.006	0.057	0.127
HIB / M	0.064	0.117	0.115	0.062	0.109	0.111	0.057	0.108	0.111
PY / M	0.031	0.062	0.058	0.033	0.064	0.062	0.026	0.065	0.064

Due to the apparent similarities in the exit solutions from the three different precursors, a further experiment was designed to investigate the possibility of switching the precursor between cycles. In order to reduce the level of apparent polymerisation occurring, 250 ppm hydroquinone was added to the original precursor solution to inhibit the polymer formation.

Experiment 28 - Recycling Mixed Acid : 7 Cycles

Experiment 28 began with a 0.5 M IC and 0.5 M NaOH solution that was decarboxylated in cycle 1. Cycle 1 was acidified with more IC and MAA was extracted before a further decarboxylation in cycle 2. The solution was then topped up with CC for the decarboxylations in cycles 3 and 4 and MC for cycles 5 and 6. After the decarboxylation in cycle 6, the concentration of CC, IC and MC was calculated and topped up with equal masses of each of the acids to top the total concentration up to 0.5 M. Cycle 7 shows the results of this mixed precursor decarboxylation.

Table 5.8 Showing the reaction conditions used in Experiment 28.

Experiment 28 Mixed Acid Recycle	
Precursor	0.5 M Itaconic Acid 0.5 M Citraconic Acid 0.5 M Mesaconic Acid
Base	0.5 M NaOH
Stabiliser	250 ppm Hydroquinone
Temperature	260 °C
Pressure	3000 psi
Precursor flow rate	1.39 ml min^{-1}
Residence time	300 s

There is a step in MAA concentration between cycle 1 and 2 (0.044 M) which can be again be attributed to the small amount of MAA carried through after extractions (0.043 M). There is some discrepancy in the conversion of the precursors to MAA. At a maximum, the concentration of MAA is 0.265 M; however this drops to 0.231 M and 0.235 M in cycles 4 and 6 respectively. These dips do not correspond to changes in the precursor isomers and so should not be attributed to a difference in selectivity of the precursor acids.

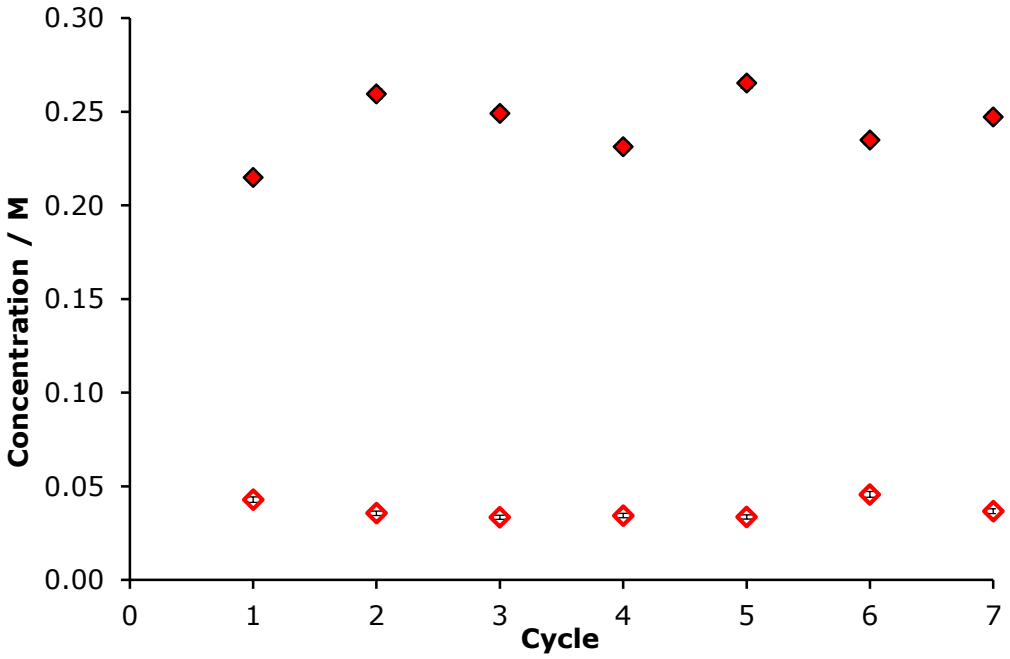


Figure 5.15 A plot to show the amount of MAA present in each decarboxylation exit solution (◆) and after three serial extractions with toluene (◇).

The extraction of MAA lay between 80 % and 87 % in this experiment, as shown in Figure 5.15. The removal of MAA from the exit solutions does not appear to be affected by the nature of the precursor used to acidify the aqueous solution and shows good agreement with the plot shown in Figure 5.6. It can also be seen from Figure 5.16 that the low levels of MAA being carried through to the next cycle do not affect the decarboxylation of the precursor isomers to form MAA. The addition of hydroquinone appeared to reduce the level of polymerisation as no strands were formed on the interface between the two phases during extraction.

Figure 5.16 shows the concentration of IC to be stable over the first four cycles, lying between 0.041 M and 0.043 M. The concentration of IC in the exit solution for cycle 5 has increased to 0.065 M and continues to rise up to 0.076 M in cycle 7. The concentration of CC shows a decrease over cycles 1 to 4, from 0.091 M down to 0.064 M. However, the concentration is boosted in cycle 5 when MC is used a precursor, up to 0.085 M before

dropping off once more to 0.070 M in cycle 7. The concentration of MC shows a similar trend to CC, dropping from 0.062 M in cycle 1 to 0.030 M in cycle 4, and then increasing to 0.049 M in cycle 5 before finishing at 0.033 M in cycle 7. These small fluctuations in the exit solution concentrations correspond to the total concentration of the three isomers in the aqueous solution before decarboxylation being slightly high in cycle 5 (0.525 M).

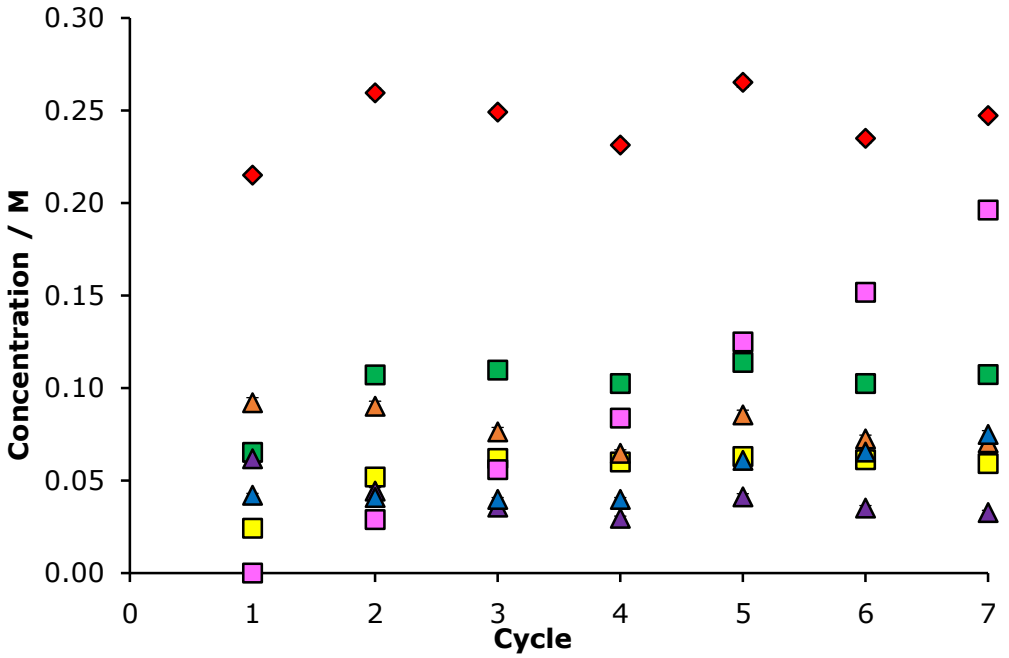


Figure 5.16 A plot to show the progressive composition of exit solutions collected after decarboxylation of CC (▲), IC (▲) and MC (▲). The results show a gradual increase in concentration of MAA (◆) during decarboxylation reactions. There is an initial increase in concentration of the hydrated version of MAA, HIB (■), and PY (□) before the concentrations of these by-products plateau after each cycle. The concentration of AA (□) continues to increase with each cycle.

There is an increase in concentration of AA that builds up through the seven cycles. After five cycles, the concentration (0.125 M) is comparable to those shown in the previous experiments. The increase reaches a maximum at 0.196 M. Conversely, the concentration of PY increases in the

first three cycles from 0.024 M to 0.076 M before levelling off at 0.059 M to 0.061 M.

The concentration of HIB shows a similar trend to that of MAA, increasing from 0.065 M to 0.107 M between cycles 1 and 2, reaching a maximum in cycle 5 at 0.114 M when the precursor was switched from CC to MC. There is also a decrease in concentration in cycles 4 and 6 to 0.102 M.

The results seen in Figure 5.15 and Figure 5.16 demonstrate that the precursor isomers can be switched during recycling experiments where necessary. It would also be possible to use a sample of mixed isomers to acidify the solution for extraction and decarboxylation without seeing a large effect on the production of MAA or extraction of the free acid product.

Once the effects of changing the precursor had been explored, the length of the experiment was investigated. Previous experiments had included up to seven cycles and so an experiment was designed to continue up to 20 cycles. During the experiment, it was noted that the conversion of IC was decreasing. It was proposed that this drop in conversion could be due to the production of strong acids with a pK_a smaller than that of the IC precursor. This would not cause problems with the extraction of MAA due to the sodium ions being associated with the strongest acids in the solution. Hence, to the exit solution of cycle 18, a small amount of NaOH was added to boost the concentration of sodium ions in the solution and examine the effect of this increased ionic presence.

Experiment 29 - Recycling Itaconic Acid : 20 Cycles

Table 5.9 Showing the reaction conditions used in Experiment 29.

Experiment 29 Itaconic Acid Recycle	
Precursor	0.5 M Itaconic Acid
Base	0.5 M NaOH
Stabiliser	250 ppm Hydroquinone
Temperature	260 °C
Pressure	3000 psi
Precursor flow rate	1.39 ml min^{-1}
Residence time	300 s
Number of repeats	2

Figure 5.17 displays the increased concentration of MAA over the first three cycles from 0.210 M to 0.276 M, as seen in previous recycling experiments. However, after cycle 5, the production of MAA decreases, with a concentration of only 0.157 M being present in the exit solution for cycle 18. This decrease in the concentration of MAA correlates with the decrease in conversion of IC, yet the addition of NaOH in cycle 18 does not appear to have an effect on the production of MAA in cycles 19 and 20.

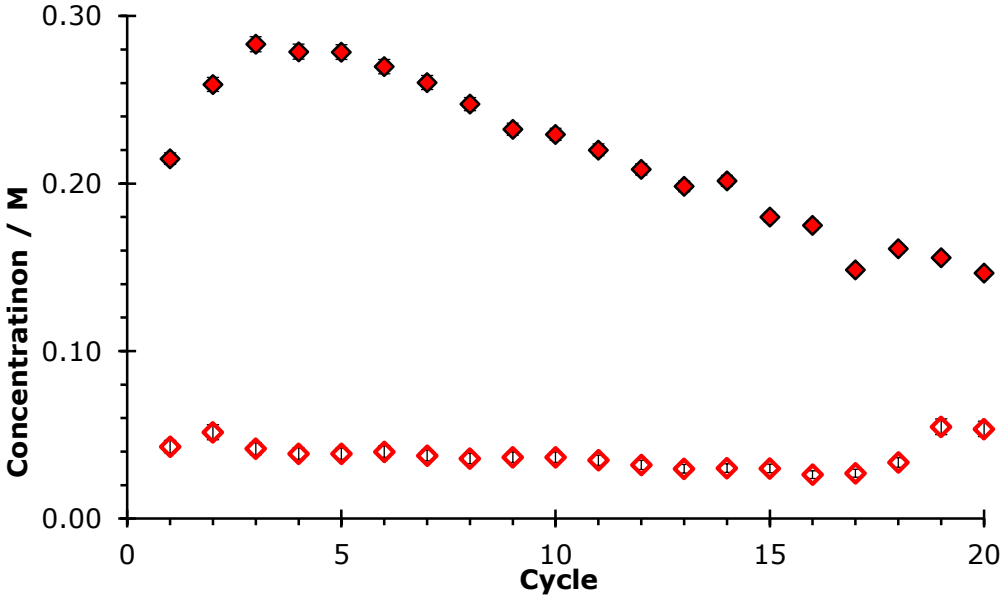


Figure 5.17 A plot to show the amount of MAA present in each decarboxylation solution (after decarboxylation ◆) and (after three serial extractions with toluene ◇).

The plot shows the extraction of MAA from the aqueous exit solutions in cycles 1 - 18 lie between 79 % and 86 %. After the addition of NaOH in

cycle 18, this drops to 64 – 65 %. This suggests the acidification prior to extractions in cycles 19 and 20 were not adequate to produce free MAA molecules and the amount of NaOH added in cycle 18 was excessive.

It can be seen in Figure 5.18 that the concentration of CC drops over sixteen cycles from 0.092 M before it levels off at 0.043 – 0.050 M between cycles 16 and 20. The concentration of MC also falls slightly over the first five cycles from 0.057 M to 0.035 M and then levels off between 0.023 M and 0.030 M. However, the concentration of the precursor acid, IC, increases significantly over the first eighteen cycles from 0.043 M to 0.194 M. This increase in IC concentration is due to a build-up of the acid in the recycled solution. Conversion calculations show that the conversion of the reaction remains high (average 71.7 %) in all cycles except the first, where the conversion lies at just 54.4 %. However, the selectivity to MAA decreases from 49.4 % in Cycles 2 and 3, to just 32.2 % in Cycle 18 and 29.6 % in Cycle 20.

There is an initial build-up of PY formed over the first four cycles, before the concentration slowly decreases from 0.064 M to 0.045 M in cycle 18. After an addition of NaOH to the exit solution of cycle 18, the concentration of PY increases to 0.076 M in cycle 20, suggesting the stability of PY is dependent on the presence of excess sodium cations. The addition of NaOH to the solution appears to increase the stability of PY in solution, allowing a secondary build-up of the acid in solution.

The concentration of HIB appears to change with the concentration of MAA in each exit solution, increasing from 0.066 M to 0.121 M over the first three cycles and dropping off to 0.061 M in cycle 17. However, the concentration of HIB increases in cycles 19 and 20 to 0.088 M, contrasting the trend shown by MAA.

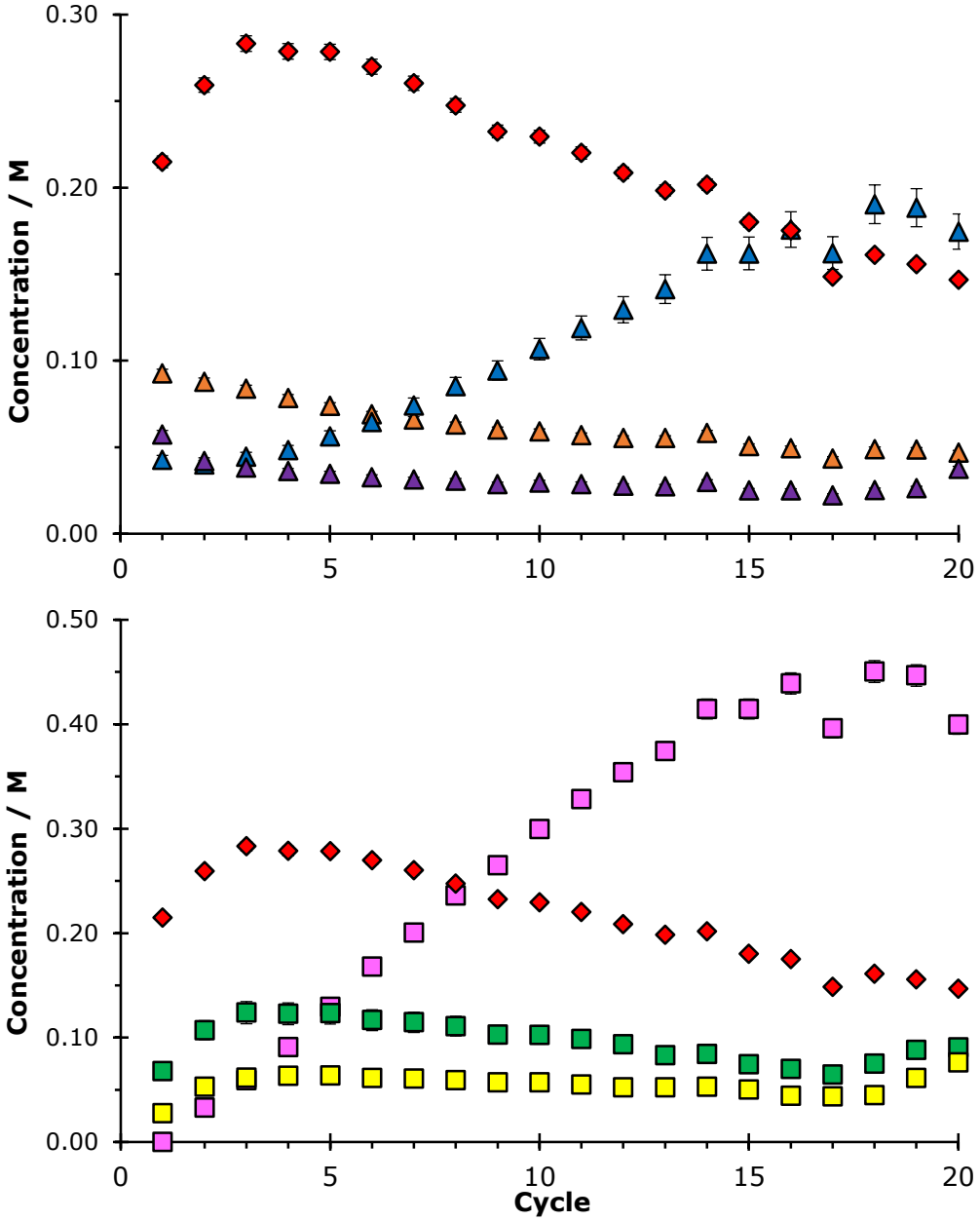


Figure 5.18 The two plots show the progressive composition of exit solutions collected after decarboxylation of IC (▲). The results show a gradual increase in concentration of MAA (◆) and HIB (■) over five cycles, before the concentration drops over the next fifteen cycles. The concentrations of CC (▲) and MC (▲) decrease over the first few cycles before reaching a steady level; however, the concentration of IC increases significantly indicating a build-up of the acid in the recycled solution. The by-product PY (□) increases slowly and levels off before increasing after the further addition of NaOH in cycle 18, while AA (□) increases rapidly until cycle 16 where the increase slows and then reverses.

A repeat of this experiment produced identical results and the drop off in selectivity remained. However, an experiment by researchers at Lucite International[123] found that at 260 °C and 3000 psi with a residence time of 480 secs, the selectivity to MAA was at a maximum (28 %) when an equimolar quantity of IC and NaOH were present, with the conversion dropping off when the amount of NaOH was increased above or decreased below this. Figure 5.19 shows the curve and the large increase in selectivity at equimolar amounts.

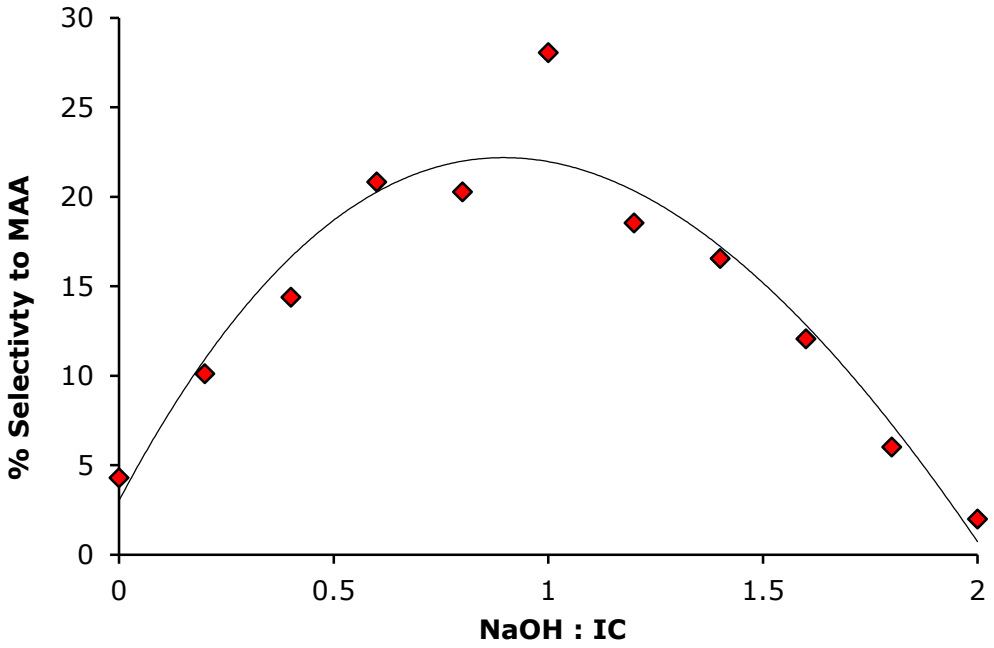


Figure 5.19 A plot to show the selectivity to MAA (◆) shown when a solution of 0.5 M IC was heated with different concentrations of NaOH.[123] The maximum conversion can be seen to occur when the ratio of NaOH to IC is 1.

When considering the results shown in Figure 5.19, achieving the maximum conversion and selectivity of IC in our recycling system would rely on IC existing as the mono-itaconate ion. As discussed in Chapter 1, Li and Brill found an increase in rate constants over several reaction temperatures when the pH of the starting solution (pH_{25}) was equal to 3.75, indicating the presence of mono-itaconate ions in the precursor solution.[69]

On a small scale, such as the one used in this research, the pH of a system can be easily monitored and altered using pH measurements taken in place of time consuming titrations. An experiment was therefore designed to show the effect of balancing the pH of the aqueous solutions prior to each decarboxylation. This was done in order to ensure the mono-itaconate ions were fed into the rig in each cycle and maintain high conversion. However, as mentioned later, the pH of the system does not appear to be as important on a larger scale. Hydroquinone was again used as a stabiliser in this reaction to reduce the level of polymerisation of MAA in solution.

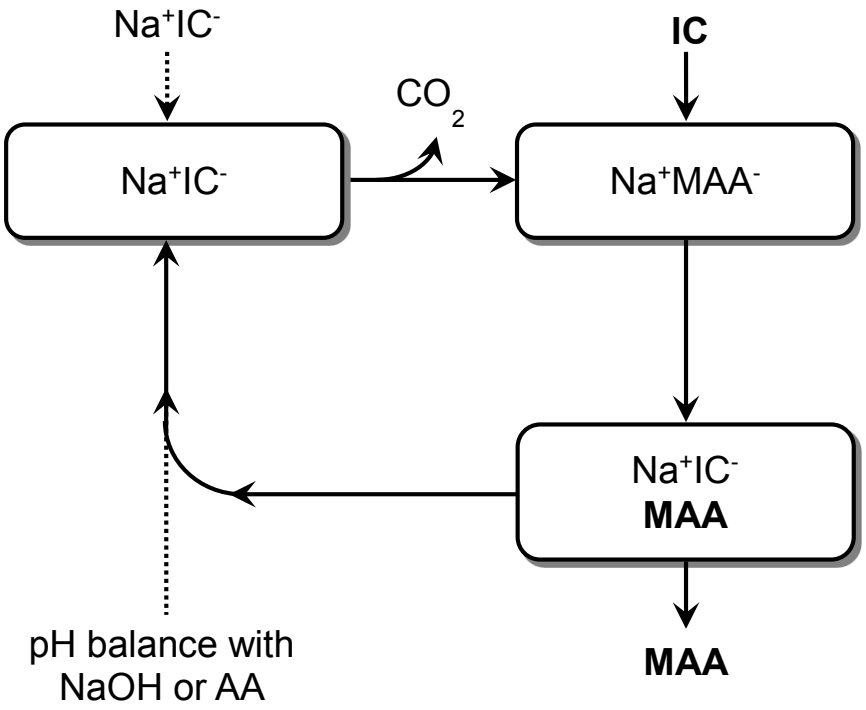


Figure 5.20 An updated route to MAA including a step to pH balance the aqueous solutions after acidification and extraction.

Experiment 30 was designed to include an extra step in the proposed route to MAA shown in Figure 5.3. Figure 5.20 shows the updated scheme and shows the addition sodium hydroxide or AA to pH balance the solution. When the pH was low, NaOH was added prior to decarboxylation and AA was used when the measured pH was high. AA was chosen for its stability

in the system, as shown by the build-up of AA in the previous recycling experiments described in this chapter.

In contrast to previous recycling experiments, pentane was used in Experiment 30 after health concerns were raised about the continued use of toluene.[124] In order to demonstrate the possibility to scale up this process, Lucite International led the move towards pentane being used as a suitable extraction solvent due to its satisfactory partition coefficient and low boiling point seen in Table 5.10. Its low boiling point meant that pentane was well suited to our previously described method of reusing the solvent for each cycle of the experiment.

Table 5.10 Common organic solvents are listed with their boiling points and partition coefficients.

Solvent	Boiling Point / °C[a]	Partition Coefficient[b]
Pentane	36	7.8
Heptane	98	5.0
Octane	126	5.0
Iso-octane	99	3.4
Nonane	151	4.5
Decane	174	4.2
Dodecane	215-217	3.7
Decalin	189-191	4.3
Toluene	111	7.2
Mixed Xylenes	136	7.3

[a] Boiling points taken from literature.[125-127]

[b] In order to calculate each partition coefficient, a series of aqueous solutions were mixed with equal weights of organic solvents, separated and the concentration of MAA in each phase measured by HPLC.

Experiment 30 - Recycling Itaconic Acid : 20 Cycles

The precursor solution was made up to contain 0.5 M IC, 0.5 M NaOH and 250 ppm hydroquinone and the pH was measured. The solution was put through the rig and the pH measured once more. After acidification and extraction, the solution was put back through the rig a second time. The exit solution for Cycle 2 was treated in the same way, with pH measurements being taken after decarboxylation, acidification and extraction. The pH at this stage of the experiment was 3.82. As Cycle 2 has shown high levels of conversion and selectivity in previous recycling experiments described in this thesis, all further cycles were pH balanced to match this solution. After the exit solution for cycle 3 had been acidified with IC and extracted with pentane, NaOH was added to increase the pH of the solution to 3.82. This was repeated with each further cycle of the experiment. Cycles 6, 8, 11, 13, 17 and 19 produced a solution after extraction that had a pH higher than the desired 3.82 and so AA was added to reduce the pH of the solution. Due to the addition of significant amounts of AA, the yield of AA is not shown on Figure 5.22.

Table 5.11 Showing the reaction conditions used in Experiment 30.

Experiment 30 Itaconic Acid Recycle	
Precursor	0.471 M Itaconic Acid
Base	0.500 M NaOH
Stabiliser	250 ppm Hydroquinone
Temperature	260 °C
Pressure	3000 psi
Precursor Flow Rate	1.39 ml min^{-1}
Residence Time	300 s

Figure 5.21 shows the concentration of MAA to fluctuate during the experiment, reaching a maximum at 0.297 M in Cycle 6 and a minimum of 0.215 M in Cycle 15. Despite these fluctuations, the concentration does not see a considerable drop off, such as the trend shown in Figure 5.17. When the solutions are pH balanced prior to decarboxylation, the concentration of MAA after twenty cycles (0.231 M) is significantly higher than that

shown in Experiment 29 (0.143 M). The concentration in Cycle 20 is slightly lower than concentrations shown in the first eight cycles, corresponding to the increase in IC concentration, suggesting a lower conversion of IC to MAA in later cycles. The concentration of HIB remains dependent on the concentration of MAA and follows the trend, reaching a maximum of 0.131 M in cycle 6 and a minimum of 0.89 M in Cycle 15.

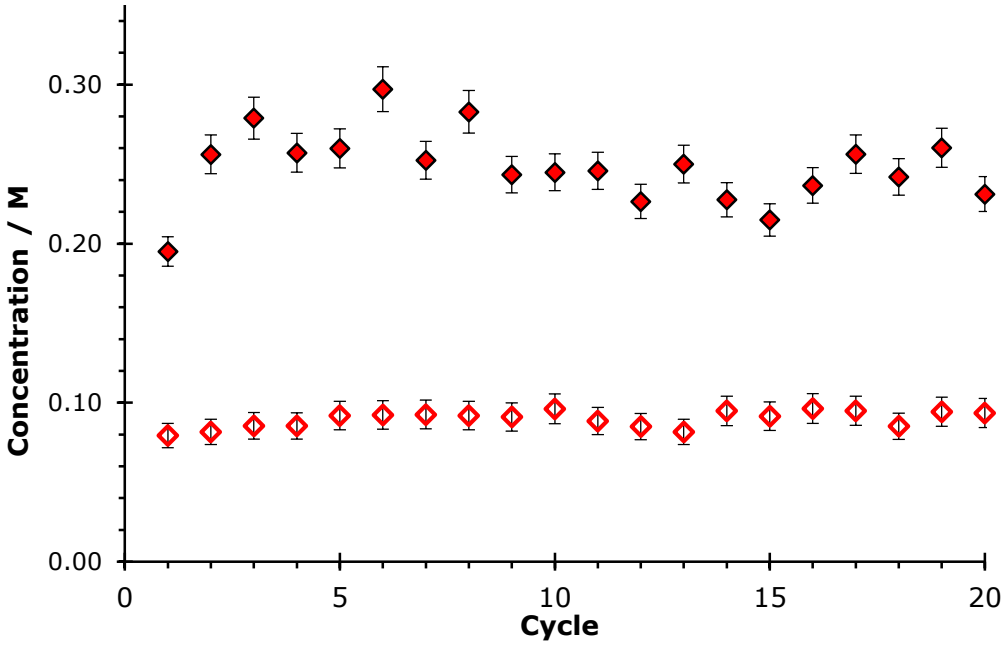


Figure 5.21 A plot to show the amount of MAA present in each decarboxylation exit solution (◆) and after three serial extractions with pentane (◇).

The extraction of MAA lies between 57 % and 69 % across the twenty cycles. This value is lower than the extractions shown previously in this chapter due to the change in extraction solvent to pentane which shows a lower partition coefficient than toluene. However, the additional MAA that is carried through to the next cycle does not seem to have an effect on the amount of MAA produced.

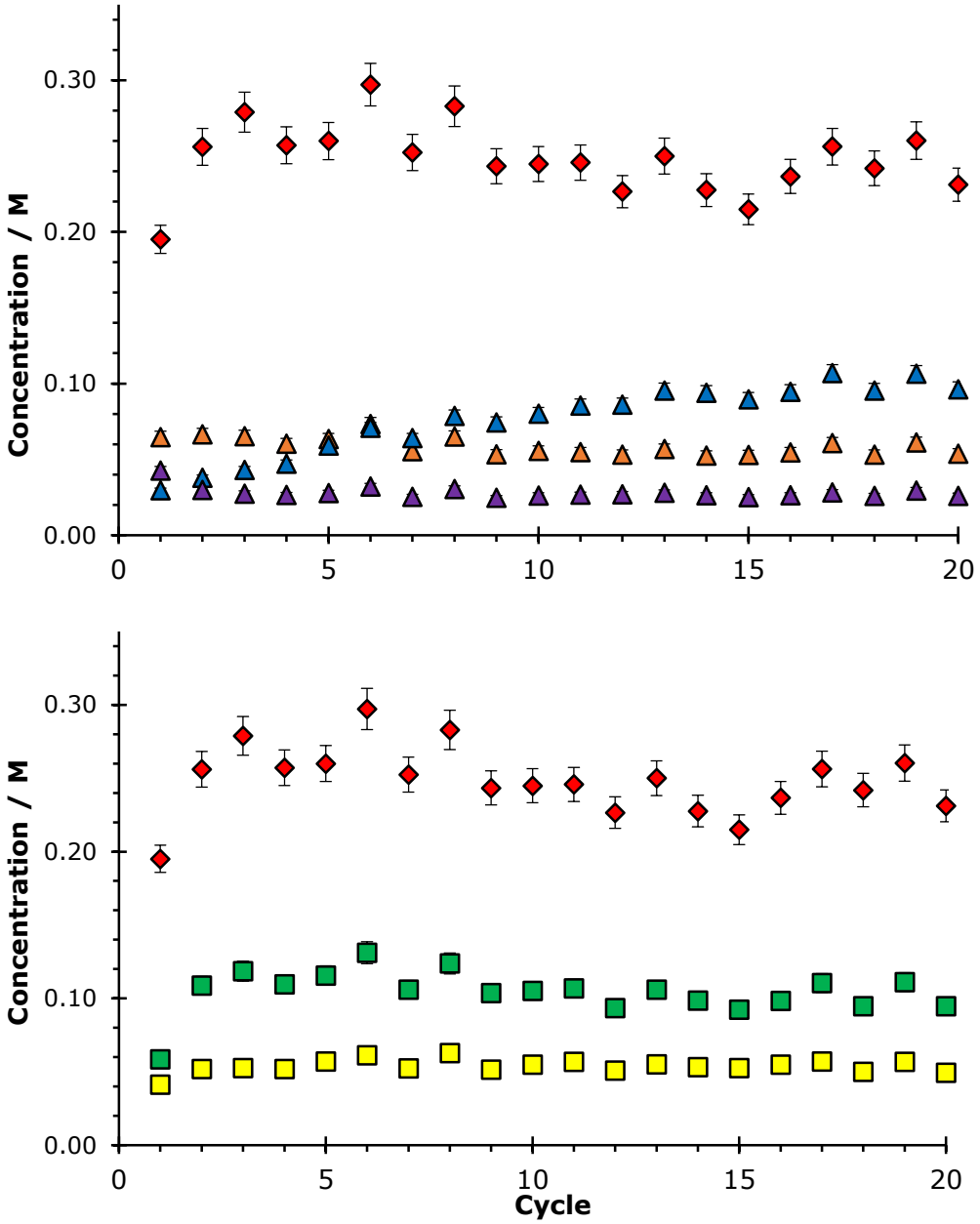


Figure 5.22 A plot to show the composition of progressive exit solutions collected after decarboxylation of IC (▲). The results show fluctuations in concentration of MAA (◆) during the reaction; however, there is not a significant decrease in MAA concentration over the 20 cycles. The concentrations of CC (▲) and MC (▲) also appear stable over the twenty cycles, while the concentration of IC increases slightly indicating a small drop in conversion. There is an initial increase in concentration of HIB (■), seemingly tracking the trend shown by MAA concentration. The concentration of by-product PY (□) remains stable.

The concentration of CC after Cycle 1 was 0.065 M and remained stable between 0.053 M and 0.067 M over the twenty cycles. After an initial concentration of 0.043 M, MC concentration dropped to between 0.025 M and 0.032 M during the remaining cycles. Unlike its isomers, the concentration of IC does increase slightly over the twenty cycles from 0.030 M to 0.095 M in Cycle 13 but then reaches a steady level between 0.090 M and 0.107 M. This is significantly lower than the concentration of IC in Experiment 29 which reached a maximum of 0.194 M, suggesting the build-up of the acid was not as great when the pH of the system was balanced. The conversion of this experiment lies slightly lower than that of the previous experiment at 67.4 %, but the selectivity remained high at 48.0 %. This shows that the pH balance improves the selectivity of the reaction, making it a more viable route to MAA.

The concentration of PY lies between 0.041 M and 0.063 M for each exit solution shown in Figure 5.22, and is similar to the concentrations shown in previous recycles described in this chapter.

It should be noted that after the addition of solid IC to aid the extraction of MAA by liquid-liquid extraction, the aqueous solutions were stirred for a period of 5 mins to ensure complete mixing has taken place. This period was more than adequate for the first ten cycles, but the solid became increasingly difficult to dissolve as each cycle passed and the stirring period had to be extended. In Cycles 19 and 20, the stirring period had to be increased to 50 mins, indicating the solution was becoming more saturated. It is recommended that the process be limited to fifteen cycles to avoid the saturation of the aqueous solution.

PMMA Production

In order to prove the usability of the whole process to completion, a sample of PMMA would need to be produced by our recycling process. As such, an experiment was designed to first esterify the collected MAA and further polymerise MMA. At present, there is no small scale commercial availability of bio-methanol and so methanol from petrochemical feedstocks was used. However, on a much larger scale, it would be possible to purchase second generation bio-methanol[128] to achieve a supply of bio-PMMA.

Experiment 31 - PMMA Synthesis

After esterification and purification of MAA (detailed in Chapter 2), a colourless sample of MMA was collected δ_H(300 MHz; D_2O) 1.79 (3 H, m, Me), 3.28 (3 H, s, Me), 5.27 (1 H, m, CH) and 5.56 (1 H, m, CH).

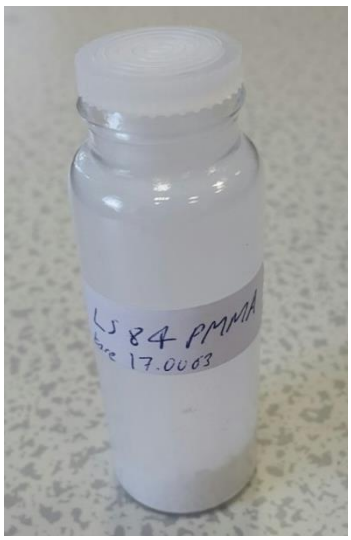


Figure 5.23 A sample of MAA collected in Experiment 30 was esterified and polymerised to form a white powder. Analysis with ^{1}H NMR confirms the production of PMMA.

The liquid was polymerised through dispersion using an azobisisobutyronitrile (AIBN) initiator. The resulting solid powder (seen in

Figure 5.23) shows a shift in the ^{1}H NMR from 3.28 to 3.16 ppm, indicating the successful polymerisation of the free MMA to PMMA. GPC analysis, shown in Table 5.12 shows the resulting PMMA to have a large molar mass and small polydispersity, as could be expected from an uncontrolled living radical polymerisation reaction of this type.

Table 5.12 Showing the data collected by GPC to describe the molar mass, M_n, mass average molar mass, M_w, and polydispersity of a sample of PMMA.

	M_n / kDa	M_w / kDa	Polydispersity
PMMA	90.2	102.9	1.141

Scale Up

To investigate the effects of a scale up, we were keen to run the recycling process on a larger scale. From this a sample of MAA was collected that was polymerised, extruded and moulded to form a sample plaque of PMMA to be compared with a sample of PMMA formed by the ACH process described in Chapter 1 of this thesis.

Experiment 32 - Recycling Itaconic Acid : 10 Cycles

Colleagues at Lucite International have since carried out a larger scale recycling experiment to investigate if concentration limits the reaction. The precursor solution was made up to contain 26 wt % (3.03 M) IC and 8 wt % (3.03 M) NaOH and was introduced to their rig (see Appendix X) containing a 96 mL C276 Hastelloy reactor under the same temperature and pressure conditions, but with a longer residence time of 460 secs. This longer residence time was used to account for heating differences found between their rig and the rig used for our research. The pH of solutions in this experiment were measured but not balanced.

Table 5.13 Showing the reaction conditions used in Experiment 32.

Experiment 32 Itaconic Acid Recycle	
Precursor	26 wt % Itaconic Acid
Base	8 wt % NaOH
Temperature	260 °C
Pressure	3000 psi
Precursor Flow Rate	9.6 ml min^{-1}
Residence Time	460 s

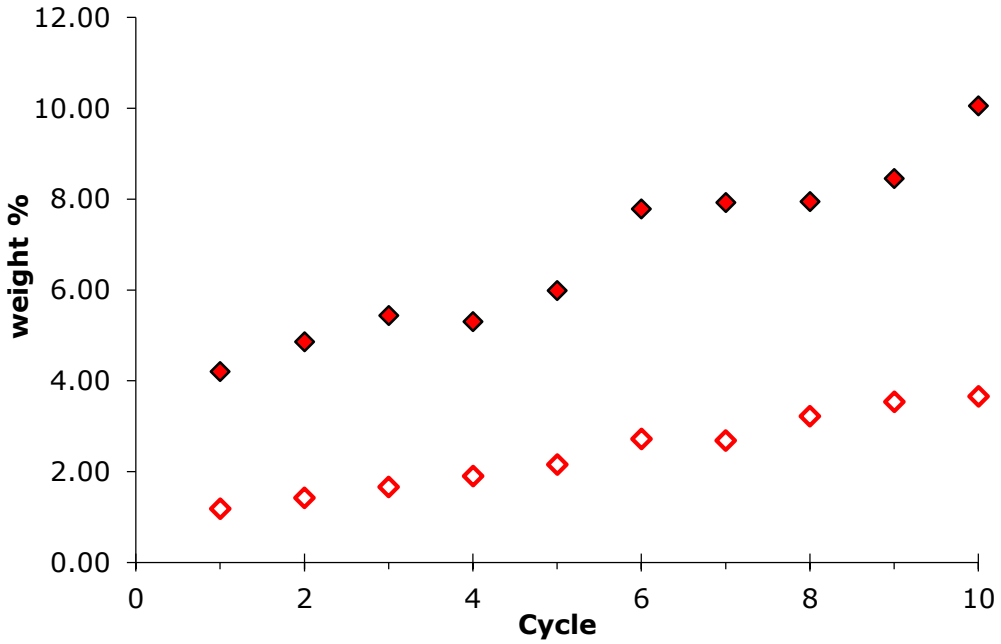


Figure 5.24 A plot to show the amount of MAA present in each decarboxylation exit solution (◆) and after three serial extractions with pentane (◇). The plot shows an increase in MAA concentration with each cycle, both before and after extraction. Errors were not calculated during this experiment.

The results seen in Figure 5.24 show an increase in the amount of MAA produced in each cycle. This is in stark contrast to the results shown earlier in this chapter. Our earlier research concluded that the concentration of MAA only increased during the first few cycles of an experiment; in fact, Experiment 29 shows that after an initial increase, the level of MAA produced decreases. Our previous results suggest that by pH balancing the system, a higher yield of MAA can be achieved. However, the pH of the

system does not appear to be as important in more concentrated solutions as results in Figure 5.24 show.

Along with the increased MAA production, Figure 5.24 shows an increase in the level of MAA carried through into subsequent cycles. This does not appear to be the cause of the increased MAA concentration of exit solutions, although it may be a contributing factor.

Figure 5.25 shows that the concentrations of the three isomers (CC, IC and MC) fluctuate throughout the experiment and do not appear to have reached equilibrium in the ten cycles completed. This is again in contrast with results previously described that showed the concentrations of the three isomers varied in initial cycles before levelling off in later cycles.

PY was produced in this experiment, but remained in low concentration throughout. By extrapolating the data collected in Experiment 30, it would be expected that the concentration of PY would lie at around 2.8 wt % when a more concentrated precursor solution was used. Figure 5.25, however, shows that the concentration of this by-product lies much lower, around 0.38 wt %.

The level of HIB increases with increasing cycles. The trend appears to be in direct correlation with the amount of MAA in solution, as found in earlier experiments. Cycle 8 produced a seemingly anomalous result, as the concentration of HIB appears much higher than expected. At the time of writing this thesis, the experiments had not been repeated at Lucite International.

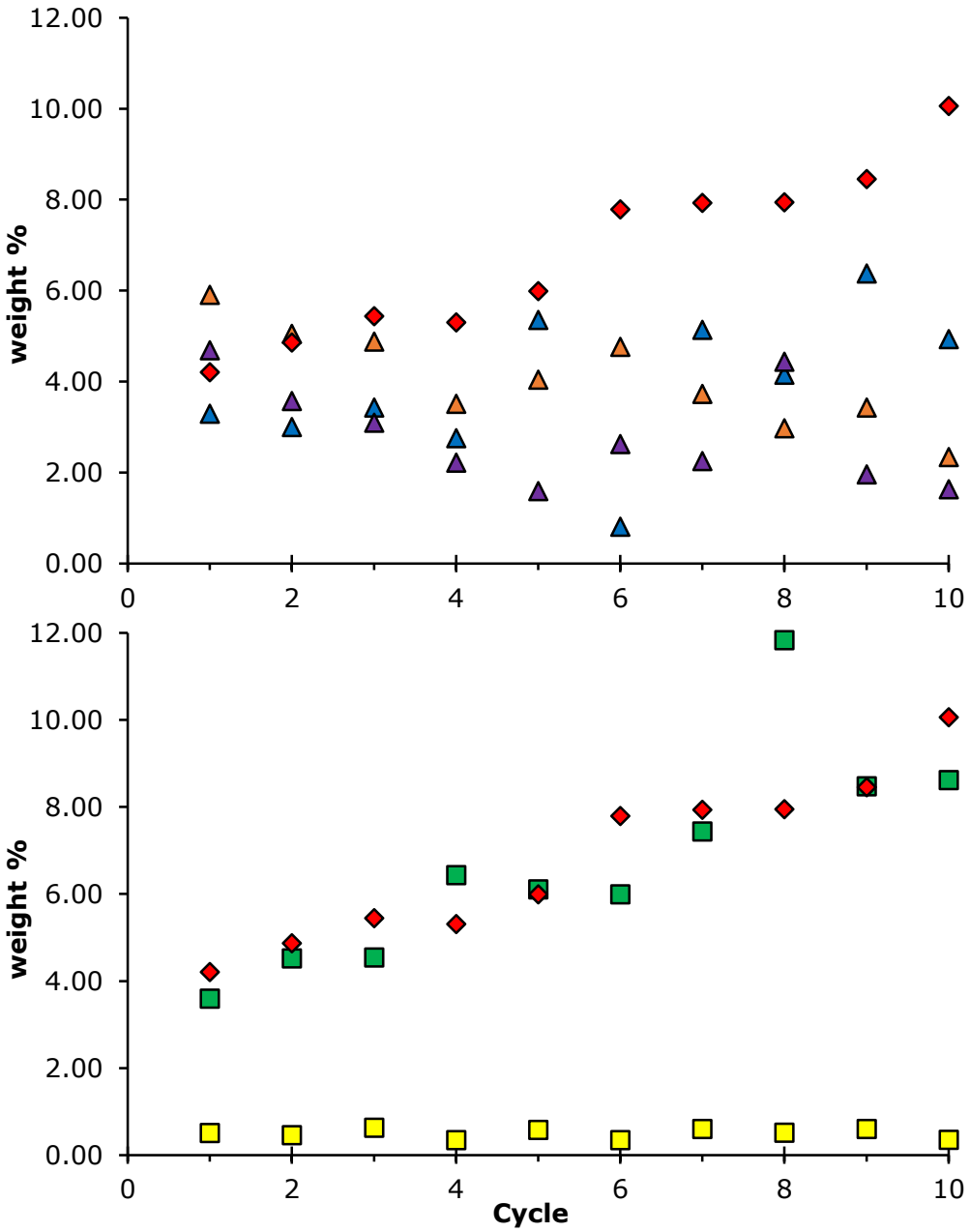


Figure 5.25 The plots show the composition of progressive exit solutions collected after decarboxylation of IC (▲). The results show an increase in concentration of MAA (◆) over the ten cycles. The concentrations of CC (▲), IC and MC (▲) fluctuate during the experiment, while the concentration of HIB (■) closely follows the trend shown by MAA, except one anomalous value from cycle eight. The concentration of by-product PY (□) remains stable throughout the cycles. Errors were not calculated during this experiment.

Colleagues at Lucite International measured the pH of the exit solutions and found them to decrease from 5.23 in Cycle 1 to 4.31 in Cycle 10. In

our Experiment 29, the pH of the exit solutions decreased from 4.84 in Cycle 1 to 4.04 in Cycle 20. This suggests that the increased concentration has an effect on the pH, as would be expected, but reinforces that the production of more acidic by-products causes the decrease in pH.

Experiment 32 shows these trends over ten cycles, in comparison to our longer recycling experiments that continued to 20 cycles. This experiment was not continued further due to concerns over the level of corrosion that appeared to be taking place during the experiment. Colleagues reported the original colourless solution turned pale green after one cycle, but after ten cycles, the collected dark green solution was opaque. ICP analysis was carried out on three samples and the results are seen in Table 5.14.

Table 5.14 ICP analysis of three solutions shows the leaching of metals into reaction solutions.

Cycle no.	Metal / ppm						
	Fe	**Ni**	**Cu**	**Cr**	**Mo**	**W**	**Total**
1	53.6	662.8	< 5	194.9	146.2	34.1	1091.7
5	113.8	1698.1	< 5	664.1	569.2	142.3	3187.5
10	202.2	2503.1	< 5	856.8	712.4	192.5	4467.0

The results of ICP show significant levels of metal ions in each solution. The concentrations of the ions increase with the number of cycles indicating that this is continuing with each pass. This supports earlier suggestions in this thesis that alternative materials should be used in the reactors (and potentially other pipework) used for these reactions.

This experiment yielded 781.62 g pure MAA (purity confirmed by GC analysis). The results show a lower conversion of IC than in our previous experiments of 34.4 % and a lower average selectivity to MAA (28.6 %). It is expected that the high levels of corrosion affected the reaction and the significant levels of metal ions hindered the reaction.

The scaled-up experiment demonstrates that this process depends on the low concentration of the solution and corrosion is minimised. Working on such a large scale would require a new reactor material that could withstand an increase in concentration before this could be viable.

Purification of the collected MAA was by distillation under reduced pressure, water washes and a further distillation under reduced pressure to yield a colourless liquid. This liquid was esterified to MMA and polymerised before a sample plaque of PMMA (Figure 5.26) was extruded. The sample plaque seen in Figure 5.26 is of comparable optical quality to PMMA produced by the ACH process, demonstrating this process as a route to bio-PMMA from easily obtained renewable feedstocks.



Figure 5.26 Two sample plaques of PMMA are shown in front of Lego figures to demonstrate clarity. (Left) A sample made by the traditional ACH process, while (right) the plaque has been manufactured by the method described in Experiment 32. The plaques display comparable optical properties, demonstrating our method as an alternative route to PMMA.

Summary

A series of five cycle experiments show consistent levels of MAA are produced (0.257 – 0.279 M) irrespective of the nature of the acidic precursor used. When extended to twenty cycles, the concentration of MAA produced falls with each cycle to 0.147 M. However, with the addition of a pH balancing step before decarboxylation, this was improved to 0.231 M after cycle 20.

Esterification and polymerisation of a sample of MAA prepared in Experiment 30 has produced a sample of PMMA with a T_g value similar to literature values. When a separate sample of bio-MAA was esterified, polymerised and extruded, the resulting plaque of PMMA showed similar optical and mechanical properties to PMMA produced by the ACH process.

Finally, this process was scaled up by colleagues at Lucite International but showed lower conversion and selectivity to earlier experiments. Different reactor materials should be investigated when conducting the experiment using these conditions to investigate the effects of corrosion on the reactions.

Chapter 6 - Conclusions and further work

The research conducted during this project began by investigating the application of previous work[67, 72, 75, 76] to the production of acrylic acid from sustainable resources. While possible, it was shown that the formation of by-products prevents the process from competing with other methods.

This thesis then described a new process for the production of MAA from di- and tri-carboxylic acid precursors, made available through known biological processes that convert biomass useful precursors. Further reactions showed the potential for scale-up of the process and for the production of bio-PMMA.

At the end of Chapter 1, the aims of this project were outlined. This final chapter concludes my research and discusses the extent to which each of the aims was reached. Further work is suggested and the future outlook of the research is described.

Aim 1

Improvements are needed into the analysis of the complex mixture of acids produced. For example, data for HIB could not be obtained with the UV detection set up in Huddle's HPLC system. By utilising a refractive index detector (RID), a more detailed and reliable set of results for each experiment can be obtained.

Progress

Early on in this project, an RID was added to the HPLC system used. This new detection method presented multiple benefits, including:

- accurate detection of UV inactive molecules was made possible. Previously, molecules such as HIB were detected by ^{1}H NMR and

using the integration values associated with the molecule compared to MAA, an estimated concentration was reported.[72] With the introduction of the RID, a single method was made possible for the detection of all compounds present in the solution, while ^{1}H NMR was used to reinforce findings;

- the detection of previously unidentified molecules was made possible. Chapter 4 describes the isolation of 3-hydroxyisobutyric acid from an exit solution that had not been detected with the UV detector, but was easily detected by the RID. Due to the low concentrations of the molecule and complex mixtures of organic molecules present in all exit solutions, the molecule had gone unnoticed in the background noise of ^{1}H NMR spectra; and
- the removal of a dilution step reduced the amount of processing required before analysis. The UV detector used with the HPLC system was easily overloaded by concentrated samples and required dilution. However, the RID was able to measure higher concentrations of the organic acids and so dilution was rendered unnecessary.

Further work

The addition of the RID enabled a more in-depth analysis into the nature and concentrations of compounds in the exit solutions. Bubbles were observed in the exit stream of almost all reactions in this thesis; however, no research was completed during this project into the nature of gaseous or volatile products. Chapter 3 describes a drop in mass balance that could be due to the formation of such by-products. It would be possible to collect exit samples in sealed bags and analyse the gaseous products by gas chromatography with mass spectrometry (GCMS) in order to identify them and propose suggestions for the reactions taking place.

Aim 2

Huddle's research will be used as a basis for a similar investigation into the production of acrylic acid. This is another monomer of interest to Lucite International and could lead to a second, independent chemical process.

Progress

Research into the production of acrylic acid from malic acid, an analogous system to the decarboxylation and dehydration of citramalic acid reported by Huddle,[72] was conducted. Reactions of malic acid in high temperature, compressed water yielded low levels of acrylic acid (0 - 46 %) and significant concentrations of unwanted by-products. There were also notable mass losses in these reactions, indicating the formation of undetected and/or unidentified products.

Investigations into the stability of acrylic acid indicate the hydration to lactic acid as a prominent side reaction. However, as with the production of HIB from MAA, it would be possible to isolate and dehydrate lactic acid to yield a second crop of acrylic acid. At higher reaction temperatures and longer residence times, the mass balance was observed to decrease, indicating the decomposition of acrylic and/or lactic acids to volatile products.

Finally, knowledge of MAA extraction was applied to acrylic acid and various solvents were tested for their efficiency as extraction solvents. Unfortunately, our research did not reveal an appropriate solvent system that offered both efficiency and selectivity.

Further work

As mentioned earlier, GCMS analysis of gaseous and volatile by-products would improve the mass balance of the results and help to gain a better understanding of any unwanted side-reactions that occur. Isolation of unidentified products would be necessary to further our knowledge of the system.

Further work into the extraction of acrylic acid would be necessary for this process. While the research in this thesis is not a comprehensive study, the solvent systems tested are not suitable and a more selective solvent than 1-octanol would be required for this process.

A decision was made to not continue with research in this area. Other, more attractive routes to bio-acrylic acid are already known[95, 98, 102, 103, 129] and our method would have to be vastly improved before it could compete in the marketplace.

Aim 3

Limited previous work has been carried out on the hydrothermal decomposition of MAA; thus the investigation into the stability of MAA at the conditions likely to be used in the process is imperative to the research. By determining the stability at a range of temperatures, residence times and concentrations of both acid precursor and base, I should be able to suggest a viable working range for the process.

Progress

Chapter 4 details the investigations into both MAA and HIB. A temperature study showed that at temperatures above 260 °C, there was more than

5 % decomposition of MAA. After investigating the effect of residence time, a set of maximum conditions (260 °C and 360 s) was proposed. Equimolar concentrations of acid : base are suggested to both minimise the amount of MAA decomposition as well as hydration of MAA to HIB.

During these investigations, it was noted that a peak appeared in HPLC-RID traces at high temperatures and long residence times that was not observed by HPLC-UV. After isolation and NMR and HPLC analysis, the peak was identified as the anti-Markovnikov hydration product of MAA, 3-hydroxyisobutyric acid.

A study of HIB stability in high temperature, compressed water revealed significant mass losses. This could be due to the production of volatile compounds that were not collected in this project. However, the results in Chapter 4 suggest that the inclusion of a base hinders the decomposition of HIB, supporting the need for a base in the decarboxylation reactions.

Further work

Again, GCMS analysis could prove useful in the detection of the decomposition products of both MAA and HIB. While the working conditions suggested do not yield significant mass loss, the identity of such products would allow for a better understanding of the overall scheme.

Aim 4

Preliminary studies by Huddle showed the possibility of recycling the sodium hydroxide and unreacted starting materials back through the rig after decarboxylation. In order to demonstrate this quantitatively, more data and more cycles are needed to show reproducibility. Recycling experiments will be

run for a range of precursors to show the versatility of the process.

Progress

The research in Chapter 5 shows the recycling of sodium hydroxide up to five times with different precursors. It was shown that any isomer of IC can be used, without any significant effect on the conversion or selectivity of the precursor. As Scheme 1.8 shows, the three isomers all pass through IC before conversion to MAA and results indicate that the rate determining step is the conversion of IC to MAA.

When the length of the experiment was increased to 20 cycles, pH appeared to negatively affect the conversion of IC. Hence, another experiment was conducted to balance the pH of the system after each cycle. The results of this pH balanced recycling experiment prove the method to be successful as the conversion did not show an overall decrease during the experiment.

Colleagues at Lucite International scaled-up the process, using both a larger reactor and higher concentrations of both precursor acid and base catalyst. Interestingly, pH did not appear to hinder the conversion of IC to MAA and the concentration of MAA in the exit solution actually increased with each cycle.

In all of the recycling experiments described in Chapter 5, large amounts of acetic acid were observed. This build-up of acetic acid, and other by-products, could begin to affect the conversion and selectivity of the reaction after more than 20 cycles. However, it is my recommendation that the process does not go beyond 20 cycles as the solution becomes increasingly saturated and the solvation of the precursor acid becomes more difficult.

Further work

Research into the continued scale-up of the reaction is needed to take the process to pilot plant-scale. It has been noted in this thesis that there has been a continued problem of corrosion. I would therefore suggest that an investigation into a more suitable reactor material be carried out as part of the scale-up process. It may be possible to utilise a glass-lined reactor vessel to reduce the corrosion of the reactor causing the discolouration of exit solutions.

Aim 5

> **Finally, using a fermentation broth, it will be demonstrated that we have found a new bio-route to PMMA from biomass precursors. The process will be run from the fermentation step, through to the polymerisation of the esterified MAA to yield a pure sample of bio-PMMA.**

Progress

Experiment 31 in Chapter 5 describes the production of PMMA from MAA collected in our recycling experiments. The collected acid was esterified using methanol and Amberlyst-15H before a suspension polymerisation with AIBN yielded PMMA. This reaction is proof-of-concept for the production of bio-PMMA using our recycling process.

Lucite International have also produced a sample of PMMA from MAA collected from their scaled-up experiment (Experiment 32). A plaque of bio-PMMA is shown in Figure 5.27 and shows similar optical properties to a plaque of PMMA made *via* the ACH process.

Further work

At the time of writing, limited analysis on the plaque of bio-PMMA had been conducted. It is suggested that the plaque should undergo mechanical testing and weathering tests to investigate the effect of any trace contaminants in the bio-PMMA. If there are significant differences caused by these contaminants, the purification of the collected MAA will need to be enhanced to remove those impurities.

Chapter 7 Final Remark

Overall, this research project has proved successful, as a sample of bio-Perspex acts as proof of concept for our method. The scaled-up reaction by colleagues at Lucite demonstrates the first step towards production at pilot plant scale and show promising results for the future development of this process. Further work is necessary and continues with colleagues at Lucite International. I wish them every success in the development of this process.

Laura Schofield

22nd July 2015

References

1. F. Aftalion, *A History of the International Chemical Industry*, Chemical Heritage Foundation, Philadelphia, 1991.
2. Chemical Industries Association, Chemical Industries Association Autumn Statement, http://www.cia.org.uk/Portals/0/Documents/CIA%20input%20to%20Autumn%20Statement.pdf, Accessed 29 July 2014.
3. Chemical Industries Association, UK Chemical and Pharmaceutical Industry Facts and Figures, http://www.cia.org.uk/Portals/0/Documents/CIA%20facts%20and%20figures%202014_MR.PDF, Accessed 25/03/2015, 2015.
4. S. Shafiee and E. Topal, *Energy Policy*, 2009, **37**, 181-189.
5. P. T. Anastas and J. C. Warner, *Green Chemistry: Theory and Practice*, Oxford University Press, New York, 1998.
6. S. L. Y. Tang, R. Smith and M. Poliakoff, *Green Chemistry*, 2005, **7**, 761-762.
7. P. T. Anastas and J. B. Zimmerman, *Environmental Science & Technology*, 2003, **37**, 94A - 101A.
8. S. L. Y. Tang, R. Bourne, R. Smith and M. Poliakoff, *Green Chemistry*, 2008, **10**, 268-269.
9. J. B. Hendrickson, *Journal of the American Chemical Society*, 1975, **97**, 5784-5800.
10. B. M. Trost, *Science*, 1991, **254**, 1471-1477.
11. R. A. Sheldon, *Chemistry & Industry (London)*, 1992, **23**, 903-906.
12. H. C. Kolb, M. G. Finn and K. B. Sharpless, *Angewandte Chemie International Edition*, 2001, **40**, 2004-2021.
13. J. E. Moses and A. D. Moorhouse, *Chemical Society Reviews*, 2007, **36**, 1249-1262.
14. R. Breinbauer and M. Köhn, *ChemBioChem*, 2003, **4**, 1147-1149.
15. V. D. Bock, H. Hiemstra and J. H. van Maarseveen, *European Journal of Organic Chemistry*, 2006, **2006**, 51-68.
16. C. D. Hein, X.-M. Liu and D. Wang, *Pharmaceutical Research*, 2008, **25**, 2216-2230.
17. B. S. Sekhon, *Journal of Pharmaceutical Education and Research*, 2012, **3**, 77-85.
18. W. Xi, T. F. Scott, C. J. Kloxin and C. N. Bowman, *Advanced Functional Materials*, 2014, **24**, 2572-2590.
19. G. G. Brundtland, *Our Common Future: The World Commision on Environmental Development*, Oxford University Press, Oxford, 1987.
20. A. Parkes, *Patents for Inventions. Abridgments of Specifications*, Oxford University Press, Oxford, 1857.
21. J. W. Hyatt Jr. and I. S. Hyatt, *US Pat.,* US105338, 1870.

22. Image taken from, http://blog.sciencemuseum.org.uk/collections/tag/parkesine/, Accessed 28 July 2014.
23. Data taken from, http://www.ecoforce.co.uk/green-facts.htm, Accessed 28 July 2014.
24. Plastics Europe, *Plastics - the facts 2014/2015*, 2015.
25. Freedonia Group, *World Bioplastics*, 2013.
26. F. Koopman, N. Wierckx, J. H. de Winde and H. J. Ruijssenaars, *Bioresource Technology*, 2010, **101**, 6291-6296.
27. I. S. Bayer, S. Guzman-Puyol, J. A. Heredia-Guerrero, L. Ceseracciu, F. Pignatelli, R. Ruffilli, R. Cingolani and A. Athanassiou, *Macromolecules*, 2014, **47**, 5135-5143.
28. B. Harris, *Ingenia*, 2010, **45**, 18-23.
29. L. E. Fitzpatrick, J. W. Y. Chan and M. V. Sefton, *Biomaterials*, 2011, **32**, 8957-8967.
30. M. Kidd, *Freeflow - Lucite International*, 2011, **9**, 4.
31. W. Bauer Jr., in *Ullmanns Encyclopedia of Industrial Chemistry*, Wiley Online, 2000.
32. A. van Ophuysen, *Eur. Pat.,* EP2698171A1, 2012.
33. R. V. Slone, in *Kirk-Othmer Encyclopedia of Chemical Technology*, John Wiley & Sons, Inc., West Sussex, 2000.
34. H. Ozaki, S. Terabe and A. Ichihara, *Journal of Chromatography A*, 1994, **680**, 117-123.
35. W. Bauer, in *Ullmann's Encyclopedia of Industrial Chemistry*, Wiley Online, 2000.
36. Asylum SFX, personal communication.
37. Merchant Research & Consulting, *Methyl Methacrylate (MMA): 2014 World Market Outlook and Forecast up to 2018*, 2014.
38. PERP Program - Methyl Methacrylate, 2006, http://www.chemsystems.com/reports/search/docs/abstracts/0405-2_abs.pdf, Accessed 4 May 2012.
39. J. W. C. Crawford, *Br. Pat.,* GB405699, 1934.
40. Sigma Aldrich, MSDS data sheet.
41. Locating and Estimating Air Emissions from Sources of Acrylonitrile, http://www.epa.gov/ttnchie1/le/acrylon.pdf, Accessed 11 May 2012.
42. M. Weber, M. Weber and M. Kleine-Boymann, in *Ullmann's Encyclopedia of Industrial Chemistry*, Wiley Online, 2000.
43. I. Gotoh and J. Endoh, *US Pat.,* US4124634, 1978.
44. T. Nakamura and T. Kita, *Chemical Economy & Engineering Review*, 1983, **15**, 23.
45. Y. Shikakura, F. Sakai and H. Shimizu, *US Pat.,* US4012449, 1977.
46. S. Umemura, K. Ohdan, K. Suzuki and T. Hisayuki, *US Pat.,* US4171328, 1979.
47. J. W. Nemec and M. S. Cholod, *US Pat.,* US4358622, 1982.

48. W. G. Shaw, P. L. Kuch and C. Paparizos, *US Pat.,* US4301031, 1981.

49. S. Umemura, K. Ohdan, F. Sakai, K. Suzuki, Y. Bando, T. Hogami and M. Fuginaga, *US Pat.,* US4364844, 1982.

50. M. Matsumoto and H. Sugi, *US Pat.,* US4467113, 1984.

51. K. Nagai, *Applied Catalysis A: General*, 2001, **221**, 367-377.

52. D. Johnson, *Chemistry & Industry*, 2009, **20**, 21.

53. G. R. Eastham, J. M. Thorpe and R. P. Tooze, *US Pat.,* US6335471B1, 2002.

54. G. R. Eastham, J. M. Thorpe and R. P. Tooze, *Eur. Pat.,* EP1003754B1, 2004.

55. R. P. Tooze, G. R. Eastham, K. Whiston and X. L. Wang, *Wo. Pat.,* WO9619434, 1996.

56. Alpha - Set to Cut MMA Manufacturing Costs by 40 %, http://www.luciteinternational.com/about-us/whats-new/2004/alpha---set-to-cut-mma-manufacturing-costs-by-40/, Accessed 30 July 2014.

57. M Kidd, *Freeflow - Lucite International*, 2011, **9**, 2.

58. V. Middlebrook, Mitsubishi Rayon Company (MRC) and SABIC to begin construction of joint venture MMA and PMMA plants in Saudi Arabia, http://blog.luciteinternational.com/mitsubishi-rayon-company-mrc-and-sabic-to-begin-construction-of-joint-venture-mma-and-pmma-plants-in-saudi-arabia/, Accessed 26/04/15.

59. K. Byrappa and M. Yoshimura, *Handbook of Hydrothermal Technology*, Noyes Publications, New Jersey, 2001.

60. S. Sōmiya, *Hydrothermal reactions for materials science and engineering*, Elsevier Applied Science, London, 1989.

61. G. W. Morey, *Journal of the American Ceramic Society*, 1953, **36**, 279-285.

62. J. García, O. Pérez, F. Fdez-Polanco and M. J. Cocero, Supercritical Water as Reaction Media: Physical Properties at Supercritical Conditions An Overview, www.isasf.net/fileadmin/files/Docs/Versailles/Papers/PTp1.pdf, Accessed 17/05/15, 2015.

63. P. Kritzer, N. Boukis and E. Dinjus, *Journal of Supercritical Fluids*, 1999, **15**, 205-227.

64. NIST, NIST fluids database, www.webbook.nist.gov/chemistry/fluid/, Accessed 20/6/2015.

65. S. A. Leeper, T. E. Ward and G. F. Andrews, *Production of Organic Chemicals via Bioconversion: A Review of the Potential*, EG&G, Idaho, 1991.

66. T. Willke and K.-D. Vorlop, *Applied Microbiology and Biotechnology*, 2001, **56**, 289-295.

67. M. Carlsson, C. Habenicht, L. C. Kam, M. J. Antal Jr., N. Bian, R. J. Cunningham and M. Jones Jr., *Industrial & Engineering Chemistry Research*, 1994, **33**, 1989-1996.

68. G. D. Cody, J. G. Blank, J. Brandes, R. Hazen and H. Yoder Jr., *Preprints Fuel Chemistry Division, 217th American Chemical Society Meeting*, 2001, **44**, 348-353.

69. J. Li and T. B. Brill, *The Journal of Physical Chemistry A*, 2001, **105**, 10839-10845.

70. A. Chapman, unpublished work,

71. D. W. Johnson, G. R. Eastham and M. Poliakoff, *Wo. Pat.,* WO2011077140A2, 2011.

72. T. A. Huddle, PhD Thesis, University of Nottingham, 2012.

73. G. R. Eastham, D. W. Johnson and M. Waugh, *Wo. Pat.,* WO2013160703A1, 2013.

74. J. Le Nôtre, S. C. M. Witte-van Dijk, J. van Haveren, E. L. Scott and J. P. M. Sanders, *ChemSusChem*, 2014, **7**, 2712-2720.

75. D. W. Johnson, G. R. Eastham, M. Poliakoff and T. A. Huddle, *Wo. Pat.,* WO2012107758A1, 2012.

76. D. W. Johnson, G. R. Eastham, M. Poliakoff and T. A. Huddle, *Wo. Pat.,* WO2012069813A1, 2012.

77. T. Robert, *Progress in Organic Coatings*, 2015, **78**, 287-292.

78. 3M, Structural Acrylic Adhesives, http://solutions.3m.com/wps/portal/3M/en_US/Adhesives/Tapes/Promotions/Structural-Acrylic-Adhesives/, Accessed 20/6/2015.

79. M. A. Kropp and Z. J. Thompson, *Wo. Pat.,* WO2013126377A1, 2013.

80. J. A. Kent, *Handbook of Industrial Chemistry and Biotechnology*, Springer US, New York, 12th ed., 2012.

81. M. J. Zohuriaan-Mehr and K. Koabiri, *17*, 2008, **6**, 451-477.

82. J. E. Potts, *US Pat.,* US4372311, 1983.

83. T. Kambayashi, H. Mekata, H. Umezu and H. Matsunaga, *US Pat.,* US5660935, 1997.

84. G. Gruber, *US Pat.,* US6828008, 2004.

85. Frogtape, http://www.frogtape.co.uk/, Accessed 08/11/2015.

86. S. Clark, Global Acrylic Market 2013 - 2020, http://www.alliedmarketresearch.com/acrylic-acid-market, Accessed 05/05/15, 2015.

87. W. E. Campbell, E. L. McDaniel, W. H. Reece, J. E. Williams and H. S. Young, *Industrial & Engineering Chemistry Product Research and Development*, 1970, **9**, 325-334.

88. T. N. Shimizu, I. I. Yanagisawa, T. M. Takata and H. T. Sato, *US Pat.,* US4147885, 1979.

89. M. A. Naylor Jr., *US Pat.,* US3271447, 1966.

90. M. W. Andersen, J. B. Myers, G. Hecquet, R. Kotwica, M. Stojanovic, C. Pham and M. Simon, *US Pat.,* US6281384B1, 2001.

91. W. Reppe, *US Pat.,* US3023237, 1962.

92. Y. Chen and J. Nielsen, *Current Opinion in Biotechnology*, 2013, **24**, 965-972.

93. X. Jiang, X. Meng and M. Xian, *Applied Microbiology and Biotechnology*, 2009, **82**, 995-1003.

94. P. Tsobanakis, X. Meng and T. W. Abraham, *US Pat.,* US008846353B2, 2014.

95. Novozymes, BASF, Cargill and Novozymes achieved another milestone in bio-based acrylic acid, http://www.novozymes.com/en/news/news-archive/Pages/BASF-Cargill-and-Novozymes-achieved-another-milestone-in-bio-based-acrylic-acid.aspx, Accessed 08/11/2015.

96. J. E. Godlewski, J. Villalobos, J. E. Velasquez and D. I. Collias, *US Pat.,* US20130274518A1, 2013.

97. J. E. Godlewski, J. Villalobos, D. I. Collias, A. Meyer, P. Dziezok and J. E. Velasquez, *US Pat.,* US20130274697A1, 2013.

98. Novozymes, Novozymes and Cargill continue bio-acrylic acid partnership as BASF exit, http://www.novozymes.com/en/news/news-archive/Pages/Novozymes-Cargill-continue-bio-acrylic-acid-partnership-BASF-exits.aspx, Accessed 22/6/2015.

99. M. Ayoub and A. Z. Abdullah, *Renewable and Sustainable Energy Reviews*, 2012, **16**, 2671-2686.

100. C. A. G. Quispe, C. J. R. Coronado and J. A. Carvalho Jr, *Renewable and Sustainable Energy Reviews*, 2013, **27**, 475-493.

101. H. W. Tan, A. R. Abdul Aziz and M. K. Aroua, *Renewable and Sustainable Energy Reviews*, 2013, **27**, 118-127.

102. J.-L. Dubois, K. Ok-Umura, Y. Kobayashi and R. Hiraoka, *Wo. Pat.,* WO2013017904A1, 2013.

103. J. Deleplanque, J. L. Dubois, J. F. Devaux and W. Ueda, *Catalysis Today*, 2010, **157**, 351-358.

104. T. A. M. Msagati, *Chemistry of Food Additives and Preservatives*, John Wiley & Sons, Ltd, West Sussex, 2013.

105. M. Kawagoe, K. Hyakumura, S.-I. Suye, K. Miki and K. Naoe, *Journal of Fermentation and Bioengineering*, 1997, **84**, 333-336.

106. S. Y. Moon, S. H. Hong, T. Y. Kim and S. Y. Lee, *Biochemical Engineering Journal*, 2008, **40**, 312-320.

107. R. M. Latanision and R. W. Shaw, *Corrosion in supercritical water oxidation systems: Workshop Summary*, Energy Laboratory, Massachusetts Institute of Technology, Massachusetts, 1993.

108. Corrosion Materials, Alloy C276 Data Sheet, https://www.google.co.uk/url?sa=t&rct=j&q=&esrc=s&source=web&cd=10&cad=rja&uact=8&ved=0CHEQFjAJ&url=http%3A%2F%2Fwww.corrosionmaterials.com%2Fdocuments%2FdataSheet%2FalloyC276DataSheet.pdf&ei=C2OWVdXXEKfP7gb9wYv4Ag&usg=AFQjCNHoISrIotkUcxn6-vtNtA0qsWitXA, Accessed 03/07/15.

109. Gilson, 221 and 221 XL Liquid Handlers User's Guide, http://www.mansci.com/pdfs/pdfid56.pdf, Accessed 11/05/12.

110. D. Volgger, A. J. Zemann, G. K. Bonn and M. J. Antal Jr., *Journal of Chromatography A*, 1997, **758**, 263-276.

111. L. Pfendt, B. Dražić, G. Popović, B. Drakulić, Ž. Vitnik and I. Juranić, *Journal of Chemical Research (S)*, 2003, **2003**, 247-248.

112. C. D. Willson and E. A. Adelberg, *The Journal of Biological Chemistry*, 1957, **229**, 1011-1018.

113. Thermo Scientific, iCAP™ Q ICP-MS, http://www.thermoscientific.com/content/tfs/en/product/icap-q-icp-ms.html, Accessed 03/07/15.

114. H. G. Joglekar, I. Rahman, S. Babu, B. D. Kulkarni and A. Joshi, *Separation and Purification Technology*, 2006, **52**, 1-17.

115. T. Ohrui, Y. Sakakibara, Y. Aono, M. Kato, H. Takao and M. Ayano, *US Pat.,* US3968153, 1976.

116. K. L. Wasewar, A. Keshav and Seema, *International Journal of Research and Reviews in Applied Sciences*, 2010, **3**, 290-302.

117. M. E. T. Alvarez, E. B. Moraes, A. B. Machado, R. Maciel Filho and M. R. Wolf-Maciel, *Applied Biochemistry and Biotechnology*, 2007, **136-140**, 451-461.

118. A. Attia, F. Mutelet, R. Solimando and M. R. Jeday, *Journal of Chemical & Engineering Data*, 2012, **57**, 2114-2120.

119. OECD-SIDS, Online Database, Methacrylic Acid, www.inchem.org/documents/sids/sids/79414.pdf, Accessed 03/05/15, 2015.

120. C. Colominas, J. Teixidó, J. Cemeli, F. J. Luque and M. Orozco, *Journal of Physical Chemistry B*, 1998, **102**, 2269-2276.

121. Dielectric Chart, http://depts.washington.edu/eooptic/linkfiles/dielectric_chart%5B1%5D.pdf, Accessed 03/05/15, 2015.

122. Carlos Colominas, Jordi Teixidó, Jose Cemelí, Francisco J Luque and Modesto Orozco, *The Journal of Physical Chemistry B*, 1998, **102**, 2269-2276.

123. M. Waugh, unpublished work, 25/05/2012.

124. Sigma Aldrich, Toluene MSDS, http://www.sigmaaldrich.com/MSDS/MSDS/DisplayMSDSPage.do?country=GB&language=en&productNumber=244511&brand=SIAL&PageToGoToURL=http%3A%2F%2Fwww.sigmaaldrich.com%2Fcatalog%2Fproduct%2Fsial%2F244511%3Flang%3Den, Accessed 03/02/15.

125. Sigma Aldrich, Dodecane MSDS, https://www.sigmaaldrich.com/MSDS/MSDS/DisplayMSDSPage.do?country=GB&language=en&productNumber=297879&brand=SIAL&PageToGoToURL=https%3A%2F%2Fwww.sigmaaldrich.com%2Fcatalog%2Fproduct%2Fsial%2F297879%3Flang%3Den, Accessed 21/07/2015.

126. Sigma Aldrich, Decalin MSDS, http://www.sigmaaldrich.com/MSDS/MSDS/DisplayMSDSPage.do?country=GB&language=en&productNumber=D251&brand=SIAL&PageToGoToURL=http%3A%2F%2Fwww.sigmaaldrich.com%2Fcatalog%2Fproduct%2Fsial%2Fd251%3Flang%3Den, Accessed 21/07/2015.

127. I. Smallwood, *Handbook of Organic Solvent Properties*, Elsevier Science, New York, 2012.

128. Nordic Green, unpublished work, 24/07/14.

129. R. Beerthuis, G. Rothenberg and N. R. Shiju, *Green Chemistry*, 2015, **17**, 1341-1361.

Chapter 8 Appendix

Please see the attached CD for the appendix.